

A Diffusion Hydrodynamic Model

U.S. Geological Survey

Water-Resources Investigations Report 87-4137



Sponsored by the
U.S. Geological Survey
No. PO 080109



[\[Back to DHM Home\]](#) [\[Back to Research\]](#) [\[Cover\]](#) [\[Table of Contents 1\]](#) [\[Table of Contents 2\]](#) [\[Table of Contents 3\]](#)
[i](#) [ii](#) [iii](#) [iv](#) [v](#) [vi](#) [vii](#) [viii](#) [ix](#) [x](#) [\[Next Page -->\]](#)

A DIFFUSION HYDRODYNAMIC MODEL
By Theodore V. Hromadka II and Chung-cheng Yen

U.S. GEOLOGICAL SURVEY
Water-Resources Investigations Report 87-4137

Contract Number--PO 080109
Name of Contractor--Williamson and Schmid
Principal Investigator--Theodore V. Hromadka II
Contract Officer's Representative--Marshall E. Jennings
Short Title of Work--Diffusion Hydrodynamic Model
Effective Date of Contract--12/9/85
Contract Expiration Date--2/3/86
Amount of Contract--\$4,500.00
Date Report is Submitted--8/10/87

Sponsored by the
U.S. Geological Survey

[\[Back to DHM Home\]](#) [\[Back to Research\]](#) [\[Cover\]](#) [\[Table of Contents 1\]](#) [\[Table of Contents 2\]](#) [\[Table of Contents 3\]](#)
[\[<-- Previous Page\]](#) [i](#) [ii](#) [iii](#) [iv](#) [v](#) [vi](#) [vii](#) [viii](#) [ix](#) [x](#) [xi](#) [\[Next Page -->\]](#)

UNITED STATES DEPARTMENT OF THE INTERIOR

Donald Paul Hodel, Secretary

Geological Survey

Dallas L. Peck, Director

For Additional Information
write to:

U.S. Geological Survey
Water Resources Division
Gulf Coast Hydroscience Center
Building 2101
NSTL, Mississippi 39529

Copies of the report can be purchased from:

Open-File Services Branch
Western Distribution Branch
U.S. Geological Survey
Box 25425, Federal Center
Denver, Colorado 80225

[\[Back to DHM Home\]](#) [\[Back to Research\]](#) [\[Cover\]](#) [\[Table of Contents 1\]](#) [\[Table of Contents 2\]](#) [\[Table of Contents 3\]](#)
[\[<-- Previous Page\]](#) [i](#) [ii](#) [iii](#) [iv](#) [v](#) [vi](#) [vii](#) [viii](#) [ix](#) [x](#) [xi](#) [xii](#) [\[Next Page -->\]](#)

CONTENTS

	Page
Abstract	1
Introduction	2
Acknowledgments	4
Model development	5
Introduction	5
Review of governing equations	5
Equation of motion	7
Diffusion hydrodynamic model	9
One-dimensional diffusion hydrodynamic model	9
Two-dimensional diffusion hydrodynamic model	12
Numerical approximation	14
Numerical solution algorithm	14
Numerical model formulation (Grid element)	15
Model timestep selection	18
Verification of diffusion hydrodynamic model	19
Introduction	19
One-dimensional analysis	22
Study approach	22
Grid spacing selection	29
Conclusions and discussions	30
Two-dimensional analysis	31
Introduction	31
K-634 modeling results and discussion	33

	Page
Program description of the diffusion hydrodynamic model	41
Introduction	41
Interface model	44
Introduction	44
Channel overflow	44
Grid overflow	44
Flooding of channel and grid	47
Applications of diffusion hydrodynamic model	48
One-dimensional model	48
Application1: Steady flow in an open channel	48
Two-dimensional model applications	50
Application2: Rain fall-runoff model	50
Application3: Small dam-break floodplain analysis	55
Application4: Small-scale flows onto a flat plain	59
Application5: Two-dimensional floodflows around a large obstruction	62
Application6: Estuary modeling	68
Application for channel and floodplain interface model	73
Application7: channel-floodplain model	73
Reduction of the diffusion hydrodynamic model to kinematic routing	80
Introduction	80
Application 8: Kinematic routing (one-dimensional)	80

	Page
Conclusions	87
References	89
Attachments	93
A. Computer program	93
Introduction	93
Input file descriptions	96
B. User's instructions	100
Introduction	100
One-dimensional analysis	100
Two-dimensional analysis	100
One-and two-dimensional interface model	100
Inflow boundary conditions	102
Outflow boundary conditions	102
Variable time step	105
Kinematic routing techniques	106
C. Computer listings	107
D. Example run (Application7)	125
Input file	125
Output file (partial results)	130

ILLUSTRATIONS

Figure	Page
1.--Continuity of unsteady flow	6
2.--Simplified representation of energy in unsteady flow	6
3.--Two-dimensional finite difference analog	16
4.--Diffusion model (☉) and k-634 model results (solid line) for 1,000-foot width channel, manning's n = 0.04, And various channel slopes, S_o	24
5.--Comparison of outflow hydrographs at 5 and 10 miles downstream from the dam-break site	25
6.--Comparison of depths of water at 5 and 10 miles downstream from the dam-break site	27
7.--Dam-break study location	32
8.--Surveyed cross section locations on owens river for use in k-634 model	34
9.--Floodplain computed from k-634 model	35
10.--Floodplain discretization for two-dimensional diffusion hydrodynamic model	37
11.--Comparison of modeled water surface elevations	38
12.--Floodplain for two-dimensional diffusion hydrodynamic model	39
13.--Diffusion hydrodynamic model one-dimensional channel elements	42
14.--Grid element nodal molecule	43
15.--Diffusion hydrodynamic interface model	45
16.--Gradually varied flow profiles	49
17.--Cucamonga creek discretization	51
18.--Design storm for cucamonga creek	52
19.--Modeled runoff hydrographs for cucamonga creek	53
20.--Vicinity map for dam-break analyses	54

ILLUSTRATIONS

	Page
Figure	
21.--Study dam-break outflow hydrograph for Orange County Reservoir	56
22.--Location map for the Orange County Reservoir dam-break problem	57
23.--Domain discretization for Orange County Reservoir	58
24.--Comparison of flood plain results for Orange County Reservoir	60
25.--Location map for L02P30 temporary retarding basin	61
26.--Flood plain for 80.5 At basin test for L02P30 temporary retarding basin	63
27.--Time of maximum flooding depth (80.5 Af basin test) for L02p30 temporary retarding basin	64
28.--Location map for Ontario Industrial Partners temporary detention basin	65
29.--Domain discretization for Ontario Industrial Partners detention basin	66
30.--Flood plain for Ontario Industrial Partners detention basin	67
31.--Time (hours) of maximum flooding depth for Ontario Industrial Partners detention basin	69
32.--A hypothetical bay	70
33.--The schematization of a hypothetical bay shown in figure 32	70
34.--Mean velocity and water surface profiles at 1-hour	70
35.--Mean velocity and water surface profiles at 5-hours	72
36.--Mean velocity and water surface profiles at 10-hours	72
37.--Diffusion hydrodynamic model discretization of a hypothetical watershed	74
38.--Inflow and outflow boundary conditions for the hypothetical watershed model	74

ILLUSTRATIONS

Figure	Page
39.--Diffusion hydrodynamic modeled floodplain at time = 1-hour	75
40.--Diffusion hydrodynamic modeled floodplain at time = 2-hours	75
41.--Diffusion hydrodynamic modeled floodplain at time = 3-hours	76
42.--Diffusion hydrodynamic modeled floodplain at time = 5-hours	76
43.--Diffusion hydrodynamic modeled floodplain at time = 7-hours	77
44.--Diffusion hydrodynamic modeled floodplain at time = 10-hours	77
45.--Maximum water depth at different cross-sections	78
46.--Bridge flow hydrographs assumed outflow relation: ($q = 10d$)	79
47.--Critical outflow hydrographs for floodplain	79
48.--Diffusion model (☉), kinematic routing (dashed line) and k-634 model results (solid line) for 1,000-foot width channel, Manning's $n = 0.040$, And various channel slopes, S_o	82
49.--Comparisons of outflow hydrographs at 5 and 10 miles downstream from the dam-break site	83
50.--Comparisons of depths of water at 5 and 10 miles downstream from the dam-break site	85
A-1.--Flow chart for diffusion hydrodynamic model	94
A-2.--Flow chart for channel and floodplain submodel	95
B-1.--One-dimensional grid elements	101
B-2.--Diffusion hydrodynamic model boundary conditions	103
B-3.--No flux boundary nodes	104
B-4.--Algorithm for the variable time step	105

TABLES

Page

Table 1.--Boundary values for flow computation in a hypothetical bay	71
--	----

ix

[\[Back to DHM Home\]](#) [\[Back to Research\]](#) [\[Cover\]](#) [\[Table of Contents 1\]](#) [\[Table of Contents 2\]](#) [\[Table of Contents 3\]](#)
[\[<-- Previous Page\]](#) [i](#) [ii](#) [iii](#) [iv](#) [v](#) [vi](#) [vii](#) [viii](#) [ix](#) [x](#) [xi](#) [xii](#) [1](#) [2](#) [3](#) [4](#) [5](#) [6](#) [7](#) [\[Next Page -->\]](#)

CONVERSION FACTORS

<u>Multiple inch-pound unit</u>	<u>By</u>	<u>To obtain SI unit</u>
inch	25.4	millimeter
inch per hour	25.4	millimeter per hour
foot (ft)	0.3048	meter
foot per hour (ft/hr)	0.3048	meter per hour
acre	0.4047	hectare
square mile	2.590	square kilometer
acre-foot (acre-ft)	0.001233	cubic hectometer
cubic foot per second (ft ³ /s , or cfs)	0.02832	cubic meter per second

x

[\[Back to DHM Home\]](#)
[\[Back to Research\]](#)
[\[Cover\]](#)
[\[Table of Contents 1\]](#)
[\[Table of Contents 2\]](#)
[\[Table of Contents 3\]](#)
[\[<-- Previous Page\]](#)
[i](#)
[ii](#)
[iii](#)
[iv](#)
[v](#)
[vi](#)
[vii](#)
[viii](#)
[ix](#)
[x](#)
[xi](#)
[xii](#)
[1](#)
[2](#)
[3](#)
[4](#)
[5](#)
[6](#)
[7](#)
[8](#)
[\[Next Page -->\]](#)

List of Symbols

<u>Symbols</u>	<u>Units</u>
a = Amplitude	ft
A = Area	ft ²
C = Chezy resistance coefficient	ft ^{1/2} /s
D = Hydraulic depth	ft
g = Acceleration of gravity	ft/s ²
h = Hydraulic (piezometric) head, or distance below water surface	ft
h _f = Head loss due to boundary friction	ft
h _x = Head loss due to local causes	ft
H = Total head or water surface elevation	ft
H = Matrix of water surface elevation	~
~	~
K = Diffusion coefficient in DHM Model	ft/s ²
K = Matrix of diffusion coefficients	~
~	~
L = Distance along channel	ft
m = Momentum quantity in DHM Model	~
M = Mean water surface	ft
n = Manning's roughness factor	~
p = Pressure	lb/ft ²
P = Wetted perimeter of channel	ft
q = Discharge per unit width	ft ² /s
Q = Discharge	ft ³ /s
R = Hydraulic radius	ft
S = Slope	~
S _a = Slope of acceleration	~

List of Symbols

<u>Symbols</u>	<u>Units</u>
S_e = Slope of energy grade line	~
S_f = Friction slope	~
S_o = Slope of bed	~
t = time	s
Δt = change in time	s
T = Top width of the channel	ft
v = Local velocity	ft/s
V = Average velocity	ft/s
W = Width	ft
x = x-direction in Cartesian Coordinate System	ft
y = y-direction in Cartesian Coordinate System	ft
z = Distance from datum to culvert invert	ft
α = Kinetic energy correction factor	~
γ = Specific weight of the fluid	lb/ft ³
Γ = Boundary of grid element	ft
δ = Width of square grid	ft
θ = Flow angle between x- and y-directions	~
ρ = Density of the fluid	slugs/ft ³
τ = Shear stress	lb/ft ²
τ_o = Shear stress at the bed	lb/ft ²
ξ = Phase lag	s

A Diffusion Hydrodynamic Model
by T. V. Hromadka II and C. C. Yen
Abstract

A diffusion (noninertial) hydrodynamic model of coupled two-dimensional overland flow and one-dimensional open-channel flow has been developed. Because the noninertial form of hydrodynamic flow equations is used, several important hydraulic effects that cannot be handled by the kinematic routing techniques--the approach employed in most watershed models--are accommodated in this model; namely, the model is capable of treating such effects as backwater, drawdown, channel overflow, storage and ponding. Although these hydraulic effects were commonly neglected in the past, they are important in drainage studies involving deficiencies of flood control channel and subtle grade differences between alluvial fan watershed boundaries.

1

[\[Back to DHM Home\]](#) [\[Back to Research\]](#) [\[Cover\]](#) [\[Table of Contents 1\]](#) [\[Table of Contents 2\]](#) [\[Table of Contents 3\]](#)
[\[<-- Previous Page\]](#) [iii](#) [iv](#) [v](#) [vi](#) [vii](#) [viii](#) [ix](#) [x](#) [xi](#) [xii](#) [1](#) [2](#) [3](#) [4](#) [5](#) [6](#) [7](#) [8](#) [9](#) [10](#) [11](#) [\[Next Page -->\]](#)

Introduction

Each year, flood control projects and storm channel systems are constructed by Federal, State, county and city governmental agencies and also by private land developers, which accumulatively cost in the tens of billions of dollars. Additionally, floodplain insurance mapping, zoning, and insurance rates are continually being prepared or modified by the Federal Emergency Management Agency. Finally, the current state-of-the-art in flood system deficiency analysis often results in the costly reconstruction of existing flood control systems. All of these flood control or protection measures are based upon widely used analysis techniques, which commonly are not adequate to represent the true hydraulic/hydrologic response of the flood control system to the standardized design storm protection level. The main drawbacks in the currently available analysis techniques lie in the ability of the current models to represent unsteady backwater effects in channels and overland flow, unsteady overflow of channel systems due to constrictions, such as culverts, bridges, and so forth, unsteady flow of floodwater across watershed boundaries due to two-dimensional (horizontal plane) backwater and ponding flow effects.

In this report is developed a diffusion hydrodynamic model, which approximates all of the above hydraulic effects for channels, overland surfaces, and the interfacing of these two hydraulic systems to represent channel overflow and return flow. The overland flow effects are modeled by a two-dimensional unsteady flow hydraulic model

based on the diffusion (noninertia) form of the governing flow equations. Similarly, channel flow is modeled using a one-dimensional unsteady flow hydraulic model based on the diffusion type equation. The resulting models both approximate unsteady supercritical and subcritical flow (without the user predetermining hydraulic controls), backwater flooding effects, and escaping and returning flow from the two-dimensional overland flow model to the channel system.

This report is organized into five sections as follows:

1. DHM model theoretical development,
2. Verification of the DHM model,
3. Program description for the DHM,
4. Applications of the DHM, and
5. Comparison between the DHM and the simpler kinematic routing technique.

In this report, the pertinent literature is cited as needed in the text. However, for a general overview, the reader is referred to the Two-Dimensional Flow Modeling Conference Proceedings of the U. S. Army Corps of Engineers (1981).

The diffusion hydrodynamic model computer code can be easily handled by most current home computers that support a FORTRAN compiler, FORTRAN listings (and documentation) are included for the reader's convenience.

In typical applications involving large scale problems, pre- and post-processors should be developed to ease the data entry demands, and graphically display the tremendous amount of modeling results generated by the computer models.

Ample applications are included in this report which hopefully demonstrate the utility of this modeling approach in many drainage engineering problems. Problems considered in this report include: (1) one-dimensional unsteady flow problem, (2) rainfall-runoff model, (3) dam-break flow analysis, (4) estuary model, and (5) channel floodplain interface model. Finally, the diffusion hydrodynamic model is modified to accommodate the kinematic routing technique, and applications are made to one-dimensional problems.

Acknowledgments

Acknowledgments are paid to United States Geological Survey, Sacramento, California, for their time and computational assistance with several sections of this report.

Model Development

Introduction

Many flow phenomena of great engineering importance are unsteady in characters, and cannot be reduced to steady flow by changing the viewpoint of the observer. A complete theory of unsteady flow is therefore required, and will be reviewed in this section. The equations of motion are not solvable in the most general case, but approximations and numerical methods can be developed which yield solutions of satisfactory accuracy.

Review of Governing Equations

The law of continuity for unsteady flow may be established by considering the conservation of mass in an infinitesimal space between two channel sections (figure 1). In unsteady flow, the discharge, Q , changes with distance, x , at a rate $\frac{\partial Q}{\partial x}$, and the depth, y , changes with time, t , at a rate $\frac{\partial y}{\partial t}$. The change in discharge volume through space dx in the time dt is $(\frac{\partial Q}{\partial x}) dx dt$. The corresponding change in channel storage in space is $T dx (\frac{\partial y}{\partial t}) dt = dx (\frac{\partial A}{\partial t}) dt$ in which $A = Ty$. Because water is incompressible, the net change in discharge plus the change in storage should be zero; that is

$$\left(\frac{\partial Q}{\partial x}\right) dx dt + T dx \left(\frac{\partial y}{\partial t}\right) dt = \left(\frac{\partial Q}{\partial x}\right) dx dt + dx \left(\frac{\partial A}{\partial t}\right) dt = 0.$$

Simplifying,

$$\frac{\partial Q}{\partial x} + T \frac{\partial y}{\partial t} = 0 \quad (1)$$

or

$$\frac{\partial Q}{\partial x} + \frac{\partial A}{\partial t} = 0 \quad (2)$$

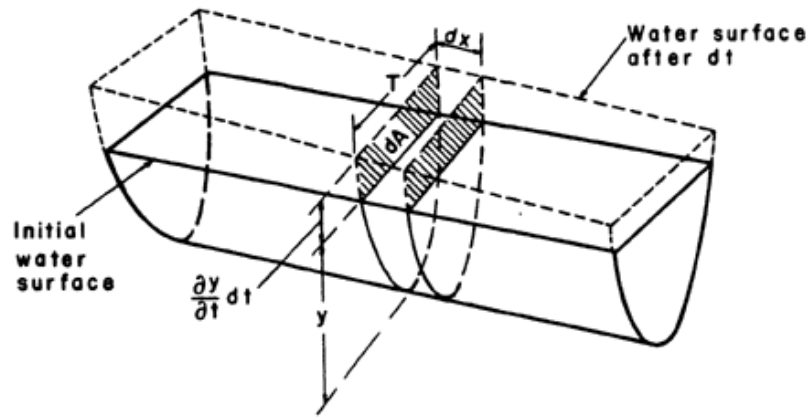


Figure 1.--Continuity of unsteady flow.

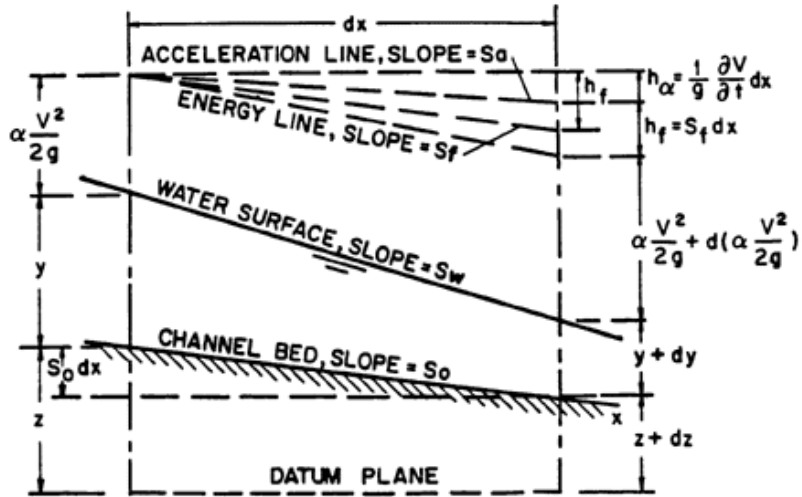


Figure 2.--Simplified Representation of Energy in Unsteady Flow.

At a given section, $Q = VA$; thus equation 1 becomes

$$\frac{\partial(VA)}{\partial x} + T \frac{\partial y}{\partial t} = 0 \quad (3)$$

or

$$A \frac{\partial V}{\partial x} + V \frac{\partial A}{\partial x} + T \frac{\partial y}{\partial t} = 0 \quad (4)$$

Because the hydraulic depth $D = A/T$ and $A = T \cdot Y$, the above equation may be written

$$D \frac{\partial V}{\partial x} + V \frac{\partial y}{\partial x} + \frac{\partial y}{\partial t} = 0 \quad (5)$$

The above equations are all forms of the continuity equation for unsteady flow in open channels. For a rectangular channel or a channel of infinite width, equation 1 may be written

$$\frac{\partial q}{\partial x} + \frac{\partial y}{\partial t} = 0 \quad (6)$$

where q is the discharge per unit width.

Equation of Motion

In a steady, uniform flow, the gradient, $\frac{dh}{dx}$, of the total energy line is equal in magnitude to the "friction slope" $S_f = V^2/(C^2 R)$ where c is the chezy coefficient and r is the hydraulic radius. Indeed this statement was in a sense taken as the definition of S_f ; however in the present context we have to consider the more general case in which the flow is nonuniform and the velocity may be changing in the downstream direction. The net force, shear force and pressure force, is no longer zero, since the flow is accelerating. Therefore, the equation of motion becomes

$$-\gamma A \Delta h - \tau_0 P \Delta x = \rho A \Delta x \left(V \frac{\partial V}{\partial x} + \frac{\partial V}{\partial t} \right)$$

that is,

$$\begin{aligned}\tau_0 &= -\gamma R \left(\frac{\partial h}{\partial x} + \frac{V}{g} \frac{\partial V}{\partial x} + \frac{1}{g} \frac{\partial V}{\partial t} \right) \\ &= -\gamma R \left(\frac{\partial H}{\partial x} + \frac{1}{g} \frac{\partial V}{\partial t} \right)\end{aligned}\quad (7)$$

where τ_0 is the shear stress, P is the hydrostatic pressure, h is the depth of water, Δh is the change of depth of water, γ is the specific weight of fluid, R is the mean hydraulic radius, and ρ is the fluid density. Substituting $\frac{\tau_0}{\gamma R} = \frac{V^2}{C^2 R}$ into equation 7, we obtain

$$\frac{\partial H}{\partial x} + \frac{1}{g} \frac{\partial V}{\partial t} + \frac{V^2}{C^2 R} = 0 \quad (8)$$

and this equation may be rewritten as

$$S_e + S_a + S_f = 0, \quad (9)$$

where the three terms of equation 9 are called the energy slope, the acceleration slope, and the friction slope respectively. Figure 2 depicts the simplified representation of energy in unsteady flow.

By substituting $H = \frac{V^2}{2g} + y + z$ and the bed slope $S_0 = -\frac{\partial z}{\partial x}$ into equation 8, we obtain

$$\begin{aligned}\frac{\partial H}{\partial x} &= \frac{\partial z}{\partial x} + \frac{\partial y}{\partial x} + \frac{V}{g} \frac{\partial V}{\partial x} \\ &= -S_0 + \frac{\partial y}{\partial x} + \frac{V}{g} \frac{\partial V}{\partial x} \\ &= -\frac{1}{g} \frac{\partial V}{\partial t} - S_f.\end{aligned}\quad (10)$$

Hence equation 8 can be rewritten as

$$S_f = S_0 - \frac{\partial y}{\partial x} - \frac{v}{g} \frac{\partial v}{\partial x} - \frac{1}{g} \frac{\partial v}{\partial t} = \frac{v^2}{C^2 R} .$$

steady →

uniform flow →

steady nonuniform flow →

unsteady nonuniform flow →

(11)

This equation may be applicable to various types of flow as indicated. This arrangement shows how the nonuniformity and unsteadiness of flows introduce extra terms into the governing dynamic equation.

Diffusion Hydrodynamic Model

One Dimensional Diffusion Hydrodynamic Model

The mathematical relationships in a one-dimensional diffusion hydro dynamic (DHM) model are based upon the flow equations of continuity (2) and momentum (11) which can be rewritten (Akan and Yen, 1981) as

$$\frac{\partial Q_x}{\partial x} + \frac{\partial A_x}{\partial t} = 0 \quad (12)$$

$$\frac{\partial Q_x}{\partial t} + \frac{\partial (Q_x^2 / A_x)}{\partial x} + g A_x \left(\frac{\partial H}{\partial x} + S_{fx} \right) = 0 , \quad (13)$$

where Q_x is the flowrate; x, t are spatial and temporal coordinates; A_x is the flow area; g is gravitational acceleration; H is the water

surface elevation; and S_{fx} is a friction slope. It is assumed that S_{fx} is approximated from Manning's equation for steady flow by (e.g. Akan and Yen, 1981)

$$Q_x = \frac{1.486}{n} A_x R^{2/3} S_{fx}^{1/2} \quad , \quad (14)$$

where R is the hydraulic radius; and n is a flow-resistance coefficient which may be increased to account for other energy losses such as expansions and bend losses. Letting m_x be a momentum quantity defined by

$$m_x = \left(\frac{\partial Q_x}{\partial t} + \frac{\partial(Q_x^2/A_x)}{\partial x} \right) / gA_x \quad , \quad (15)$$

then equation 13 can be rewritten as

$$S_{fx} = - \left(\frac{\partial H}{\partial x} + m_x \right) \quad . \quad (16)$$

In equation 15, the subscript x included in m_x indicates the directional term. The expansion of equation 13 to the two-dimensional case leads directly to the terms (m_x, m_y) except that now a cross-product of flow velocities are included, increasing the computational effort considerably.

Rewriting equation 14 and including equations 15 and 16, the directional flow rate is computed by

$$Q_x = - K_x \left(\frac{\partial H}{\partial x} + m_x \right) \quad , \quad (17)$$

where Q_x indicates a directional term, and K_x is a type of conduction parameter defined by

$$K_x = \frac{1.486}{n} A_x R^{2/3} \left/ \left| \frac{\partial H}{\partial x} + m_x \right|^{1/2} \right. . \quad (18)$$

In equation 18, K_x is limited in value by the denominator term being checked for a smallest allowable magnitude, (such as $\left| \frac{\partial H}{\partial x} + m_x \right|^{1/2} > 10^{-3}$).

Substituting the flow rate formulation of equation 17 into equation 12 gives a diffusion type of relationship

$$\frac{\partial}{\partial x} K_x \left(\frac{\partial H}{\partial x} + m_x \right) = \frac{\partial A_x}{\partial t} . \quad (19)$$

The one-dimensional model of Akan and Yen (1981) assumes $m_x = 0$ in equation 18. Thus, the one-dimensional DHM is given by

$$\frac{\partial}{\partial x} K_x \frac{\partial H}{\partial x} = \frac{\partial A_x}{\partial t} , \quad (20)$$

where K_x is now simplified as

$$K_x = \frac{1.486}{n} A_x R^{2/3} \left/ \left| \frac{\partial H}{\partial x} \right|^{1/2} \right. . \quad (21)$$

For a channel of constant width, W_x , equation 20 reduces to

$$\frac{\partial}{\partial x} K_x \frac{\partial H}{\partial x} = W_x \frac{\partial H}{\partial t} . \quad (22)$$

Assumptions other than $m_x = 0$ in equation 19 result in a family of models:

$$m_x = \begin{cases} \frac{\partial(Q_x^2/A_x)}{\partial x} / gA_x, & \text{(convective acceleration model)} \\ \frac{\partial Q_x}{\partial t} / gA_x, & \text{(local acceleration model)} \\ \left(\frac{\partial Q_x}{\partial t} + \frac{\partial(Q_x^2/A_x)}{\partial x} \right) / gA_x, & \text{(fully dynamic model)} \\ 0. & \text{(DHM)} \end{cases} \quad (23)$$

Two Dimensional Diffusion Hydrodynamic Model

The set of (fully dynamic) 2-D unsteady flow equations consists of one equation of continuity

$$\frac{\partial q_x}{\partial x} + \frac{\partial q_y}{\partial y} + \frac{\partial H}{\partial t} = 0 \quad (24)$$

and two equations of motion

$$\frac{\partial q_x}{\partial t} + \frac{\partial}{\partial x} \left(\frac{q_x^2}{h} \right) + \frac{\partial}{\partial y} \left(\frac{q_x q_y}{h} \right) + gh \left(S_{fx} + \frac{\partial H}{\partial x} \right) = 0, \quad (25)$$

$$\frac{\partial q_y}{\partial t} + \frac{\partial}{\partial y} \left(\frac{q_y^2}{h} \right) + \frac{\partial}{\partial x} \left(\frac{q_x q_y}{h} \right) + gh \left(S_{fy} + \frac{\partial H}{\partial y} \right) = 0, \quad (26)$$

in which q_x, q_y are flow rates per unit width in the x,y-directions; S_{fx}, S_{fy} represent friction slopes in x,y-directions; H, h, g stand for water-surface elevation, flow depth, and gravitational acceleration, respectively; and x,y,t are spatial and temporal coordinates.

The above equation set is based on the assumptions of constant fluid density without sources or sinks in the flow field, and of hydrostatic pressure distributions.

The local and convective acceleration terms can be grouped together and equations 25 and 26 are rewritten as

$$m_z + \left(S_{fz} + \frac{\partial H}{\partial z} \right) = 0, \quad z = x, y, \quad (27)$$

where m_z represents the sum of the first three terms in equations 25 or 26 divided by gh . Assuming the friction slope to be approximated by the Manning's formula, one obtains, in the U.S. customary units for flow in the x or y direction,

$$q_z = \frac{1.486}{n} h^{5/3} S_{fz}^{1/2}, \quad z = x, y. \quad (28)$$

Equation 28 can be rewritten in the general case as

$$q_z = -K_z \frac{\partial H}{\partial z} - K_z m_z, \quad z = x, y, \quad (29)$$

where

$$K_z = \frac{1.486}{n} h^{5/3} \left/ \left| \frac{\partial H}{\partial S} + m_S \right|^{1/2} \right., \quad z = x, y. \quad (30)$$

The symbol S in equation 30 indicates the flow direction which makes an angle of $\theta = \tan^{-1} (q_y/q_x)$ with the positive x -direction.

Values of m are assumed negligible by several investigators (Akan and Yen, 1981, Hromadka et al., 1985, and Xanthopoulos and Koutitas, 1975), resulting in the simple diffusion model,

$$q_z = -K_z \frac{\partial H}{\partial z}, \quad z = x, y. \quad (31)$$

The proposed 2-D DHM is formulated by substituting equation 31 into equation 24

$$\frac{\partial}{\partial x} K_x \frac{\partial H}{\partial x} + \frac{\partial}{\partial y} K_y \frac{\partial H}{\partial y} = \frac{\partial H}{\partial t}. \quad (32)$$

If the momentum term groupings were retained, equation 32 would be written as

$$\frac{\partial}{\partial x} K_x \frac{\partial H}{\partial x} + \frac{\partial}{\partial y} K_y \frac{\partial H}{\partial y} + S = \frac{\partial H}{\partial t}, \quad (33)$$

where

$$S = \frac{\partial}{\partial x} (K_x m_x) + \frac{\partial}{\partial y} (K_y m_y),$$

and K_x, K_y are also functions of m_x, m_y respectively.

Numerical Approximation

Numerical Solution Algorithm

The following steps are taken in the one-dimensional model where the flow path is assumed initially discretized by equally spaced nodal points with a Manning's n , an elevation, and an initial flow depth (usually zero) defined:

- (1) between nodal points, compute an average Manning's n , and average geometric factors,
- (2) assuming $m_x = 0$, estimate the nodal flow depths for the next timestep, $(t + \Delta t)$ by using equations 20 and 21 explicitly,

- (3) using the flow depths at time t and $(t + \Delta t)$, estimate the mid timestep value of m_x selected from equation 23,
- (4) recalculate the conductivities K_x using the appropriate m_x values,
- (5) determine the new nodal flow depths at time $(t + \Delta t)$ using equation 19, and
- (6) return to Step (3) until K_x matches mid timestep estimates.

The above algorithm steps can be used regardless of the choice of definition for m_x from equation 23. Additionally, the above program steps can be directly applied to a two-dimensional diffusion model with the selected (m_x, m_y) relations incorporated.

Numerical Model Formulation (Grid element)

For uniform grid elements, the integrated finite difference version of the nodal domain integration (NDI) method (Hromadka et al., 1981) is used. For grid elements, the NDI nodal equation is based on the usual nodal system shown in figure 3. Flow rates across the boundary Γ are estimated by assuming a linear trial function between nodal points.

For a square grid of width δ ,

$$q|_{\Gamma_E} = - \left(K_x|_{\Gamma_E} \right) \left(H_E - H_C \right) / \delta \quad , \quad (34)$$

where

$$K_x|_{\Gamma_E} = \begin{cases} \left(\frac{1.486}{n} h^{5/3} \right)_{\Gamma_E} / \left| \frac{H_E - H_C}{\delta \cos \theta} \right|^{1/2} & ; |H_E - H_C| \geq \epsilon \\ 0 & ; |H_E - H_C| < \epsilon \end{cases} \quad (35)$$

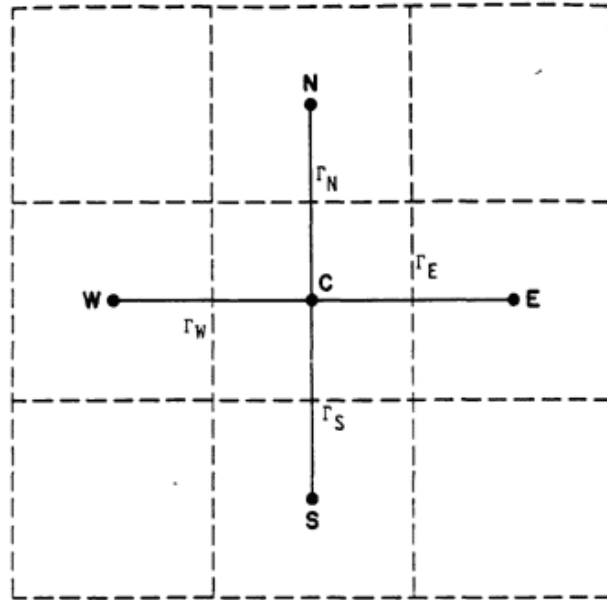


Figure 3.--Two-dimensional finite difference anaolg.

In Equation 35, h (depth of water) and n (the Manning's coefficient) are both the average of their respective values at C and E, i.e. $h = (h_C + h_E)/2$ and $n = (n_C + n_E)/2$. (Additionally, the denominator of K_x is checked such that K_x is set to zero if $|H_E - H_C|$ is less than a tolerance ϵ such as 10^{-3} ft.)

The net volume of water in each grid element between timestep i and $i+1$ is $\Delta q_C^i = q|_{\Gamma_E} + q|_{\Gamma_W} + q|_{\Gamma_N} + q|_{\Gamma_S}$ and the change of depth of water is $\Delta H_C^i = \Delta q_C^i * \Delta t / \delta^2$ for timestep i and $i+1$ with Δt interval. Then the model advances in time by an explicit approach

$$H_C^{i+1} = \Delta H_C^i + H_C^i \quad (36)$$

where the assumed input flood flows are added to the specified input nodes at each timestep. After each timestep, the hydraulic conductivity parameters of equation 35 are reevaluated, and the solution of equation 36 reinitiated.

Model Timestep Selection

The sensitivity of the model to timestep selection is dependent upon the slope of the discharge hydrograph ($\frac{\partial Q}{\partial t}$) and the grid spacing. Increasing the grid spacing size introduces additional water storage to a corresponding increase in nodal point flood depth values. Similarly, a decrease in timestep size allows a refined calculation of inflow and outflow values and a smoother variation in nodal point flood depths with respect to time. The computer algorithm may self-select a timestep by increments of halving (or doubling) the initial user-chosen timestep size so that a proper balance of inflow-outflow to control volume storage variation is achieved. In order to avoid a matrix solution for flood depths, an explicit timestepping algorithm is used to solve for the time derivative term. For large timesteps or a rapid variation in the dam-break hydrograph (such as $\frac{\partial Q}{\partial t}$ is large), a large accumulation of flow volume will occur at the most upstream nodal point. That is, at the dam-break reservoir nodal point, the lag in outflow from the control volume can cause unacceptable error in the computation of the flood depth. One method that offsets this error is the program to self-select the timestep until the difference in the rate of volume accumulation is within a specified tolerance.

Due to the form of the DHM in equation 22, the model can be extended into an implicit technique. However, this extension would require a matrix solution process which may become unmanageable for two dimensional models which utilize hundreds of nodal points.

VERIFICATION OF DIFFUSION HYDRODYNAMIC MODEL

Introduction

An unsteady flow hydraulic problem of considerable interest is the analysis of dam-breaks and their downstream hydrograph. In this section, the main objective is to evaluate the diffusion form of the flow equations for the estimation of flood depths (and the flood plain) resulting from a specified dam-break hydrograph. The dam-break failure mode is not considered in this section. Rather, the dam-break failure mode may be included as part of the model solution (such as for a sudden breach) or specified as a reservoir outflow hydrograph.

The use of numerical methods to approximately solve the flow equations for the propagation of a flood wave due to an earthen dam failure has been the subject of several studies reported in the literature. Generally, the flow is modeled using the one-dimensional equation wherever there is no significant lateral variation in the flow. Land (1980a,b) examines four such dam-break models in his prediction of flooding levels and flood wave travel time, and compares the results against observed dam failure information. In dam-break analysis, an assumed dam-break failure mode (which may be part of the solution) is used to develop an inflow hydrograph to the downstream flood plain. Consequently, it is noted that a considerable sensitivity in modeling results is attributed to the dam-break failure rate assumptions. Ponce and Tsivoglou (1981) examine the gradual failure of an earthen embankment (caused by an overtopping flooding event) and present detailed analysis for each part of the total system: sediment transport, unsteady channel hydraulics, and earth embankment failure.

In another study, Rajar (1978) studied a one-dimensional flood wave propagation from an earthen dam failure. His model solves the St. Venant equations by means of either a first-order diffusive or a second-order Lax-Wendroff numerical scheme. A review of the literature indicates that the most frequently used numerical scheme is the method of characteristics (to solve the governing flow equations) such as described in Sakkas and Strelkoff (1973), Chen (1980), and Chen and Armbruster (1980).

Although many dam-break studies involve flood flow regimes which are truly two-dimensional (in the horizontal plane), the two dimensional case has not received much attention in the literature. Katopodes and Strelkoff (1978) use the method of bicharacteristics to solve the governing equations of continuity and momentum. The model utilizes a moving grid algorithm to follow the flood wave propagation, and also employs several interpolation schemes to approximate the nonlinearity effects. In a much simpler approach, Xanthopoulos and Koutitas (1976) use a diffusion model (i.e. the inertia terms are assumed negligible in comparison to the pressure, friction, and gravity components) to approximate a two-dimensional flow field. The model assumes that the flow regime in the flood plain is such that the inertia terms (local and convective acceleration) are negligible. In a one-dimensional model, Akan and Yen (1981) also use the diffusion approach to model hydrograph confluences at channel junctions. In the latter study, comparisons of modeling results were made between the diffusion model, a complete dynamic wave model solving the total equation system, and the basic kinematic wave equation model (that is, the inertia and pressure terms are assumed negligible in comparison to the friction and gravity terms). The differences between the diffusion model and the dynamic wave model were small, showing only minor discrepancies.

The kinematic-wave flow model has been recently used in the computation of dam-break flood waves (Hunt, 1982). Hunt concludes in his study that the kinematic-wave solution is asymptotically valid. Since the diffusion model has a wider range of applicability for varied bed slopes and wave periods than the kinematic model (Ponce et al., 1978), the diffusion model approach should provide an extension to the referenced kinematic model.

Because the diffusion modeling approach leads to an economic two-dimensional dam-break flow model (with numerical solutions based on the usual integrated finite-difference or finite element techniques), the need to include the extra components in the momentum equation must be ascertained. For example, evaluating the convective acceleration terms in a two-dimensional flow model requires approximately an additional 50-percent of the computational effort required in solving the entire two-dimensional model with the inertia terms omitted. Consequently, including the local and convective acceleration terms increases the computer execution costs significantly. Such increases in computational effort may not be significant for one-dimensional case studies; however, two-dimensional case studies necessarily involve considerably more computational effort and any justifiable simplifications of the governing flow equations is reflected by a significant decrease in computer software requirements, costs and computer execution time.

Ponce (1982) examines the mathematical expressions of the flow equations which lead to wave attenuation in prismatic channels. It is concluded that the wave attenuation process is caused by the interaction of the local acceleration term with the sum of the terms of friction slope and channel slope. When local acceleration is considered negligible, wave attenuation is caused by the interaction of the friction slope and channel slope terms with the pressure gradient or convective acceleration terms

(or a combination of both terms). Other discussions of flow conditions and the sensitivity to the various terms of the flow equations are given in Miller and Cunge (1975), Morris and Woolhiser (1980), and Henderson (1963).

It is stressed that the ultimate objective of this paper is to develop a two-dimensional diffusion model for use in estimating flood plain evolution such as occurs due to drainage system deficiencies. Prior to finalizing such a model, the requirement of including the inertia terms in the unsteady flow equations needs to be ascertained. The strategy used to check on this requirement is to evaluate the accuracy in predicted flood depths produced from a one-dimensional diffusion model with respect to the one-dimensional U.S.G.S K-634 dam-break model which includes all of the inertia term components.

One-Dimensional Analysis

Study Approach

In order to evaluate the accuracy of the one-dimensional diffusion model (equation 22) in the prediction of flood depths, the U.S.G.S. fully dynamic flow model K-634 (Land, 1980a,b) is used to determine channel flood depths for comparison purposes. The K-634 model solves the coupled flow equations of continuity and momentum by an implicit finite difference approach and is considered to be a highly accurate model for many unsteady flow problems. The study approach is to compare predicted: (1) flood depths, and (2) discharge hydrographs from both the K-634 and the diffusion hydrodynamic model (equation 22) for various channel slopes and inflow hydrographs.

It should be noted that different initial conditions are used for these two models. The U.S.G.S. K-634 model requires a base flow to start the simulation; therefore, the initial depth of water cannot be zero. Next, the normal depth assumption is used to generate an initial water depth before the simulation starts. These two steps are not required by the DHM.

In this case study, two hydrographs are assumed; namely, peak flows to 120,000 cfs and 600,000 cfs. A baseflow of 5,000 cfs and 40,000 cfs was used for hydrographs with peaks of 120,000 and 600,000 cfs respectively for all K-634 simulations. Both hydrographs are assumed to increase linearly from zero (or the base flow) to the peak flow rate at time of 1-hour, and then decrease linearly to zero (or the baseflow) at time of 6-hours (see figure 4 inset). The study channel is assumed to be a 1000 feet width rectangular section of Manning's n equal to 0.040, and various slopes S_o in the range of 0.001_ S_o _0.01. Figures 4 shows the comparison of modeling results. From the figure, various flood depths are plotted along the channel length of up to 10-miles. Two reaches of channel lengths of up to 30-miles are also plotted in figure 4 which correspond to a slope $S_o = 0.0020$. In all tests, grid spacing was set at 1000-feet intervals. Time steps were 0.01 hours for K-634 and 7.2 seconds for DHM.

From figure 4 it is seen that the diffusion model provides estimates of flood depths that compare very well to the flood depths predicted from the K-634 model. For downstream distances at up to 30 miles, differences in predicted flood depths are less than 3 percent for the various channel slopes and peak flow rates considered.

In figures 5 and 6, good comparisons between the diffusion hydrodynamic and the K-634 models are observed for water depths and outflow hydrographs at 5 and 10 miles down stream from the dam-break site. It should be noted that the test conditions are purposefully severe in order to bring out potential inaccuracies in the diffusion hydrodynamic model results. Less severe test conditions should lead to more favorable comparisons between the two model results. Although offsets do occur in timing, volume continuity is preserved when allowances are made for differences in baseflow volumes.

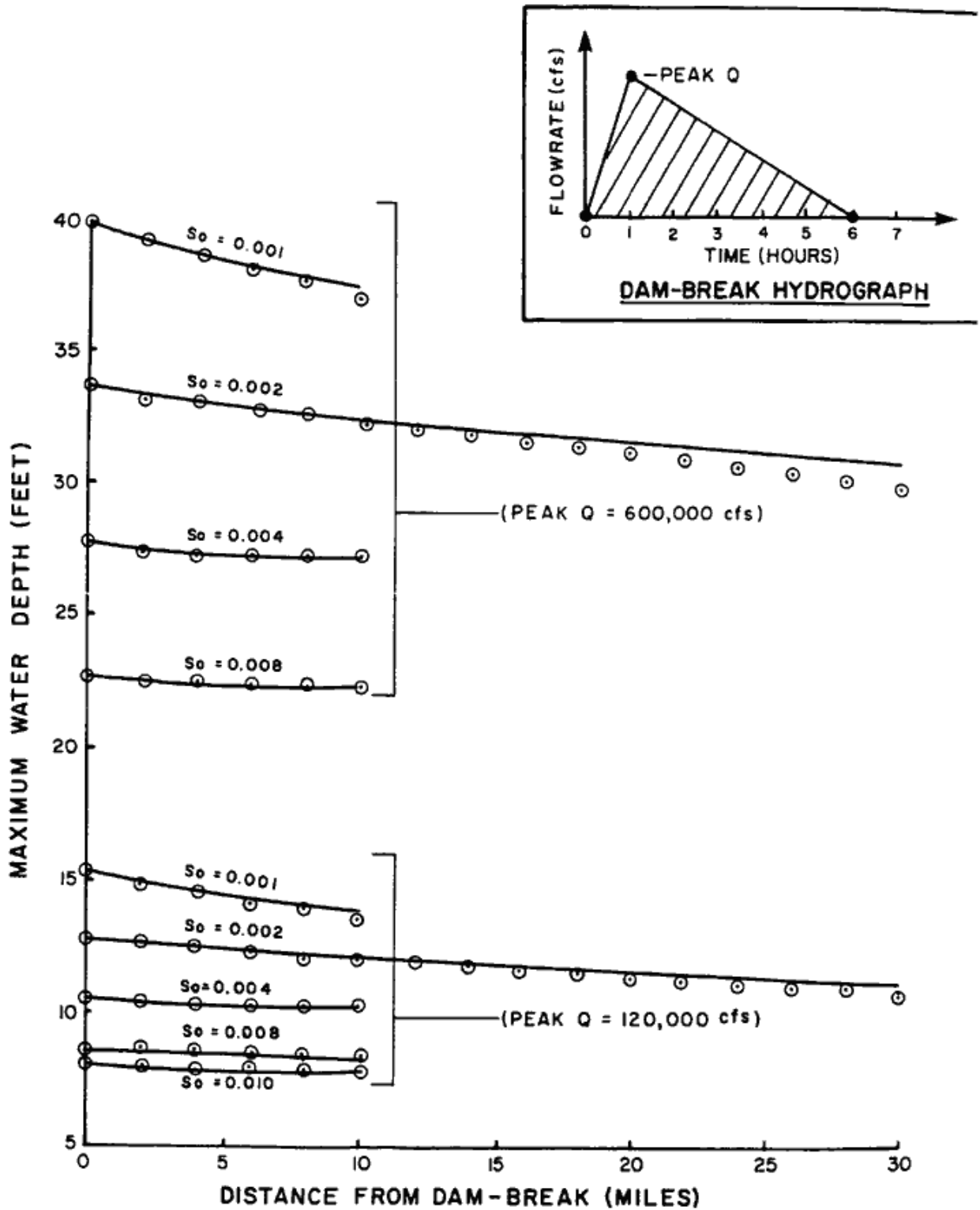
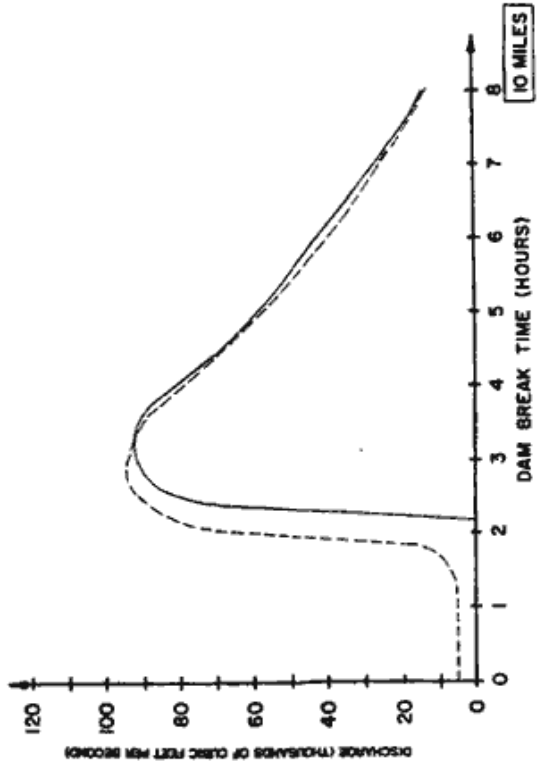
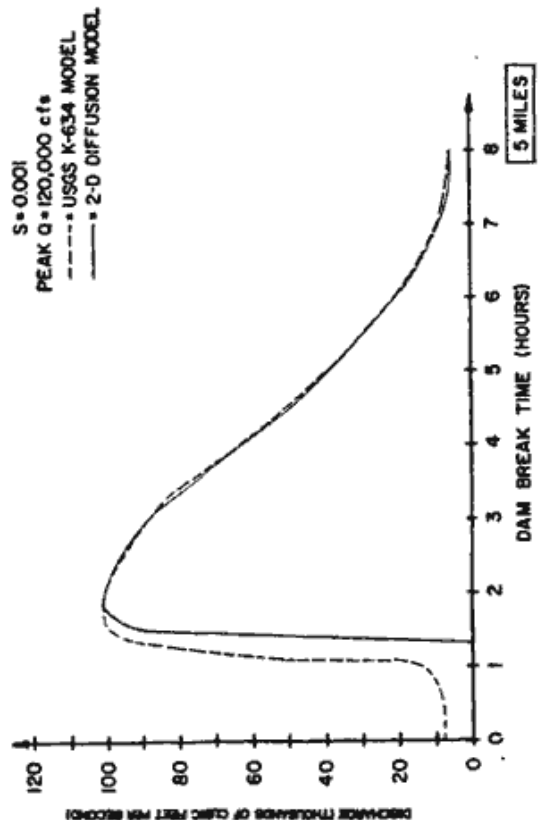
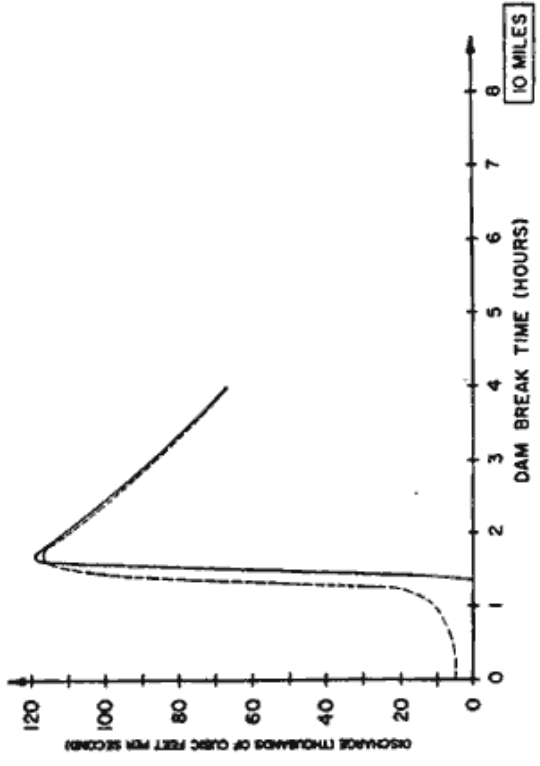
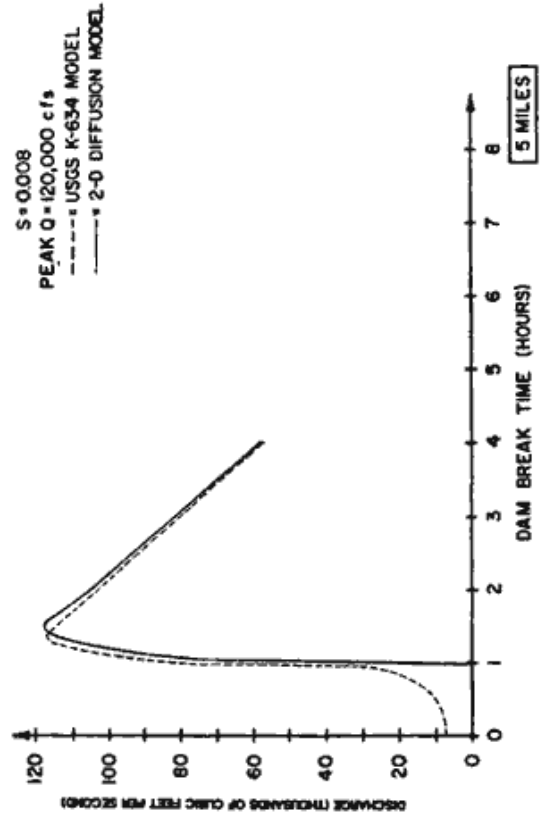


Figure 4.--Diffusion hydrodynamic model (⊙) and K-634 model results (solid line) for 1,000-foot width channel, Manning's $n = 0.040$, and various channel slopes, S_0 .

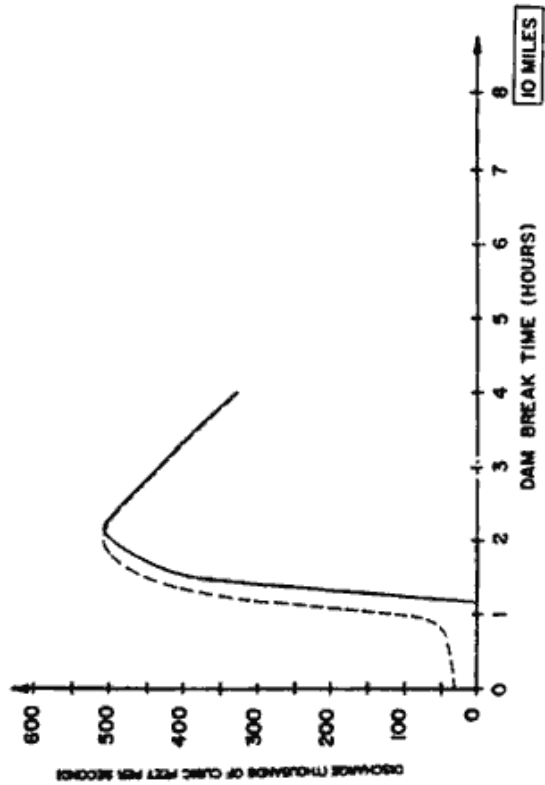
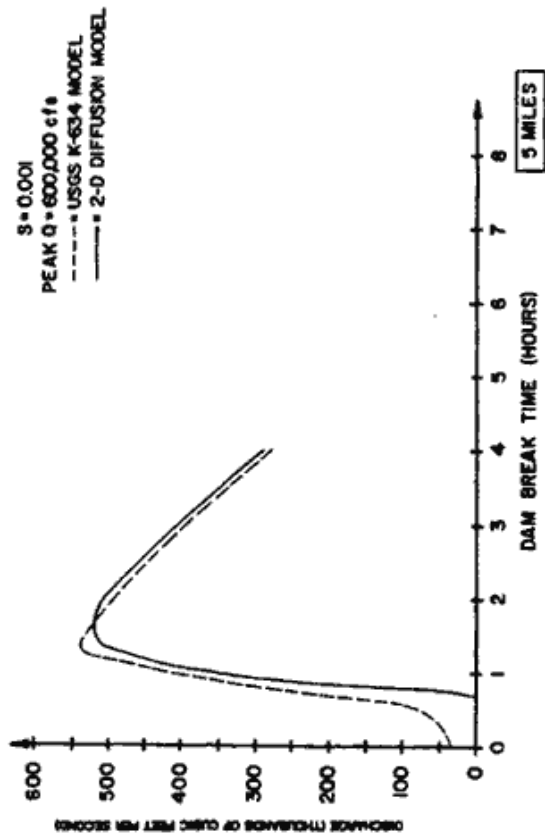


(A)

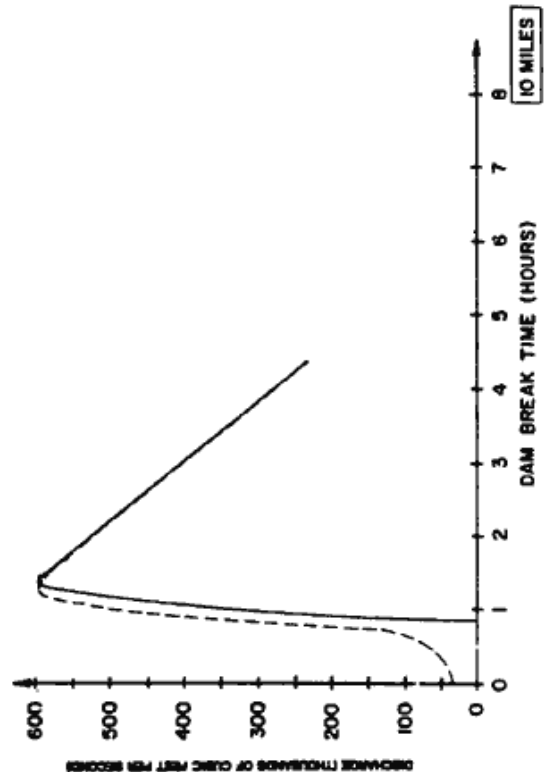
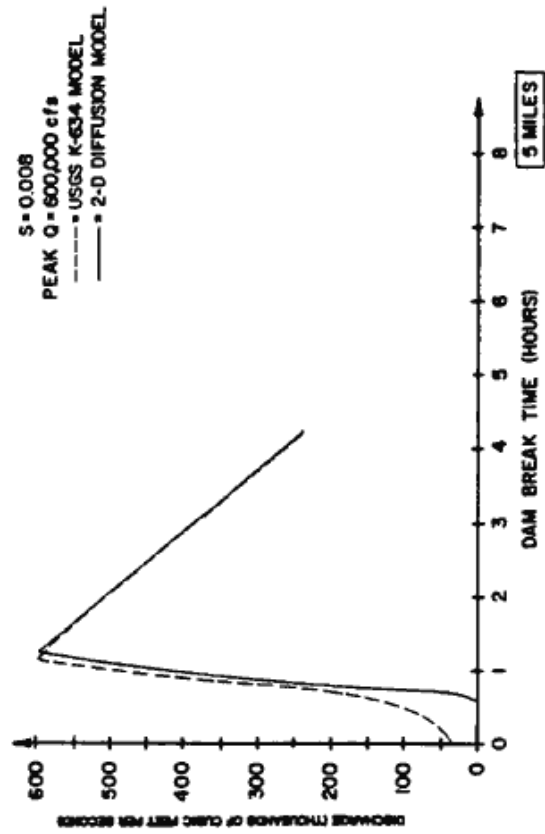


(B)

Figure 5.--Comparisons of outflow hydrographs at 5 and 10 miles downstream from the dam-break site.



(C)



(D)

Figure 5.--Comparisons of outflow hydrographs at 5 and 10 miles downstream from the dam-break site.--(Continued)

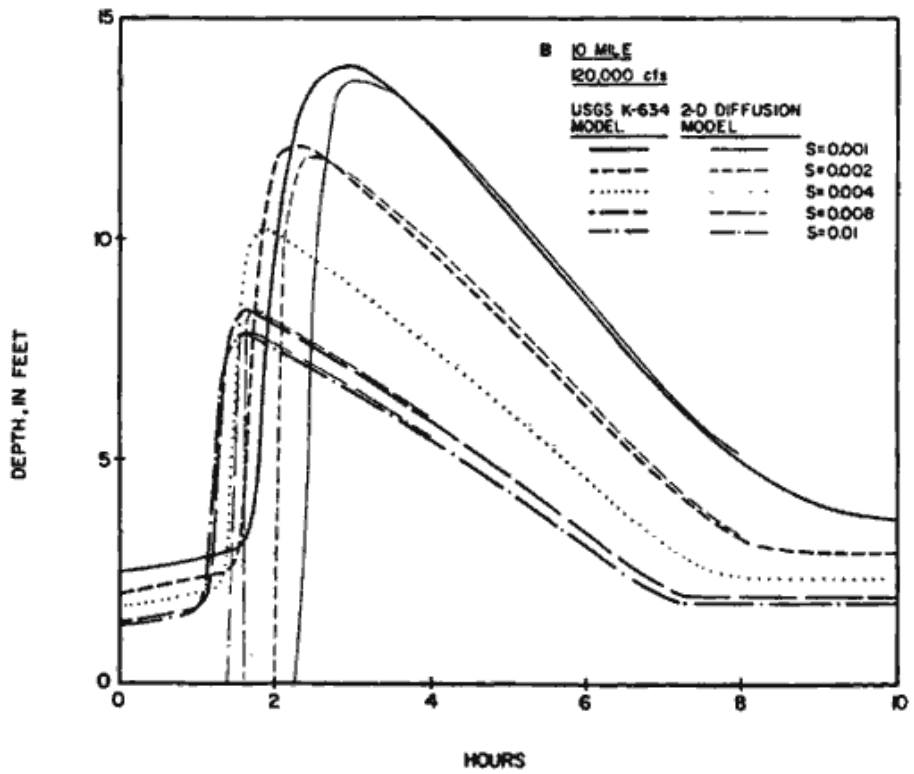
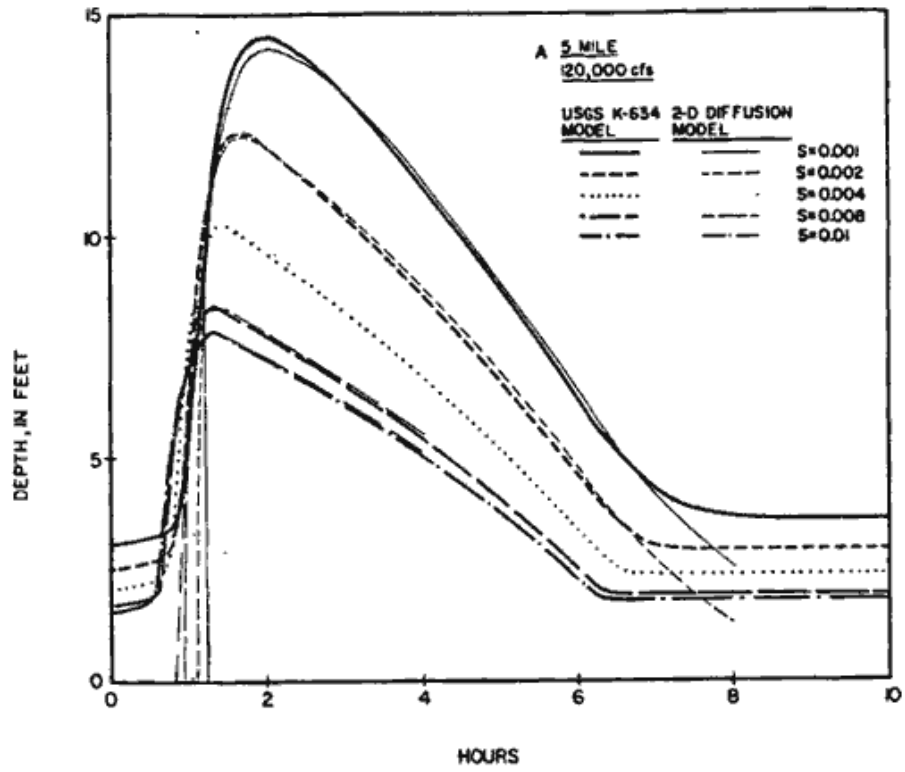


Figure 6.--Comparisons of depths of water at 5 and 10 miles downstream from the dam-break site.

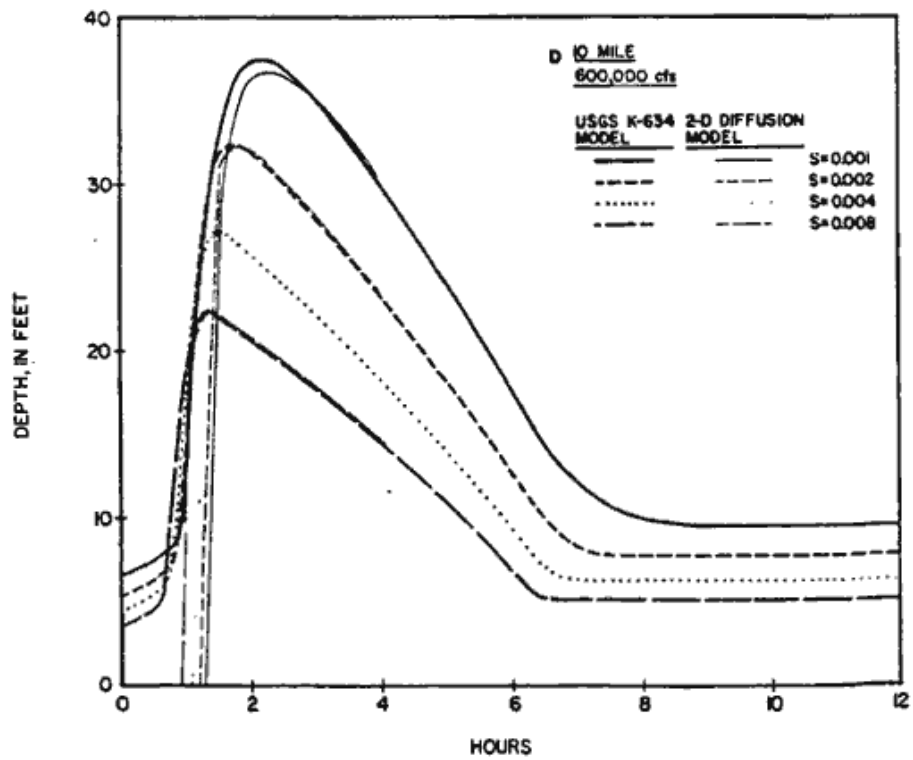
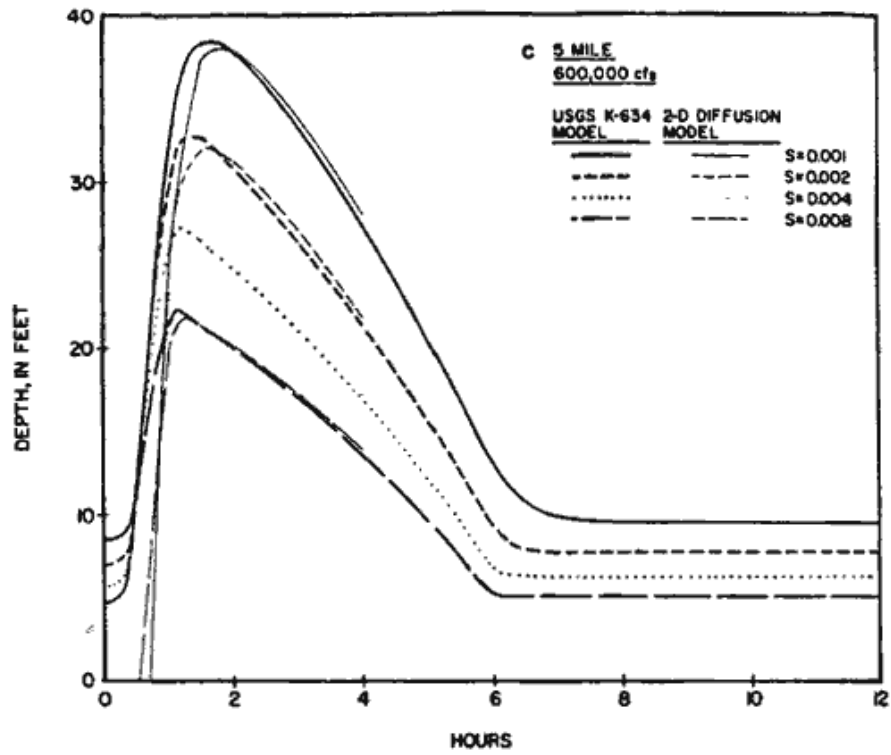


Figure 6.--Comparisons of depths of water at 5 and 10 miles downstream from the dam-break site.--(Continued)

Grid Spacing Selection

The choice of timestep and grid size for an explicit time advancement is a relative matter and is theoretically based on the well-known Courant condition (Basco, 1978). The choice of grid size usually depends on available topographic data for nodal elevation determination and the size of the problem. The effect of the grid size (for constant timestep for 7.2 seconds) on the diffusion model accuracy can be shown by example where nodal spacings of 1,000, 2,000 and 5,000-feet are considered. The predicted flood depths varied only slightly from choosing the grid size between 1,000-feet and 2,000-feet. However, an increased variation in results occurs when a grid size in 5,000-feet is selected. For the example of peak flow rate test hydrograph of 600,000 cfs, the differences of simulated flow depths between 1,000-feet and 5,000-feet grid are 0.03 feet, 0.06 feet and 0.17 feet at 1 mile, 5 miles and 10 miles, respectively, downstream from the dam-break site for the maximum flow depth with the magnitude of 30 feet.

Because the algorithm presented is based upon an explicit timestepping technique, the modeling results may become inaccurate should the timestep size versus grid size ratio become large. A simple procedure to eliminate this instability is to half the timestep size until convergence in computed results is achieved. Generally, such a timestep adjustment may be directly included in the computer program for the dam-break model. For the cases considered in this section, timestep size of 7.2 second was found to be adequate when using the 1,000-feet to 5,000-feet grid sizes.

Conclusions and Discussion

For the dam-break hydrographs considered and the range of channel slopes modeled, the simple diffusion dam-break model of equation 12 provides estimates of flood depths and outflow hydrographs which compare favorably to the results determined by the well-known K-634 one-dimensional dam-break model. Generally speaking, the difference between the two modeling approaches is found to be less than a 3 percent variation in predicted flood depths.

The presented diffusion dam-break model is based upon a straightforward explicit timestepping method which allows the model to operate upon the nodal points without the need to use large matrix systems. Consequently, the model can be implemented on most currently available microcomputers. However, as compared to implicit solution methods, time steps for DHM use are extremely small. Thus, relatively short simulation times must be used.

The diffusion model of equation 22 can be directly extended to a two-dimensional model by adding the y-direction terms which are computed in a similar fashion as the x-direction terms. The resulting two-dimensional diffusion model is tested by modeling the considered test problems in the x-direction, the y-direction, and along a 45-degree trajectory across a two-dimensional grid aligned with the x-y coordinate axis. Using a similar two-dimensional model, Xanthopoulos and Koutitas (1976) conceptually verify the diffusion modeling technique by considering the evolution of a two-dimensional flood plain which propagates radially from the dam-break site.

From the above conclusions, use of the diffusion approach, equation 22, in a two-dimensional DHM may be justified due to the low variation in predicted flooding depths (one-dimensional) with the exclusion of the inertia terms. Generally speaking, a two-dimensional model would be employed when the expansion nature of flood flows is anticipated. Otherwise, one of the available one-dimensional models would suffice for the analysis.

Two-Dimensional Analysis

Introduction

In this section, a two-dimensional DHM is developed. The model is based on a diffusion approach where gravity, friction, and pressure forces are assumed to dominate the flow equations. Such an approach has been used earlier by Xanthopoulos and Koutitas (1976) in the prediction of dam-break flood plains in Greece. In those studies, good results were also obtained by using the two-dimensional model for predicting one-dimensional flow quantities. In the preceding section a one-dimensional diffusion model has been considered and it has been concluded that for most velocity flow regimes (such as Froude Number less than approximately 4), the diffusion model is a reasonable approximation of the full dynamic wave formulation.

An integrated finite difference grid model is developed which equates each cell-centered node to a function of the four neighboring cell nodal points. To demonstrate the predictive capacity of the flood plain model, a study of a hypothetical dam-break of the Crowley Lake dam near the City of Bishop, California (figure 7) is considered (Hromadka, et al., 1985).

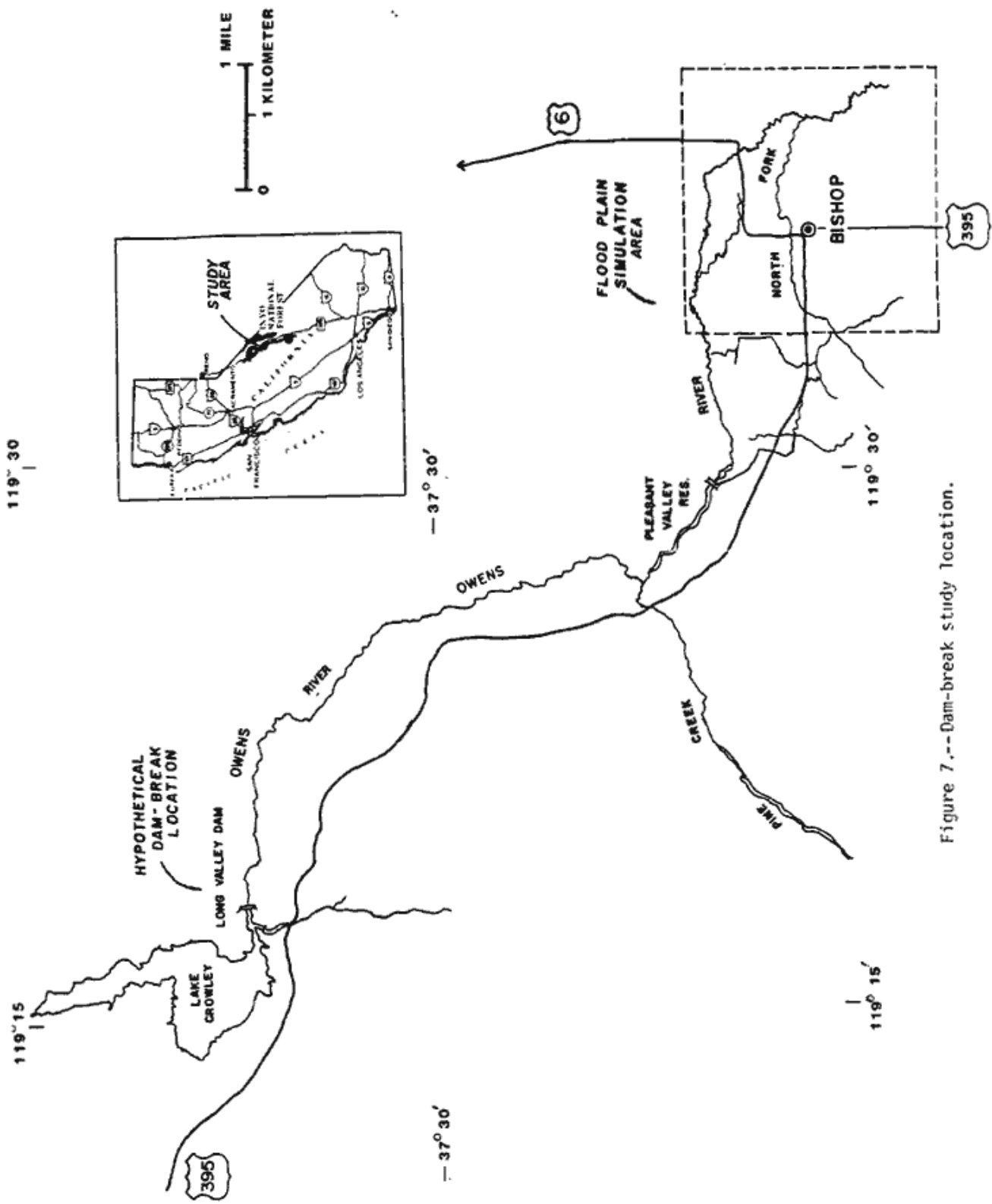


Figure 7.--Dam-break study location.

The steepness and confinement of the channel right beneath the Crowley Lake dam results a translation of outflow hydrograph in time. Therefore, the dam-break analysis is only conducted on the neighborhood near City of Bishop where the gradient of topography is mild.

K-634 Modeling Results and Discussion

Using the K-634 model for computing the two-dimensional flow was attempted by means of the one-dimensional nodal spacing (figure 8). Cross sections were obtained by field survey, and the elevation data were used to construct nodal point flow-width versus stage diagrams. A constant Manning's roughness coefficient of 0.04 was assumed for study purposes. The assumed dam failure reached a peak flow rate of 420,000 cfs within one hour, and returned to zero flow 9.67 hours later. Figure 9 depicts the K-634 flood plain limits. To model the flow break-out, a slight gradient was assumed for the topography perpendicular to the main channel. The motivation for such a lateral gradient is to limit the channel flood-way section in order to approximately conserve the one-dimensional momentum equations. Consequently, fictitious channel sides are included in the K-634 model study which results in an artificial confinement of the flows. Hence, a narrower flood plain is delineated in figure 9 where the flood flows are falsely retained within a hypothetical channel confine. An examination of the flood depths given in figure 11 indicates that at the widest flood plain expanse of figure 9, the flood depth is about 6-feet, yet the

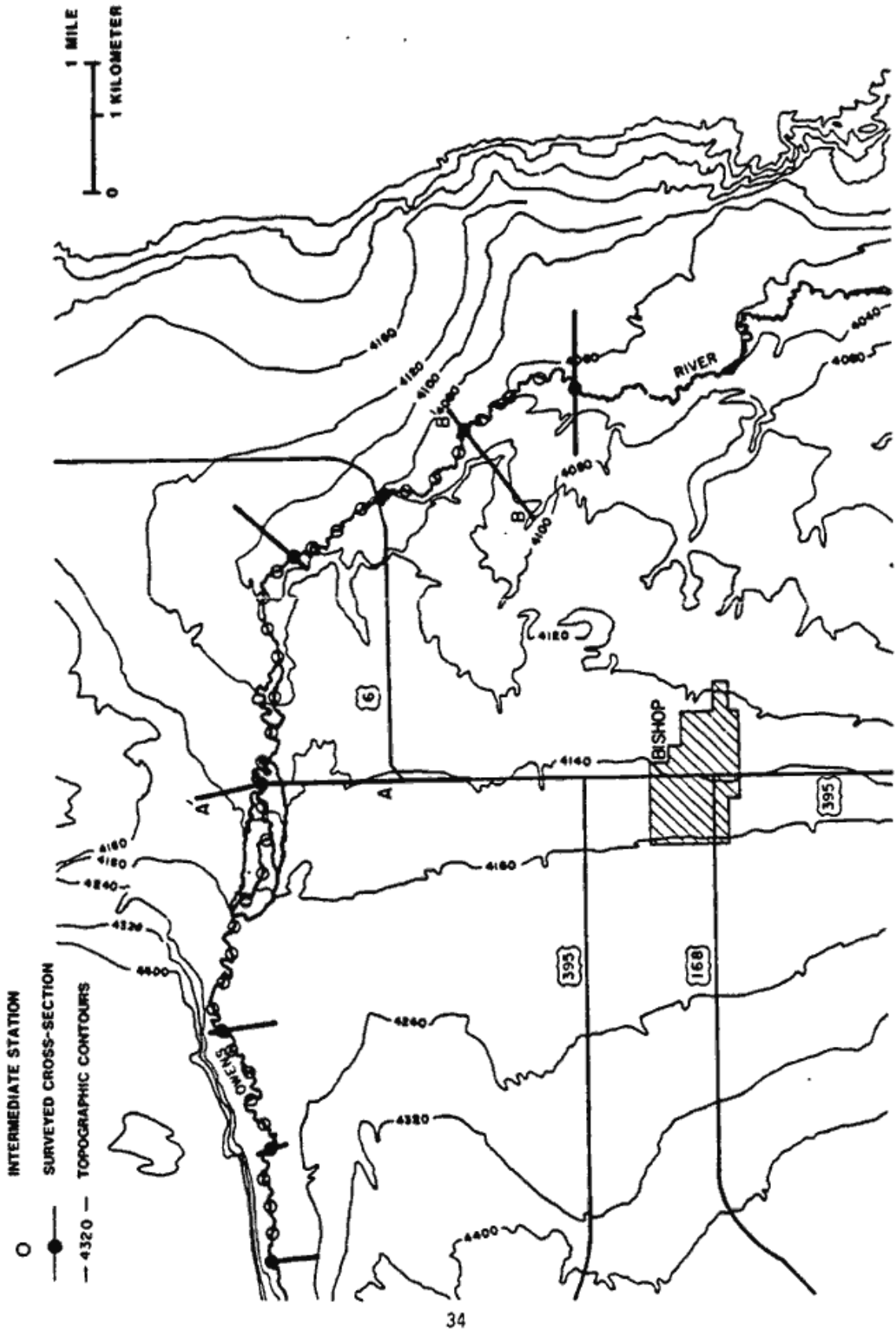


Figure 8.--Surveyed cross section locations on Owens River for use in K-634 model.

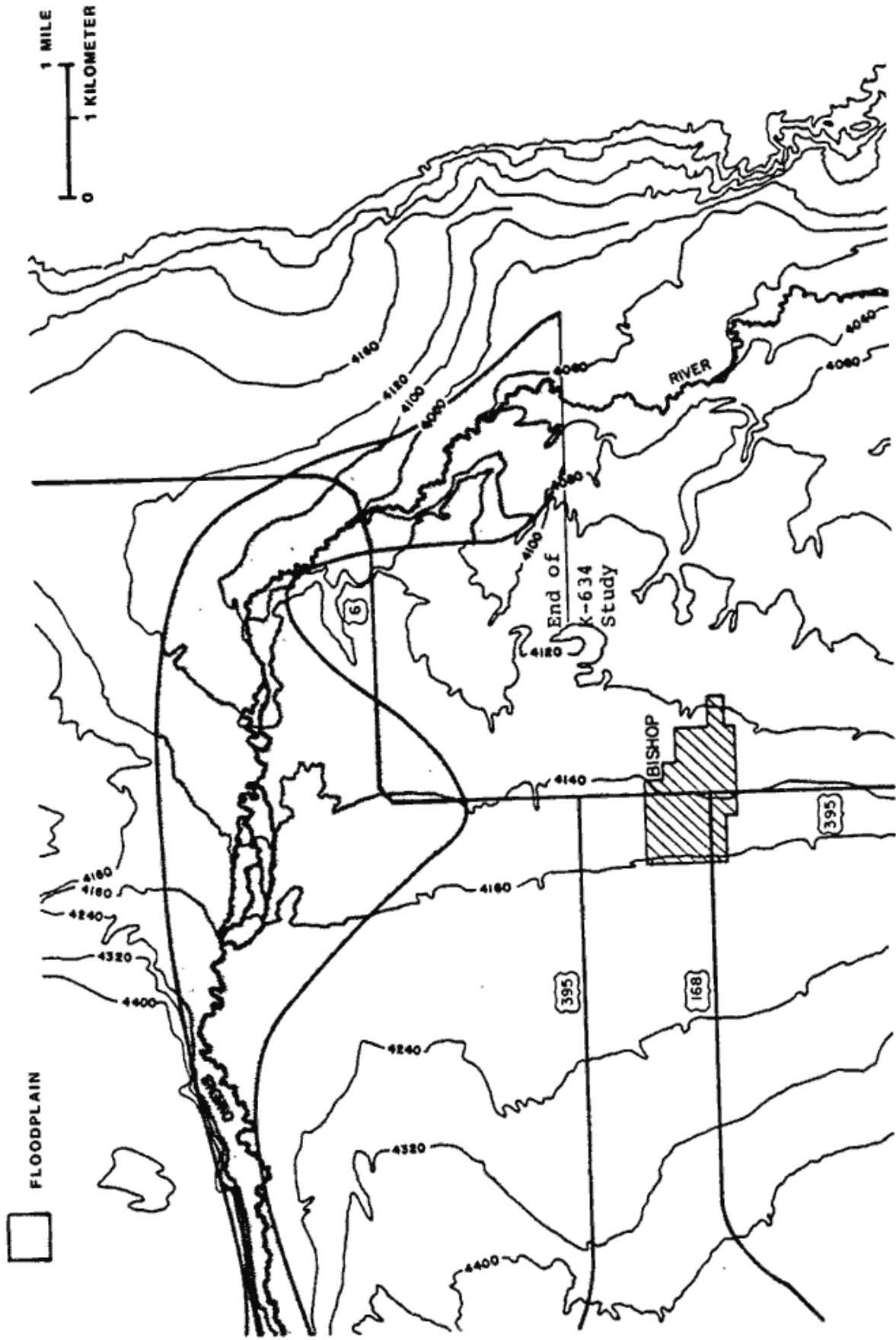


Figure 9.--Floodplain computed from K-634 model.

flood plain is not delineated to expand southerly, but is modeled to terminate based on the assumed gradient of the topography towards the channel. Such complications in accommodating an expanding flood plain when using a one-dimensional model are obviously avoided by using a two-dimensional approach.

The two-dimensional diffusion hydrodynamic model is now applied to the hypothetical dam-break problem using the grid discretization shown in figure 10. The same inflow hydrograph used in K-634 model is also used for the diffusion hydrodynamic model. Again, the Manning's roughness coefficient at 0.04 was used. The resulting flood plain is shown in figure 12 for the 1/4 square-mile grid model.

The two approaches are comparable except at cross-sections shown as A-A and B-B in figure 8. Cross-section A-A corresponds to the predicted breakout of flows away from the Owens River channel with flows traveling southerly towards the City of Bishop. As discussed previously, the K-634 predicted flood depth corresponds to a flow depth of 6 feet (above natural ground) which is actually unconfined by the channel. The natural topography will not support such a flood depth and, consequently, there should be southerly breakout flows such as predicted by the two-dimensional model. With such breakout flows included, it is reasonable that the two-dimensional model would predict a lower flow depth at cross-section A-A.

At cross-section B-B, the K-634 model predicts a flood depth of approximately 2 feet less than the two-dimensional model. However at this location, the K-634 modeling results are based on cross-sections which traverse a 90-degree bend. In this case K-634 model will over-estimate the true channel storage, resulting in an underestimation of flow-depths.

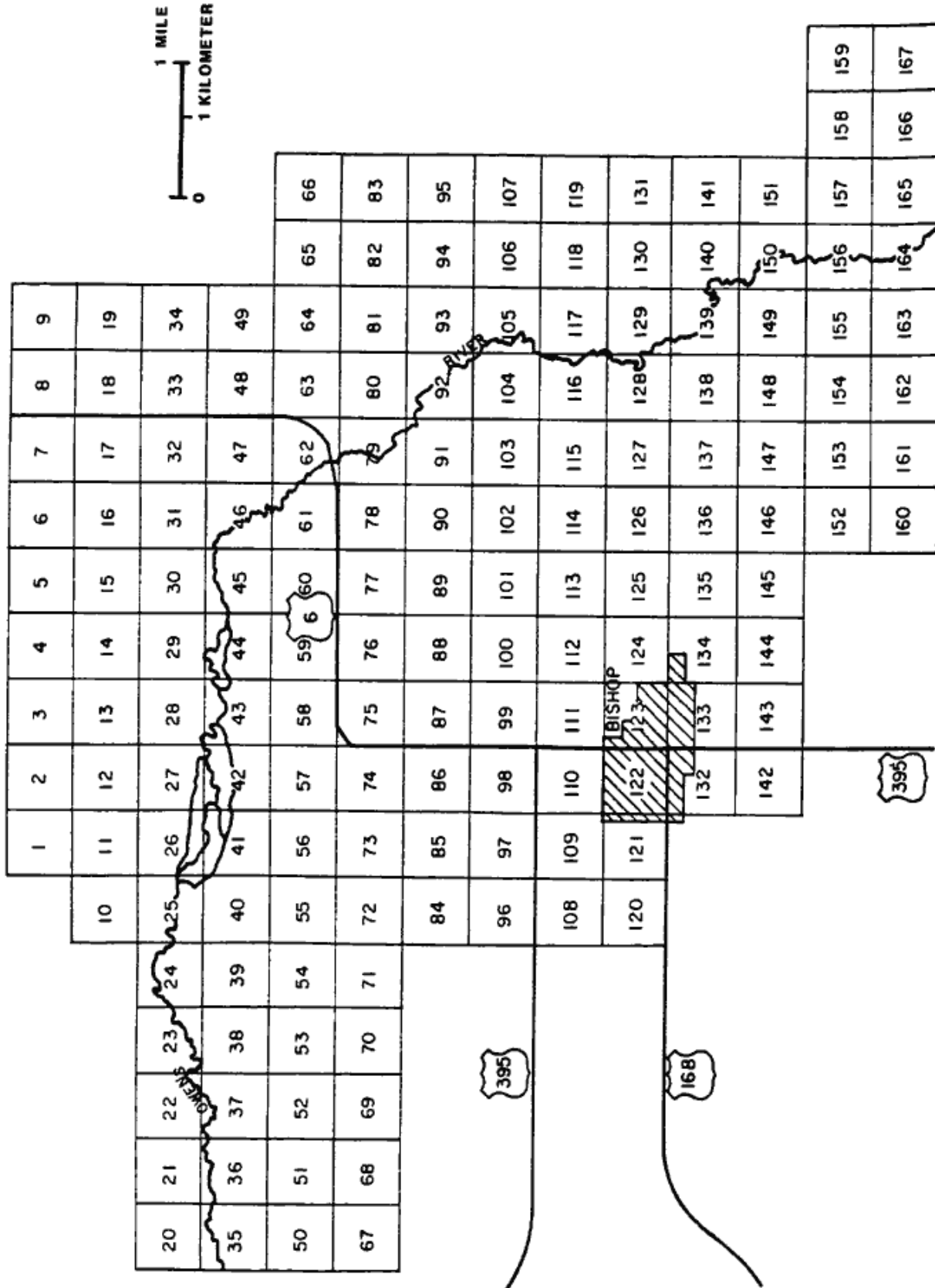


Figure 10.--Floodplain discretization for two-dimensional diffusion hydrodynamic model.

PREDICTED WATER SURFACE ELEVATIONS

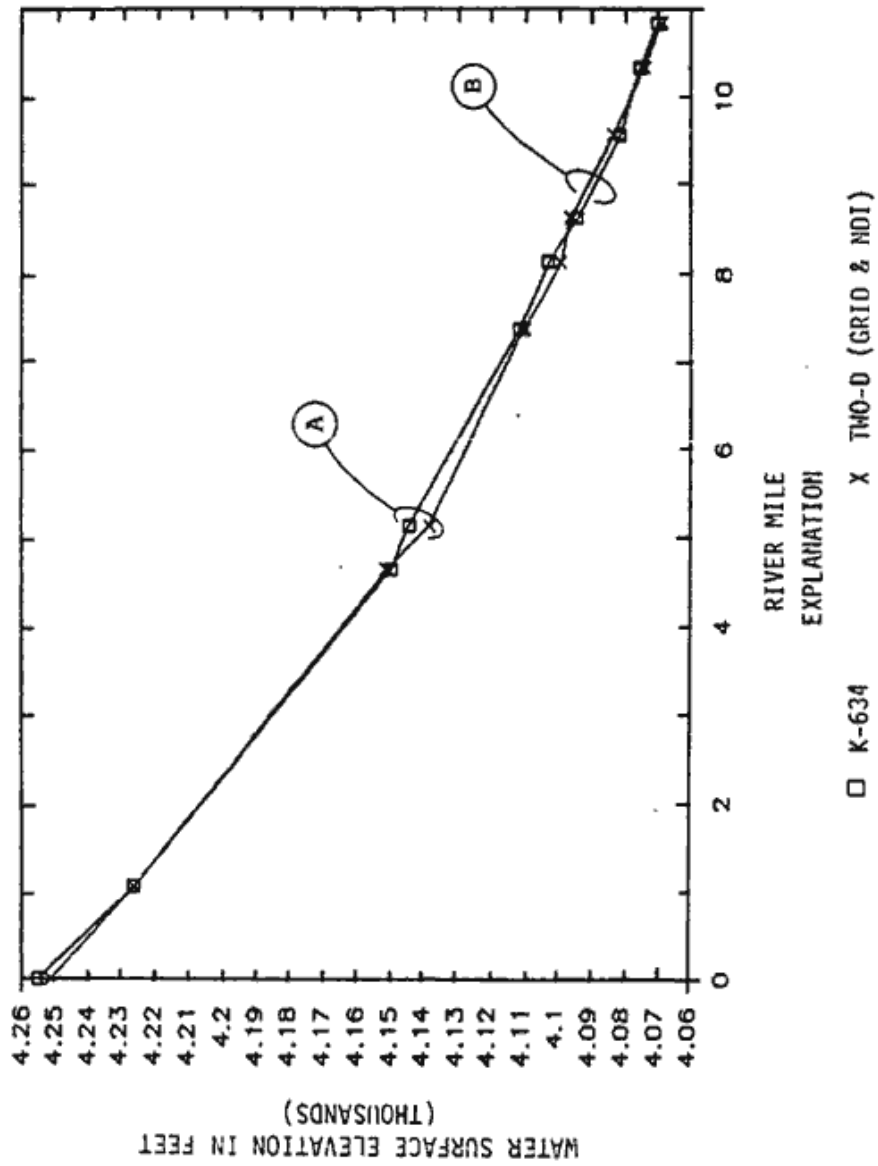


Figure 11.--Comparison of modeled water surface elevations.

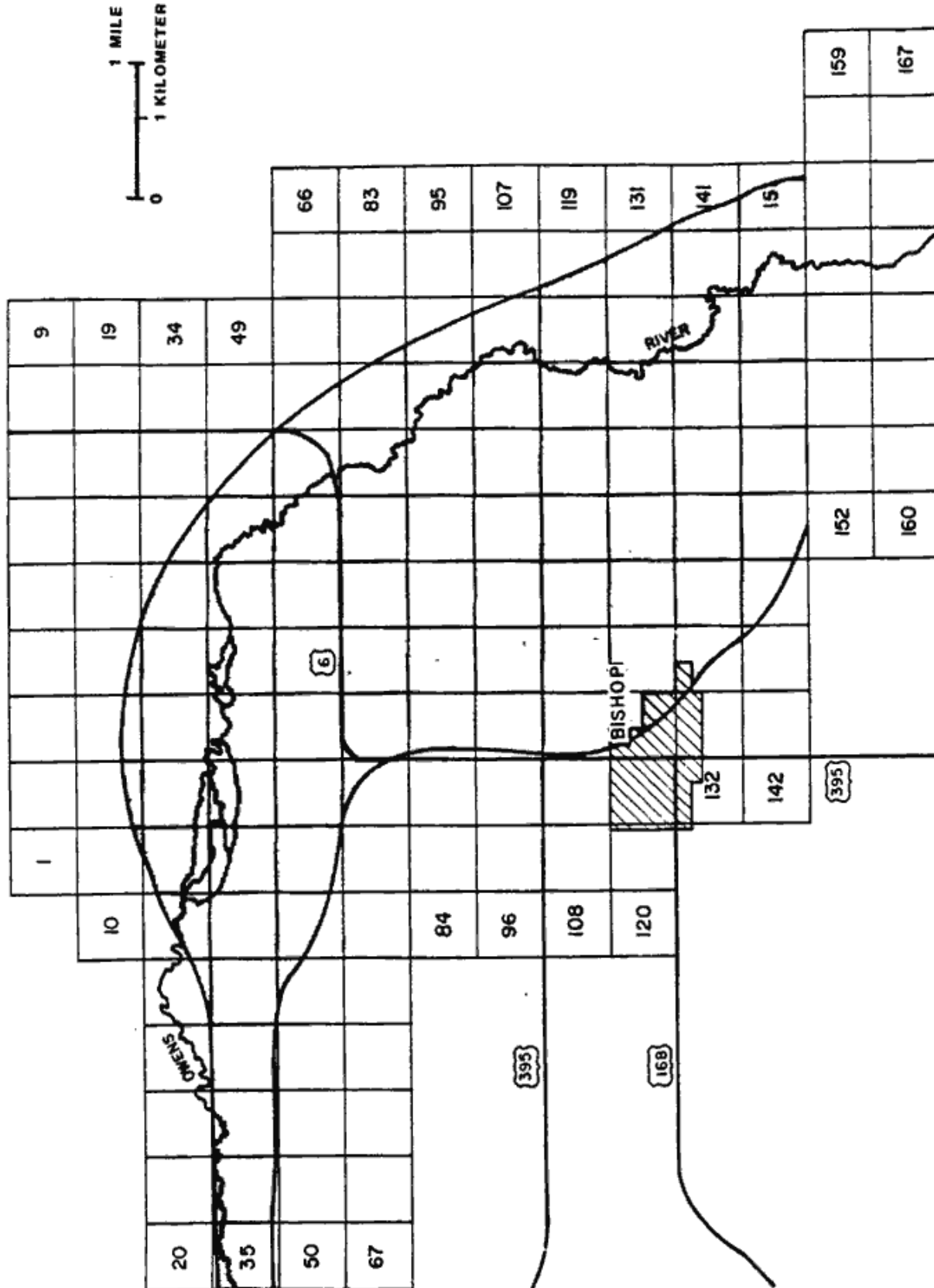


Figure 12.--Floodplain for two-dimensional diffusion hydrodynamic model.

In comparing the various model predicted flood depths and delineated plains, it is seen that the two-dimensional diffusion hydrodynamic model predicted more reasonable flood plain boundary, which is associated with broad, flat plains such as found at the study site, than the one-dimensional model. The diffusion hydrodynamic model approximates channel bends, channel expansions and contractions, flow breakouts, and the general area of inundation. Additionally, the diffusion hydrodynamic model approach allows for the inclusion of return flows (to the main channel), which were the result of upstream channel breakout, and other two-dimensional flow effects, without the need for special modeling accommodations that would be necessary with using a one-dimensional model.

PROGRAM DESCRIPTION OF THE DIFFUSION HYDRODYNAMIC MODEL

Introduction

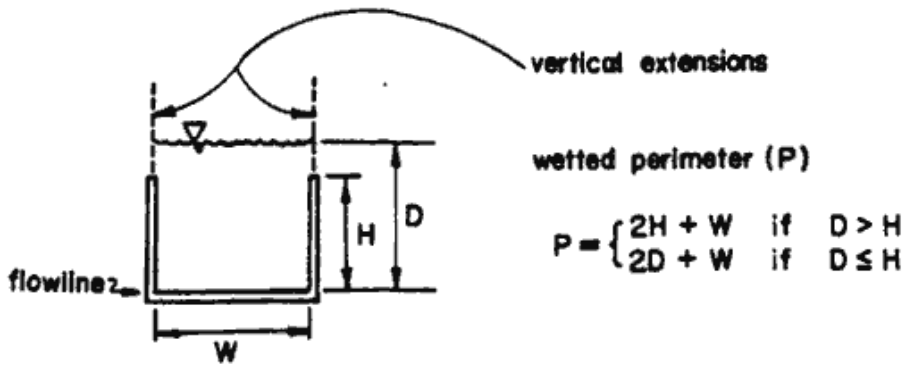
A computer program for the two-dimensional diffusion hydrodynamic model which is based on the diffusion form of the St. Venant equations where gravity, friction, and pressure forces are assumed to dominate the flow equation will be discussed in this section.

The DHM model consists of a 1-D channel and 2-D flood plain models, and an interface sub-model. The one-dimensional channel element utilizes the following assumptions:

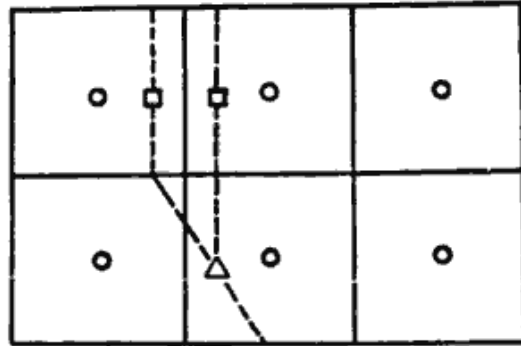
- (1) infinite vertical extensions on channel walls (figure 13),
- (2) wetted perimeter is calculated as shown on figure 13a,
- (3) volumes due to channel skew is ignored (figure 13b), and
- (4) all overflow water is assigned to one grid element (figure 14).

The interface model calculates the excess amount of water either from the channel element or from the flood plain element. This excess water is redistributed to the flood plain element or the channel element according to the water surface elevation.

This FORTRAN program has the capabilities to simulate both one-and two-dimensional surface flow problems, such as the one-dimensional open channel flow and two-dimensional dam-break problems illustrated in the preceding pages. Engineering applications of the program will be presented in the next section.



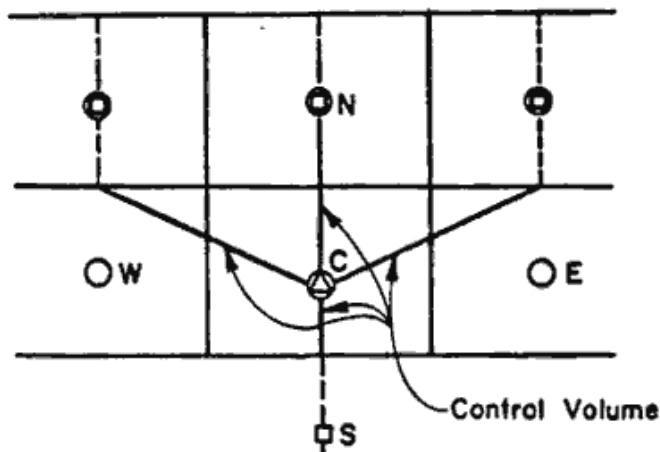
a. Element Geometrics



Legend

- - grid node
- - channel node
- △ - channel junction

b. Element Associations to Grid Elements



Assumptions

- Ignore volume differences due to channel skew
- All overflow assigned to one grid element (see interface model)

c. Channel Element Connections

Figure 13.--Diffusion hydrodynamic model one-dimensional channel elements.

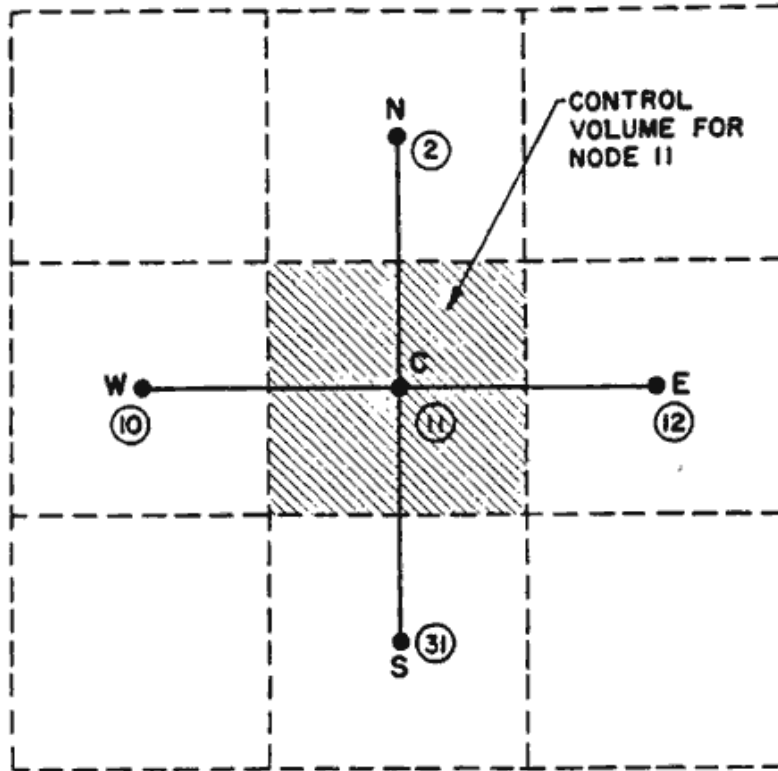


Figure 14.--Grid element nodal molecule.

Interface Model

Introduction

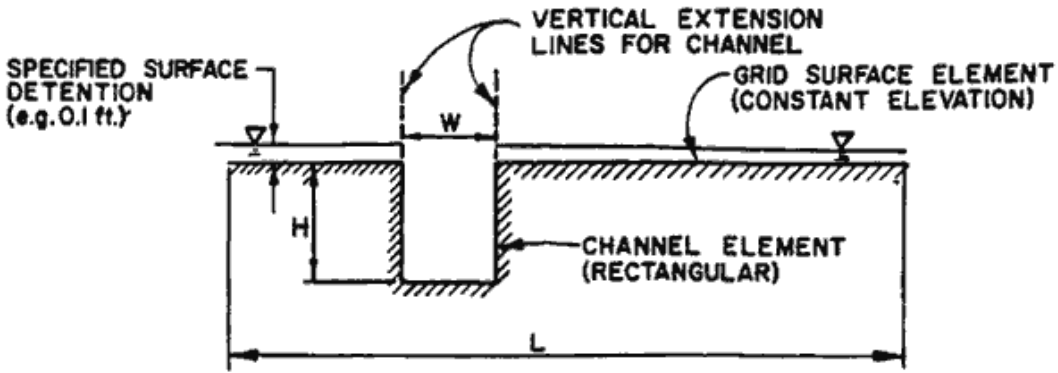
The interface model modifies the water surface elevations of flood plain grids and channel elements at specified time intervals (update intervals). There are three cases of interface situations: (1) channel overflow, (2) grid overflow, and (3) flooding of channel and grid elements.

Channel Overflow

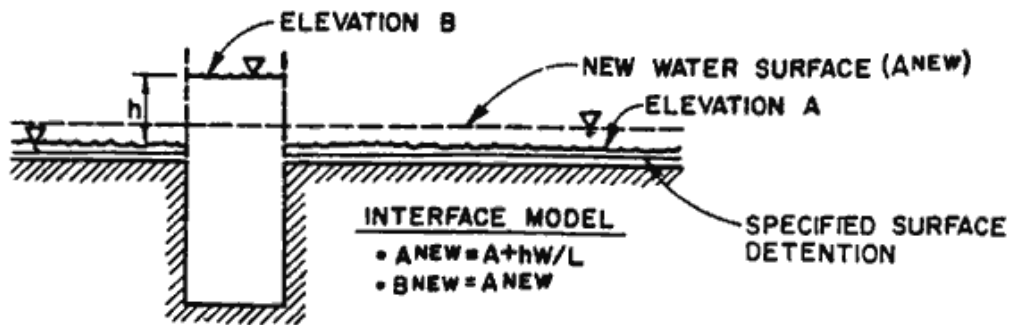
When the channel is overflowing; the excess water is temporarily stored in the vertically extended space (figure 15b). Actually, it is the volume per unit length. This excess water is the product of the depth of water, width of the channel and length of the channel and is subsequently uniformly distributed over the grid elements. In other words, the new grid water surface elevation is equal to the old water surface elevation plus a depth of hw/L , and the channel water surface elevation now matches the parent grid water surface elevation.

Grid Overflow

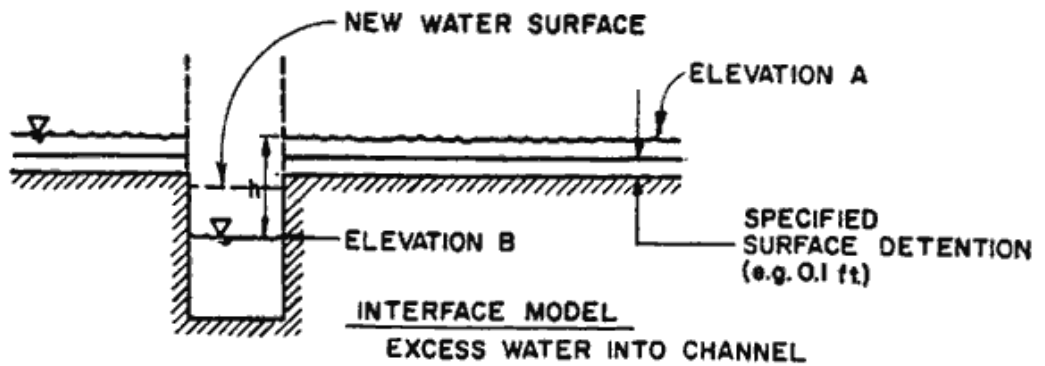
When the water surface elevation of the grid element is greater than a specified surface detention (figure 15a), the excess water drains into the channel element and the new water surface elevation is changed according to the following two conditions (figure 15c), (a) if $v > v'$, where v denotes the excess volume of water per unit length and v' denotes the available volume per unit length, the new water surface of the grid element is $A^{NEW} = A^{OLD} - (v-v')/L$ and the new water surface elevation of the channel element is also equal to A^{NEW} ; (b) if $v \leq v'$, the new water surface elevation of the grid element is $A^{NEW} = A^{OLD} - h$ and the new water surface elevation of the channel element is $B^{NEW} = B^{OLD} + v/w$.



a. MODEL INTERFACE GEOMETRICS

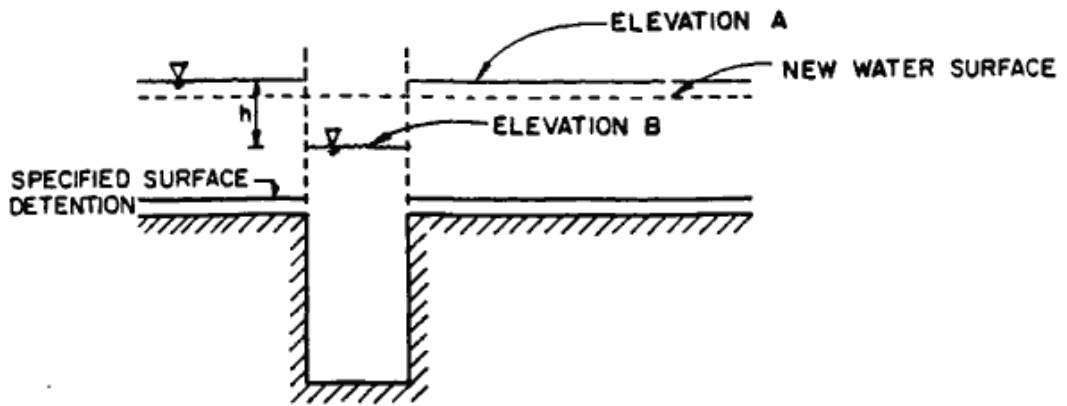


b. CHANNEL OVERFLOW INTERFACE MODEL

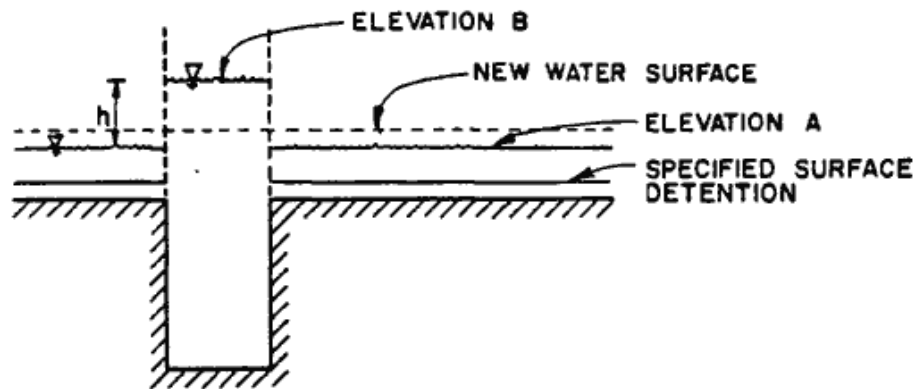


c. GRID OVERFLOW INTERFACE MODEL

Figure 15.--Diffusion hydrodynamic interface model.



d. GRID-CHANNEL FLOODING INTERFACE MODEL



e. CHANNEL-GRID FLOODING INTERFACE MODEL

Figure 15.--Diffusion hydrodynamic interface model.--(Continued)

Flooding of Channel and Grid

When flooding occurs, the water surface elevations of the grid and channel elements are both greater than the specified surface detention elevation. Two cases have to be considered as follows:

- (1) If $A > B$ (figure 15d), the new water surface elevation of the grid element is $A^{NEW} = B^{OLD} + h(L-w)/L$ and the new water surface elevation of the channel element is equal to A^{NEW} .
- (2) If $A < B$ (figure 15e), the new water surface elevation of the grid element is $A^{NEW} = A^{OLD} + h \cdot w/L$ and the new water surface elevation of the channel element is equal to A^{NEW} .

APPLICATIONS OF THE DIFFUSION HYDRODYNAMIC MODEL

One-Dimensional Model

Application 1: Steady Flow in an Open Channel

Because the DHM is anticipated for use in modeling watershed phenomena, it is important that the channel models represent known flow characteristics. Unsteady flow is examined in the previous section. For steady flow, a steady-state, gradually varied flow problem is simulated by the 2-D diffusion model. Figure 16 depicts both the water levels from the 2-D diffusion model and from the gradually varied flow equation. For an 8000 cfs constant inflow rate, the water surface profiles from both the 2-D diffusion model and the gradually varied flow equation match quite well. The discrepancies of these profiles occur at the break points where the upstream channel slope and downstream channel slope change. At the first break point where the upstream channel slope is equal to 0.001 and the downstream channel slope is equal to 0.005, the water surface level is assumed to be equal to the critical depth. However, Henderson (1966), notes that brink flow is typically less than the critical depth (D_c). The DHM water surface closely matches the $0.72 D_c$ brink depth.

It is clear to see that the DHM cannot simulate the hydraulic jump, but rather smoothes out the usually assumed "shock front". However, when considering unsteady flow, the DHM may be a reasonable approach for approximating the jump profile. For a higher inflow rate, 20,000 cfs, the surface water levels differ in the most upstream reach. Again, this is due to the downstream control, critical depth, of the gradually varied flow equation.

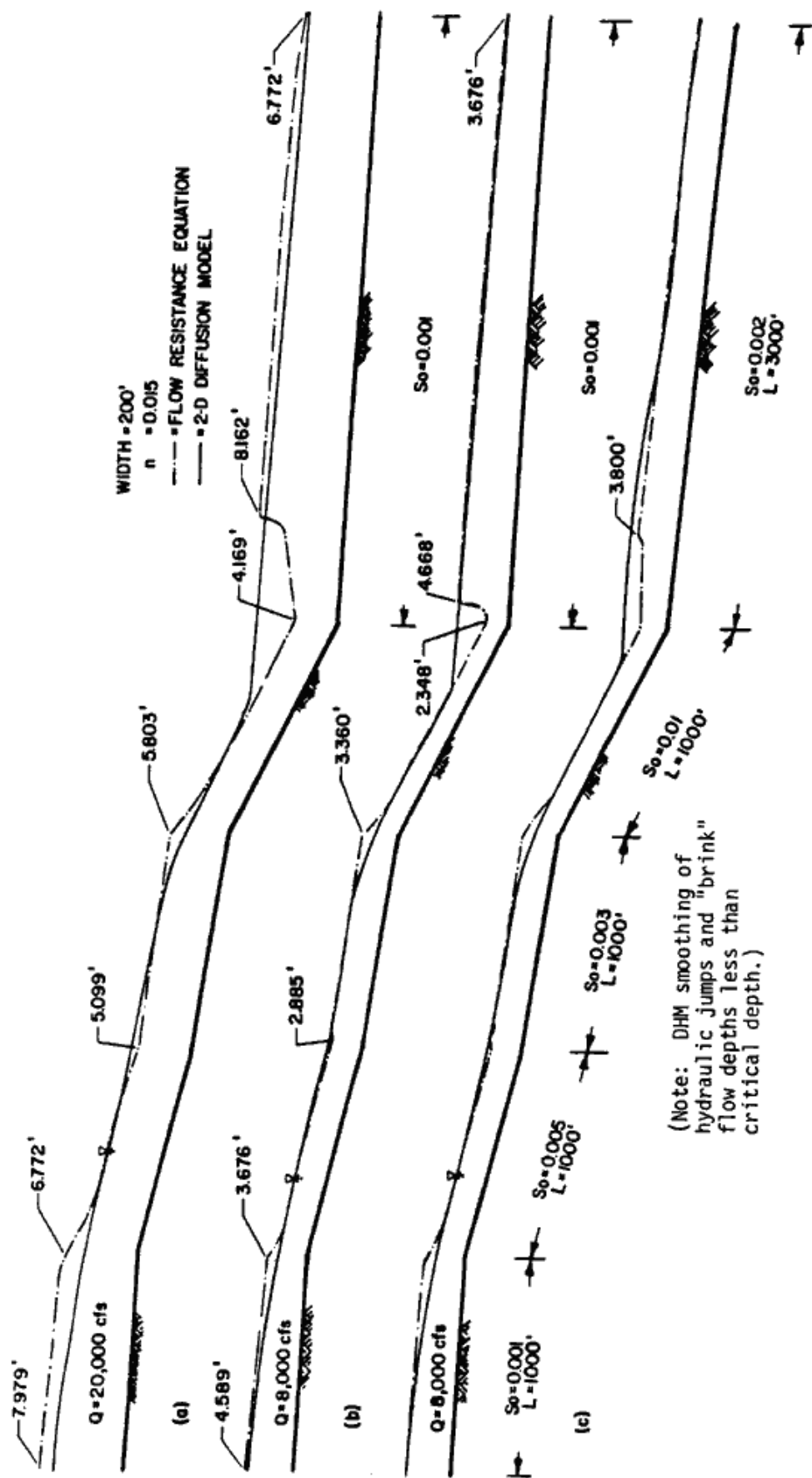


Figure 16.--Gradually varied flow profiles.

Two-Dimensional Applications

Application 2: Rainfall-Runoff Model

The DHM can be used to develop a runoff hydrograph given the time distribution of effective rainfall. To demonstrate the DHM runoff hydrograph generation (Hromadka and Nestlinger, 1985), the DHM is used to develop a synthetic S-graph for a watershed where overland flow is the dominating flow effect.

To develop the S-graph, a uniform effective rainfall is assumed to uniformly occur over the watershed. For each timestep (5-seconds), an incremental volume of water is added directly to each grid-element based on the assumed constant rainfall intensity, resulting in an equivalent increase in the nodal point depth of water. Runoff flows to the point of concentration according to two-dimensional diffusion hydrodynamics model.

The 10 square mile Cucamonga Creek watershed (California) is shown, discretized by 1000-foot grid elements, in figure 17. A design storm (figure 18) was applied to the watershed and resulting runoff hydrographs are depicted in figure 19 for DHM model and synthetic unit hydrograph method. From figure 19, the diffusion model generates runoff quantities which are in good agreement with the values computed using synthetic unit hydrograph method derived from stream gage data.

Next, the DHM is applied to three hypothetical dam-failures in Orange County, California (see figure 20). Applications of the DHM illustrates its use in a municipal setting where flood flow patterns are affected by railroad, bridge undercrossings, and other man-made obstacles to flow.

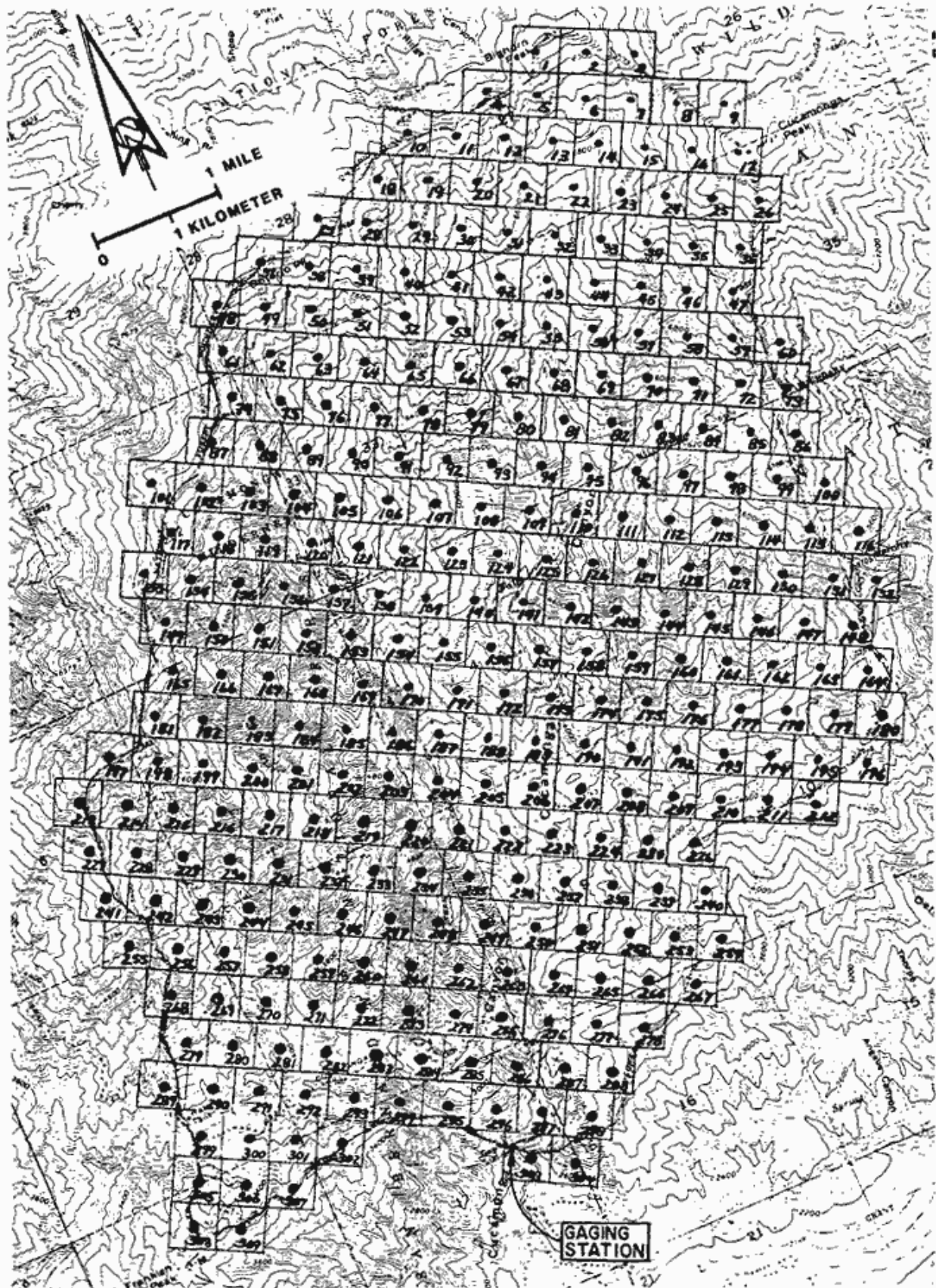
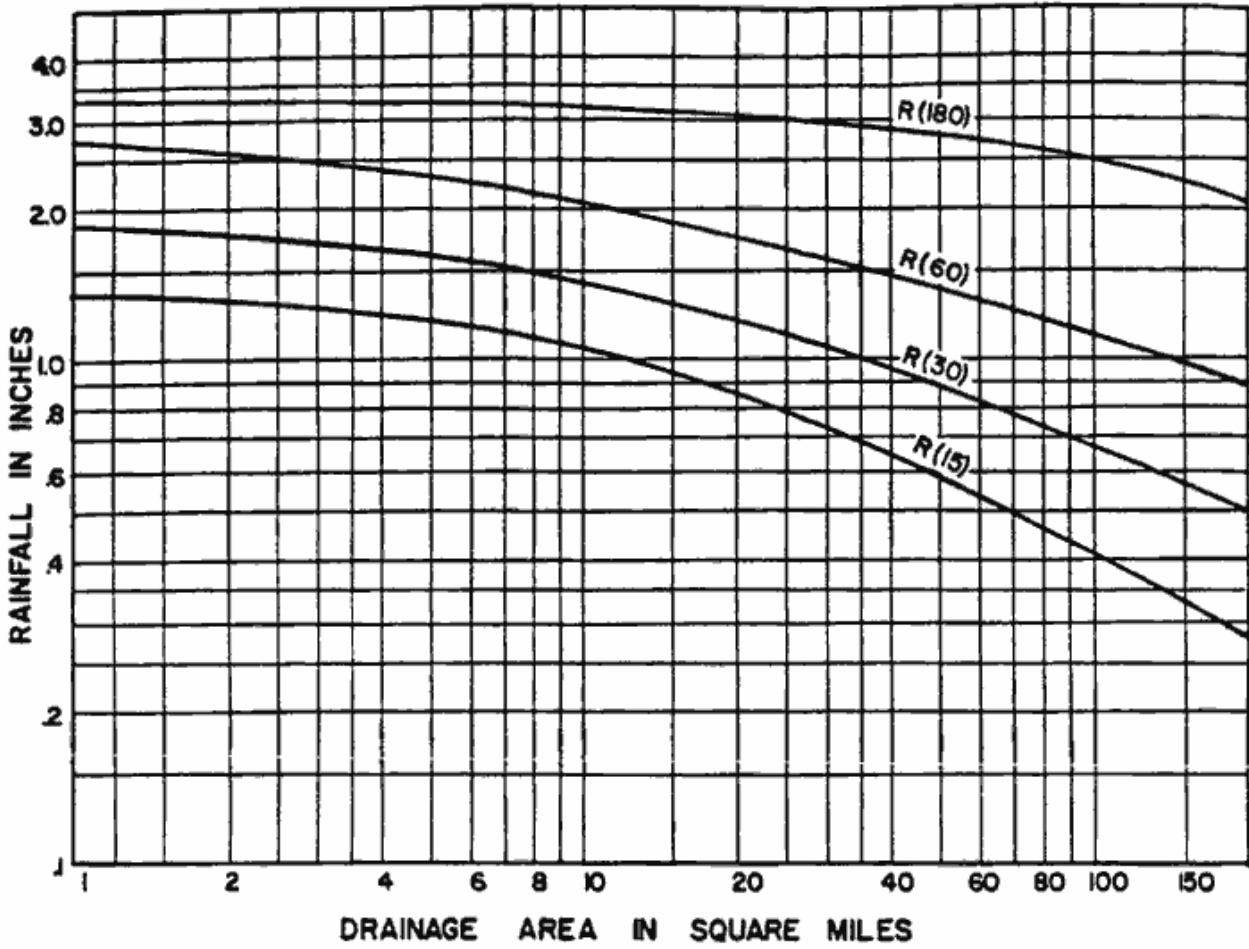


Figure 17.--Cucamonga Creek Discretization
51



HYETOGRAPH COMPUTATION

UNIT PERIOD	AMOUNT
1	.07 (R(180)-R(60))
2	.05 (R(180)-R(60))
3	.11 (R(180)-R(60))
4	.05 (R(180)-R(60))
5	.20 (R(180)-R(60))
6	.22 (R(180)-R(60))
7	.14 (R(180)-R(60))
8	.16 (R(180)-R(60))
9	.48 (R(60)-R(30))
10	.52 (R(60)-R(30))
11	1.00 (R(15))
12	1.00 (R(30)-R(15))

Note:
R(15) = Rainfall (inches) in 15-minute duration

LOCAL PROJECT STORM
DEPTH AREA DURATION CURVES

Figure 18.--Design storm for Cucamonga Creek.

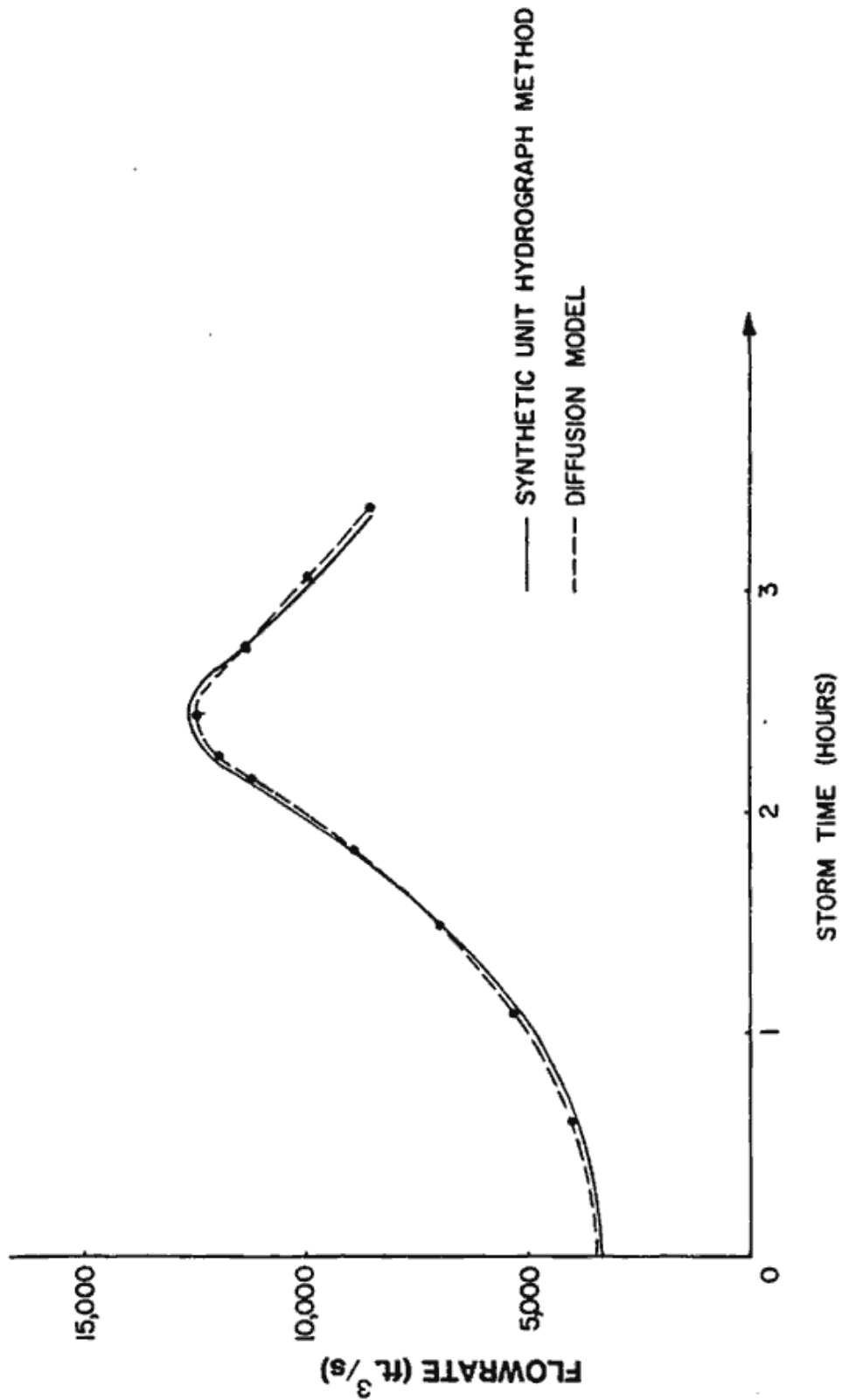


Figure 19.--Simulated runoff hydrographs for Cucamonga Creek.

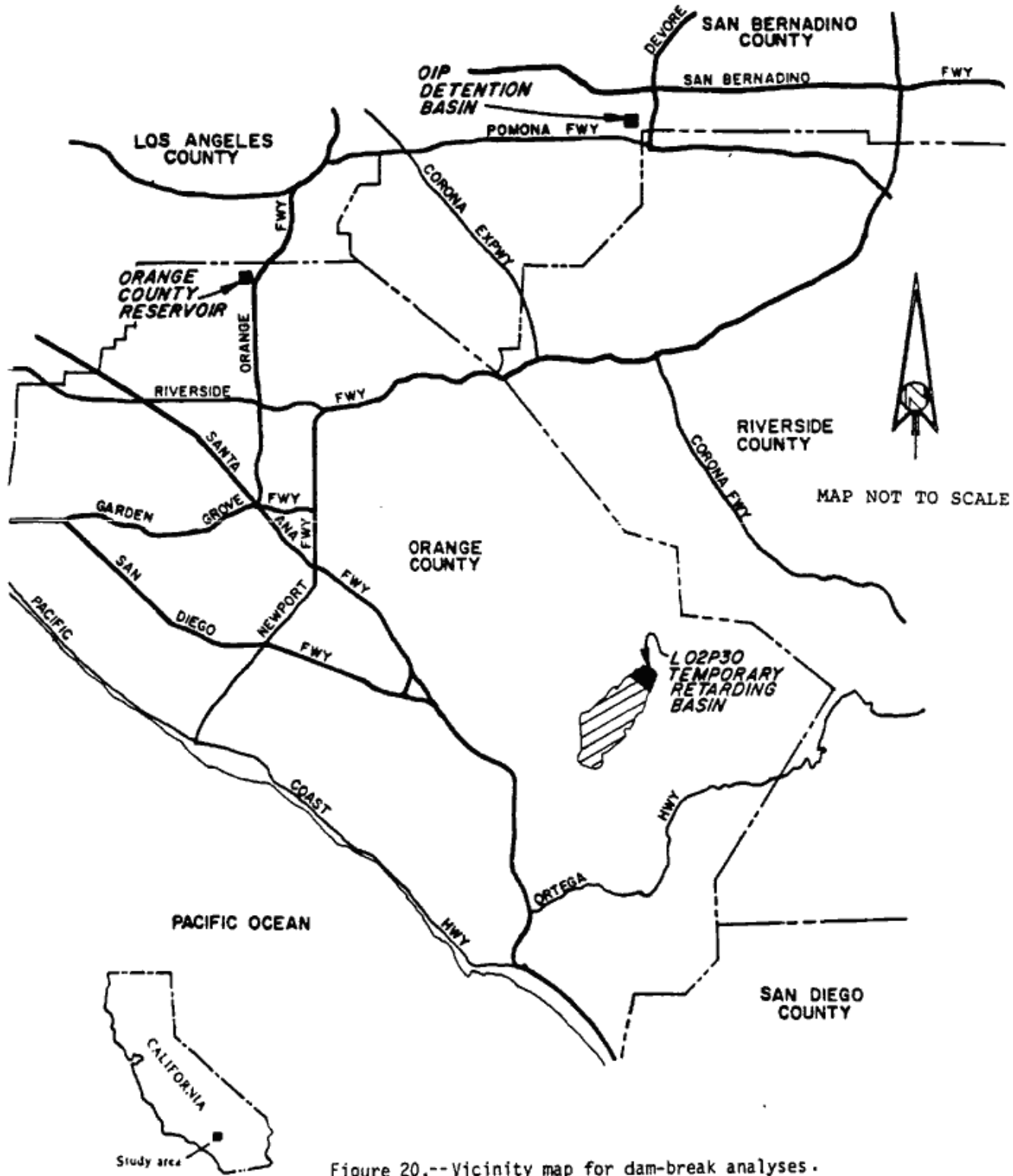


Figure 20.--Vicinity map for dam-break analyses .

Major assumptions used in these assumptions are as follows:

- (1) In each grid, an area-averaged ground elevation was estimated based on the topographic map and a Manning's roughness coefficient was used for each application
- (2) All storm drain systems provide negligible draw off of the dam-break flows. This assumption accommodates a design storm in progress during the dam failure. This assumption also implies that storm water runoff provides a negligible increase to the dam-break flow hydrograph.
- (3) All canyon damming effects due to culvert crossings provide negligible attenuation of dam-break flows. This assumption is appropriate due to the concurrent design storm assumption, and due to sediment deposition from transport of the reservoir earthen dam materials.
- (4) The reservoir failure yields an outflow hydrograph as depicted in figure 21.

Application 3: Small-Scale Dam-Break Flood Plain Analysis

Study of a hypothetical failure of the Orange County Reservoir north-east of the City of Brea, California (figure 22) was conducted by Hromadka and Lai (1985). Using current USGS topographic quadrangle map (photo-revised, 1981), a 500-foot grid discretization was prepared (figure 23), and nodal-area ground elevations were estimated based on the map. A Manning's roughness coefficient of $n = 0.040$ was used throughout the study, except in canyon reaches and grassy plains, where n was selected as 0.030 and 0.050, respectively. In this study, the resulting flood plain and the comparison of the model-simulated flood plain to a previous study by the Metropolitan Water District of Southern California (1973), are shown in

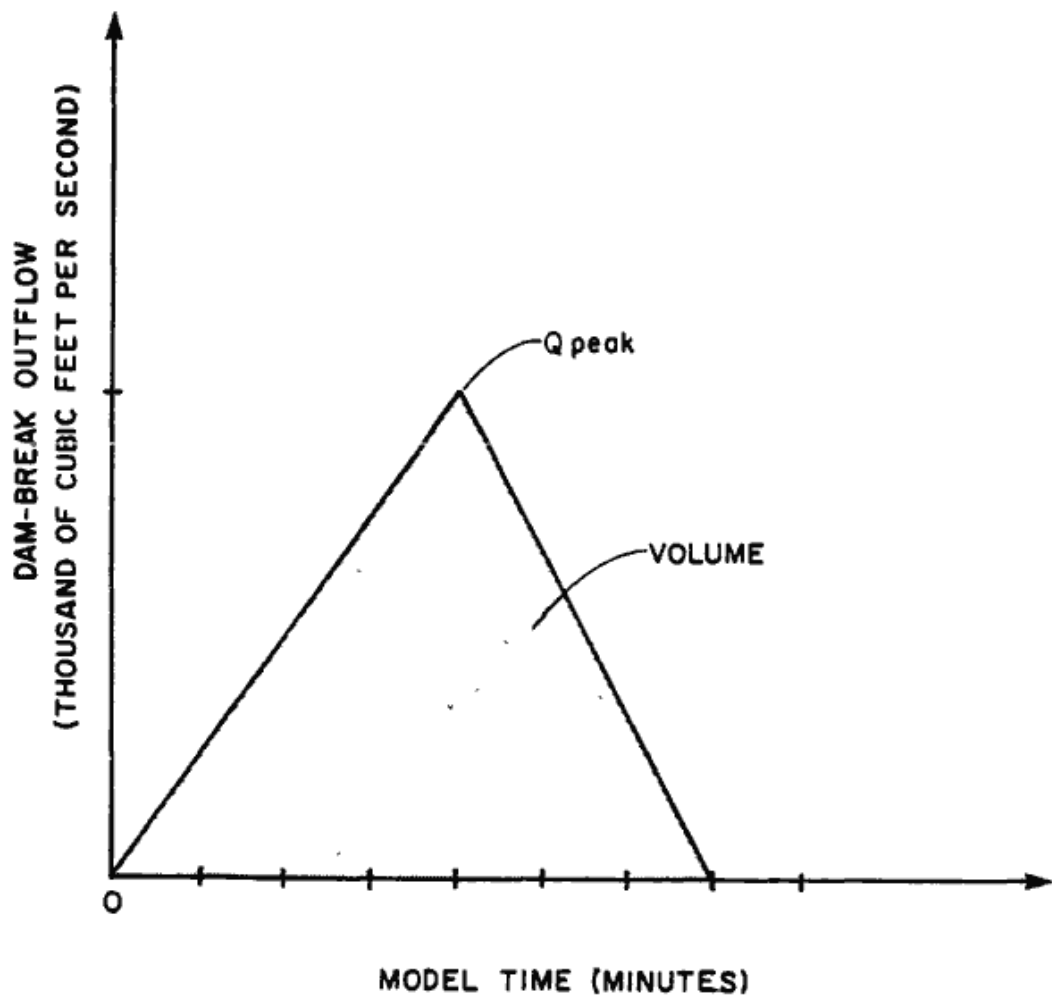


Figure 21.-- Study dam-break outflow hydrograph for Orange County Reservoir.

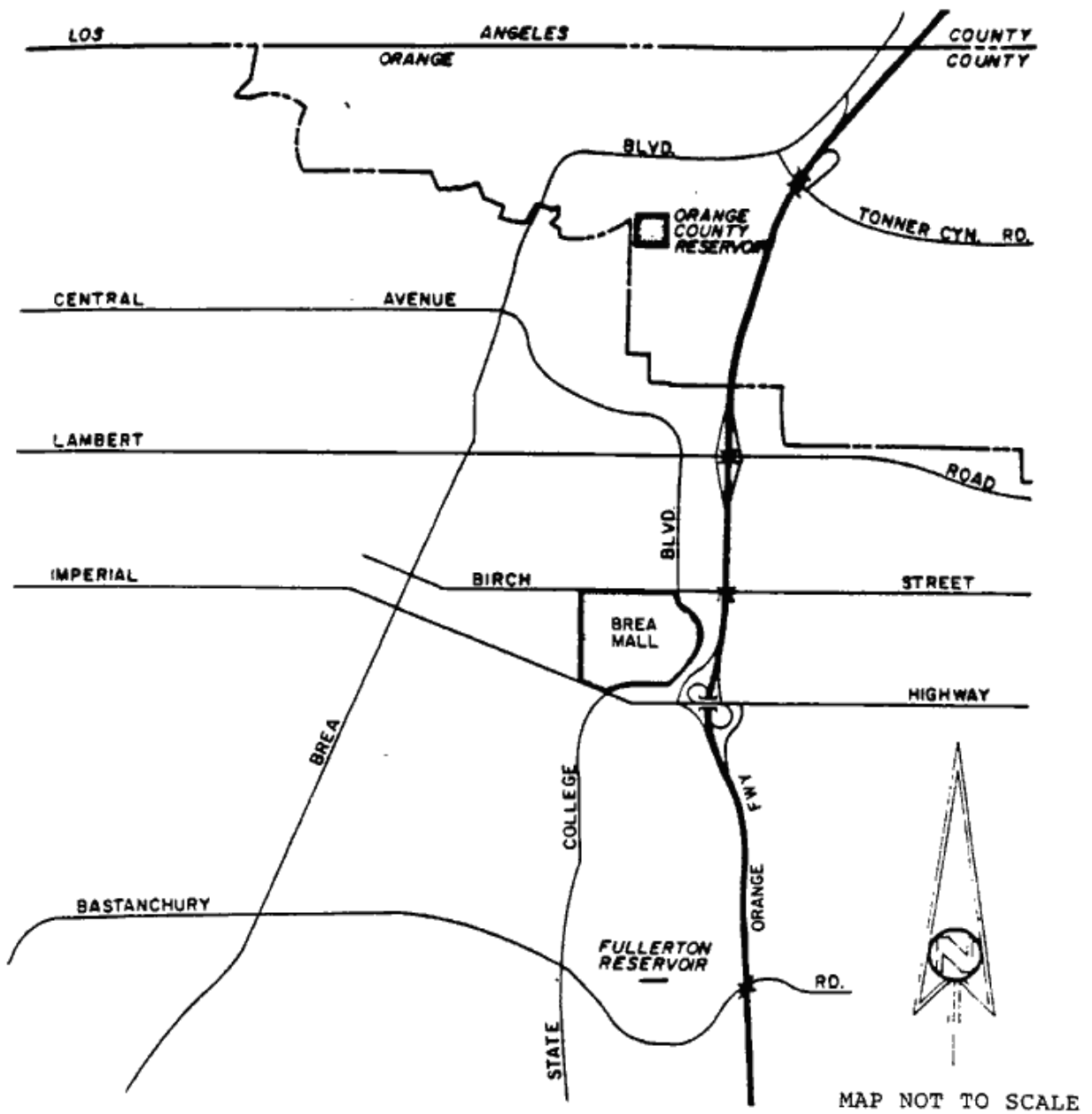


Figure 22.--Location map for the Orange County Reservoir dam-break problem.

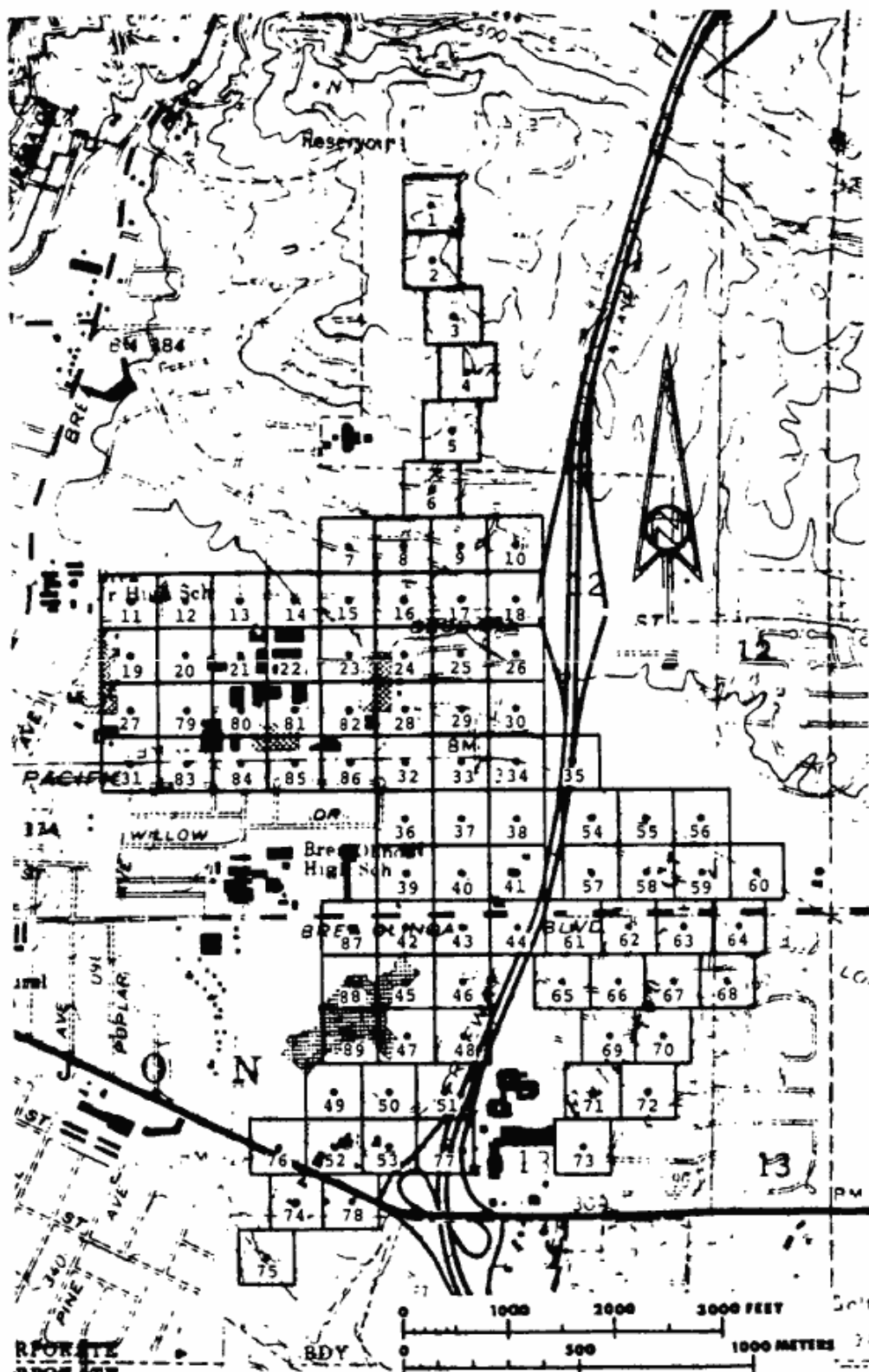


Figure 23.-- Domain Discretization for Orange County Reservoir.

figure 24. The main difference in the estimated flood plains is due to the dynamic nature of the DHM model, which accounts for the storage effects resulting from flooding, and the attenuation of a flood wave because of 2-D routing effects. From this study, the estimated flood plain is judged to be reasonable.

Application 4: Small-Scale Flows Onto a Flat Plain

A common civil engineering problem is the use of temporary detention basins to offset the effects of urbanization on watershed runoff. A problem, however, is the analysis of the basin failure; especially, when the floodflows enter a wide expanse of land surface with several small channels. This application is to present study conclusions in estimating the flood plain which may result from a hypothetical dam-failure of the LO2P3O Temporary Retarding Basin. The results of this study are to be used to estimate the potential impacts of the area if the retention basin berm were to fail.

The study site includes the area south of Plano Trabuco, Phase I. It is bounded on the north of LO2P3O Retarding Basin Berm, on the east and south of Portola Parkway and on the west by the Arroyo Trabuco bluffs (see figure 25).

Using a 1" = 300' topographic map, a 200-foot grid control volume discretization was constructed as shown in figure 26. In each grid, an area-averaged ground elevation was estimated based on the topographic map. A Manning's roughness coefficient of $n = 0.030$ was used throughout the study.

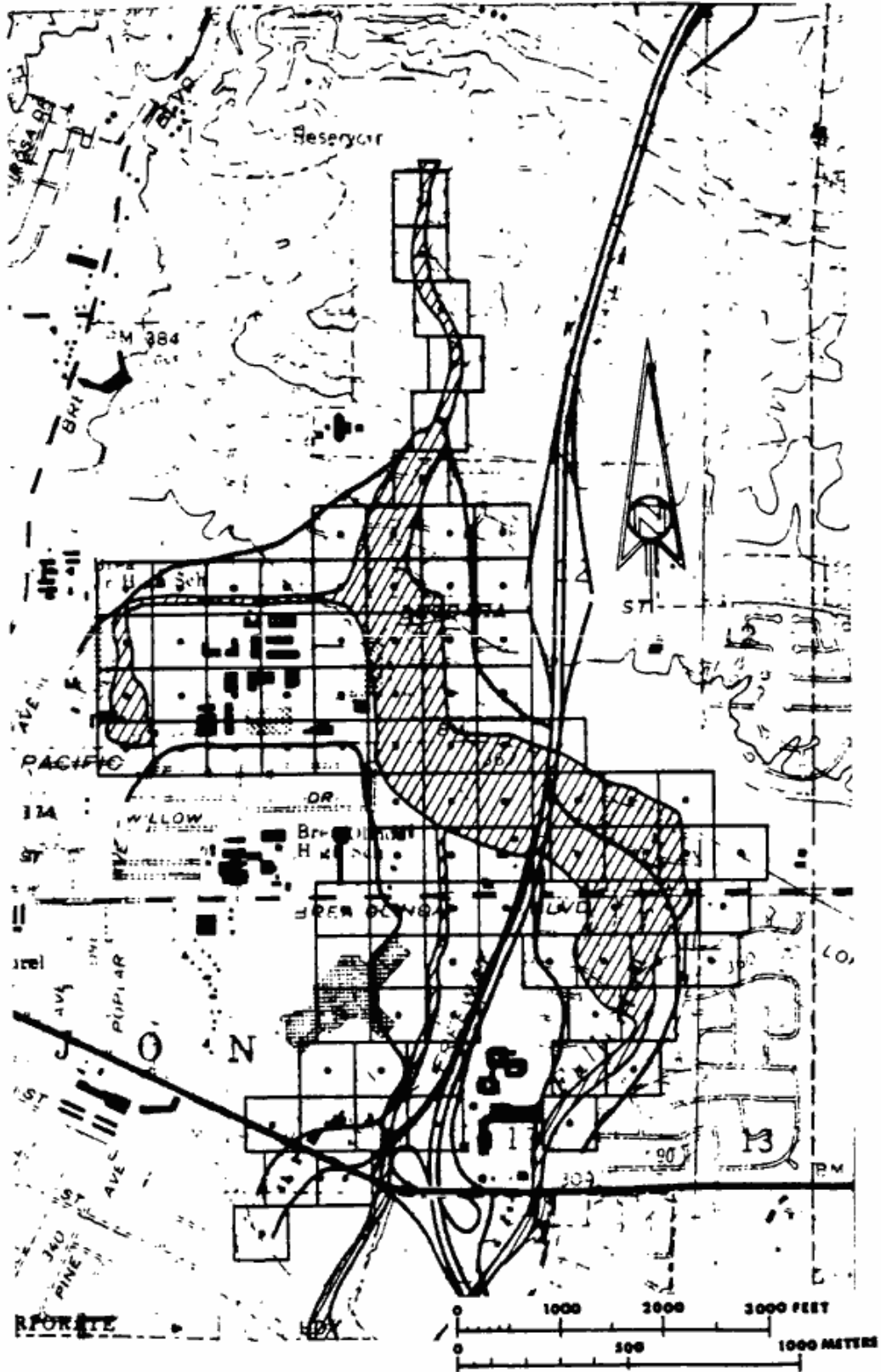


Figure 24.--Comparison of flood plain results for Orange County Reservoir.

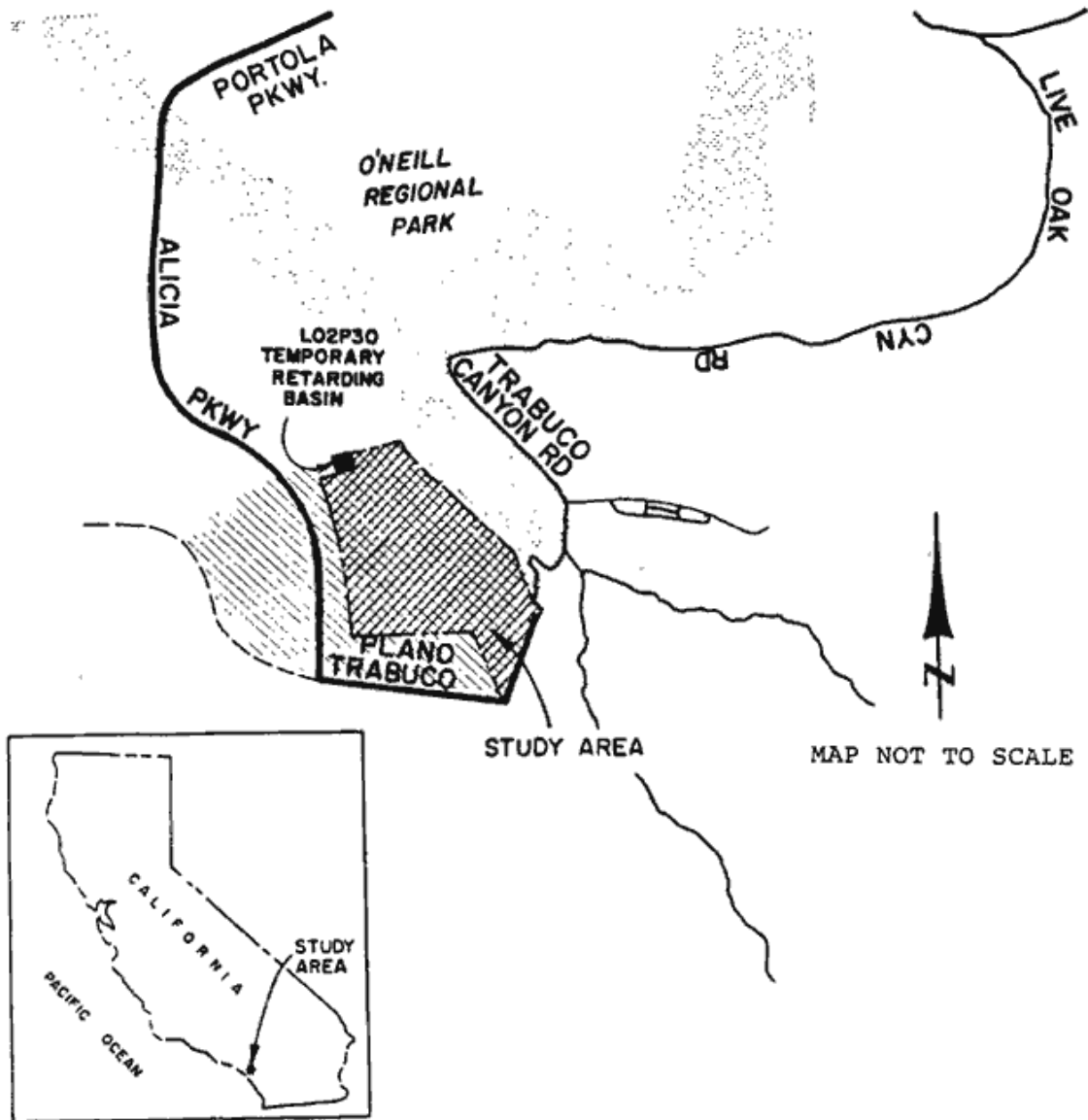


Figure 25.--Location map for L02P30 temporary retarding basin.

The profile of Portola Parkway varies approximately 2 feet above and below the adjacent land. Consequently, minor ponding may occur where Portola Parkway is high and sheet flow across Portola Parkway will occur at low points. It should be noted that depths along Portola Parkway are less than 1 foot (figure 26). Figure 27 shows lines of arrival times for the basin study. It is concluded that Portola Parkway is essentially unaffected by a hypothetical failure of the LO2P3O Temporary Retarding Basin.

Application 5: Two-Dimensional Floodflows Around a Large Obstruction

In another temporary detention basin site, floodflows (from a dam-break) would pond upstream of a landfill site, and then split, when waters are deep enough, to flow on either side of the landfill. An additional complication is a railroad berm located downstream of the landfill, which forms a channel for floodflows. The study site (see figure 28) is bounded on the north by a temporary berm approximately 300 feet north of the Union Pacific Railroad, bounded on the east by Milliken Avenue, bounded on the south by the Union Pacific Railroad and bounded on the west by Haven Avenue.

A 200-foot grid control volume discretization was constructed as depicted in figure 29. In each grid, an area-averaged ground elevation was estimated based on the topographic map. A Manning's roughness coefficient of $n = 0.030$ was used throughout the study.

From figure 30 it is seen that flood plain spreads out laterally and flows around the landfill. The flow ponds up around the landfill; along the north side of the landfill, the water ponds as high as 9.2 feet, and along the east and west sides of the landfill, the water ponds up to 5.1 feet high. As the flow travels south, it ponds up to a depth of 4.8

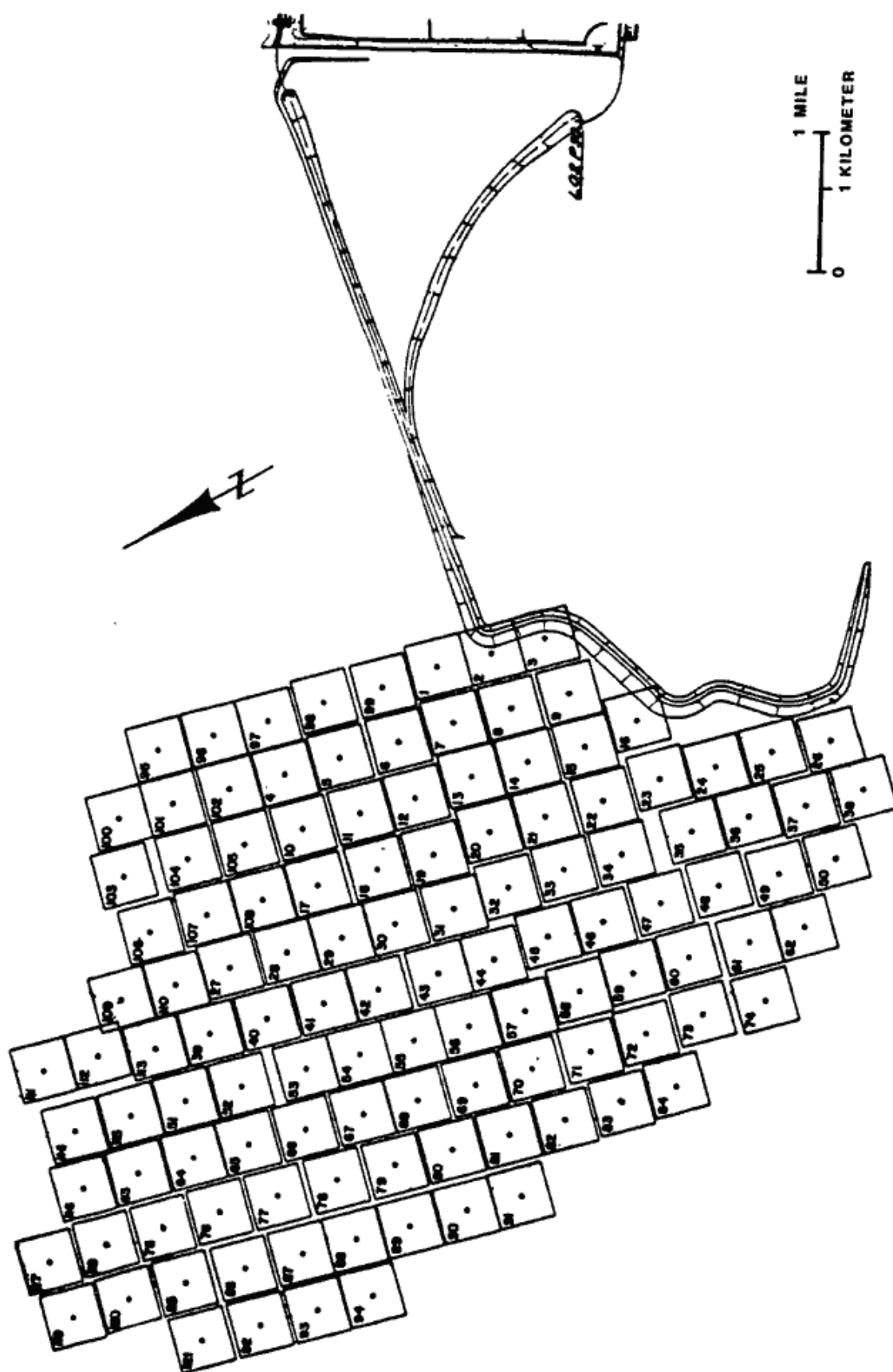


Figure 26.--Domain discretization of L02P30 temporary retarding basin.

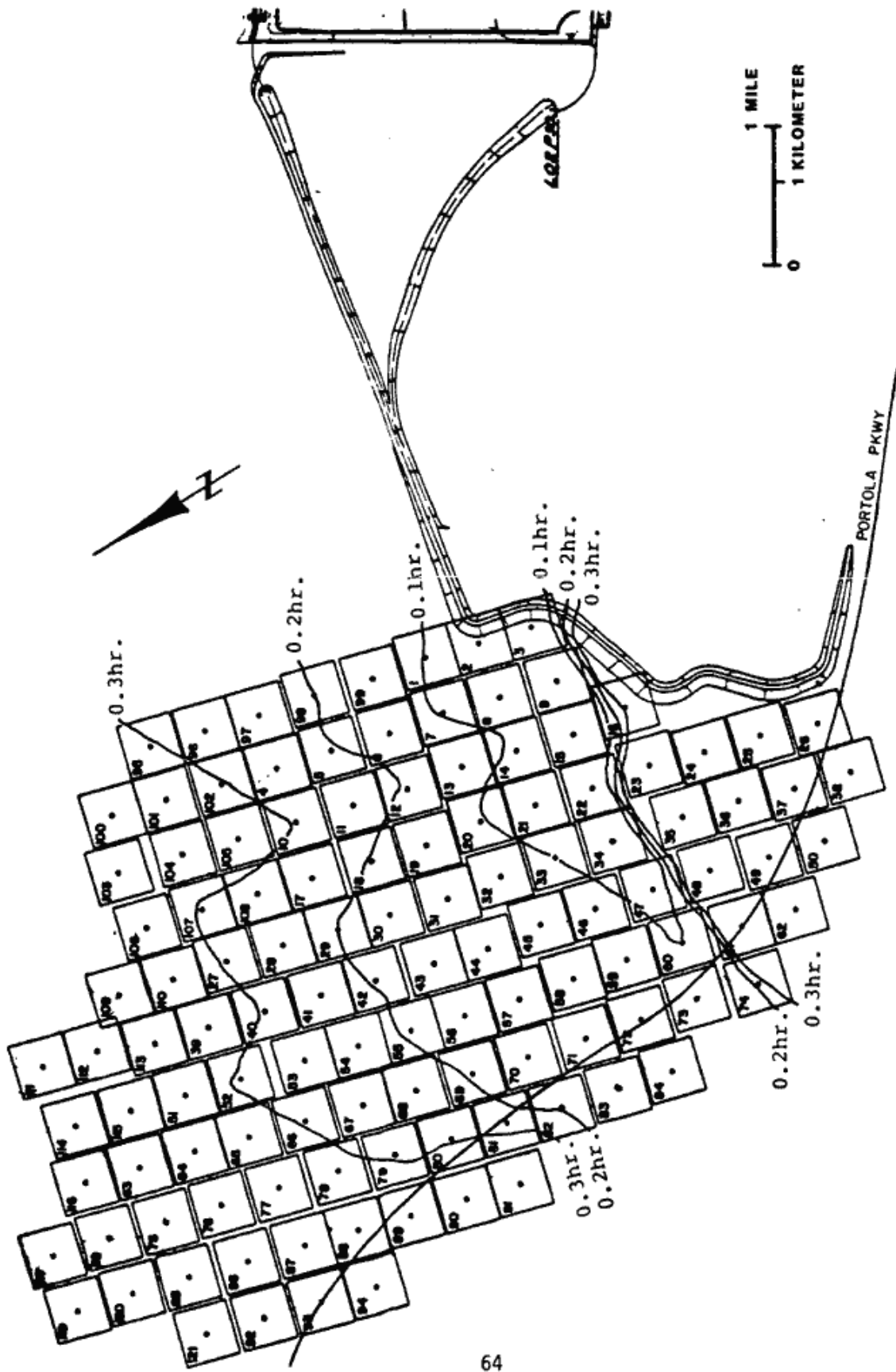
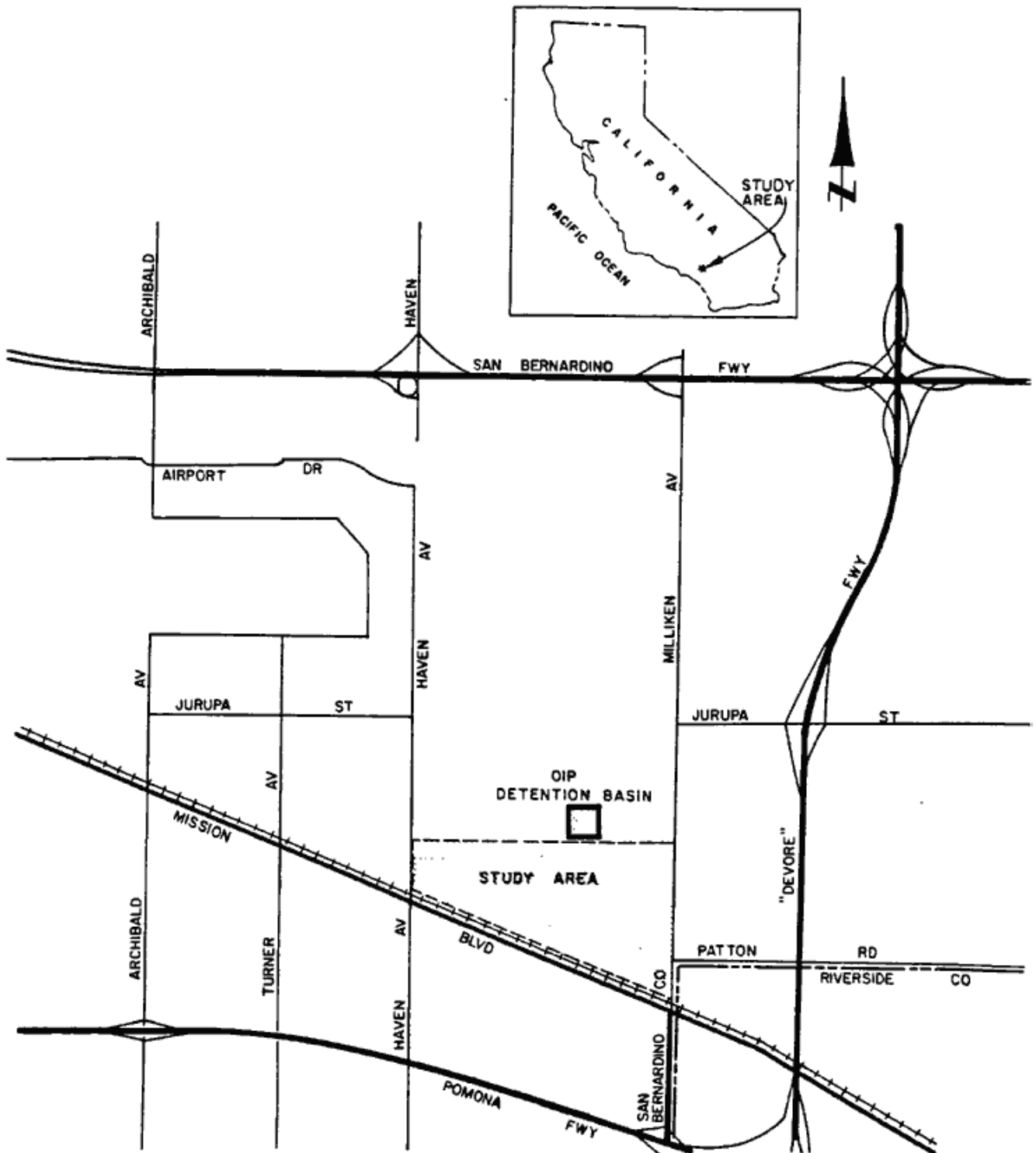


Figure 27.--Time of maximum flooding depth (80.5 Acre-Feet basin test) for L02P30 temporary retarding basin.



MAP NOT TO SCALE

Figure 28.--Location map for Ontario Industrial Partners temporary detention basin.

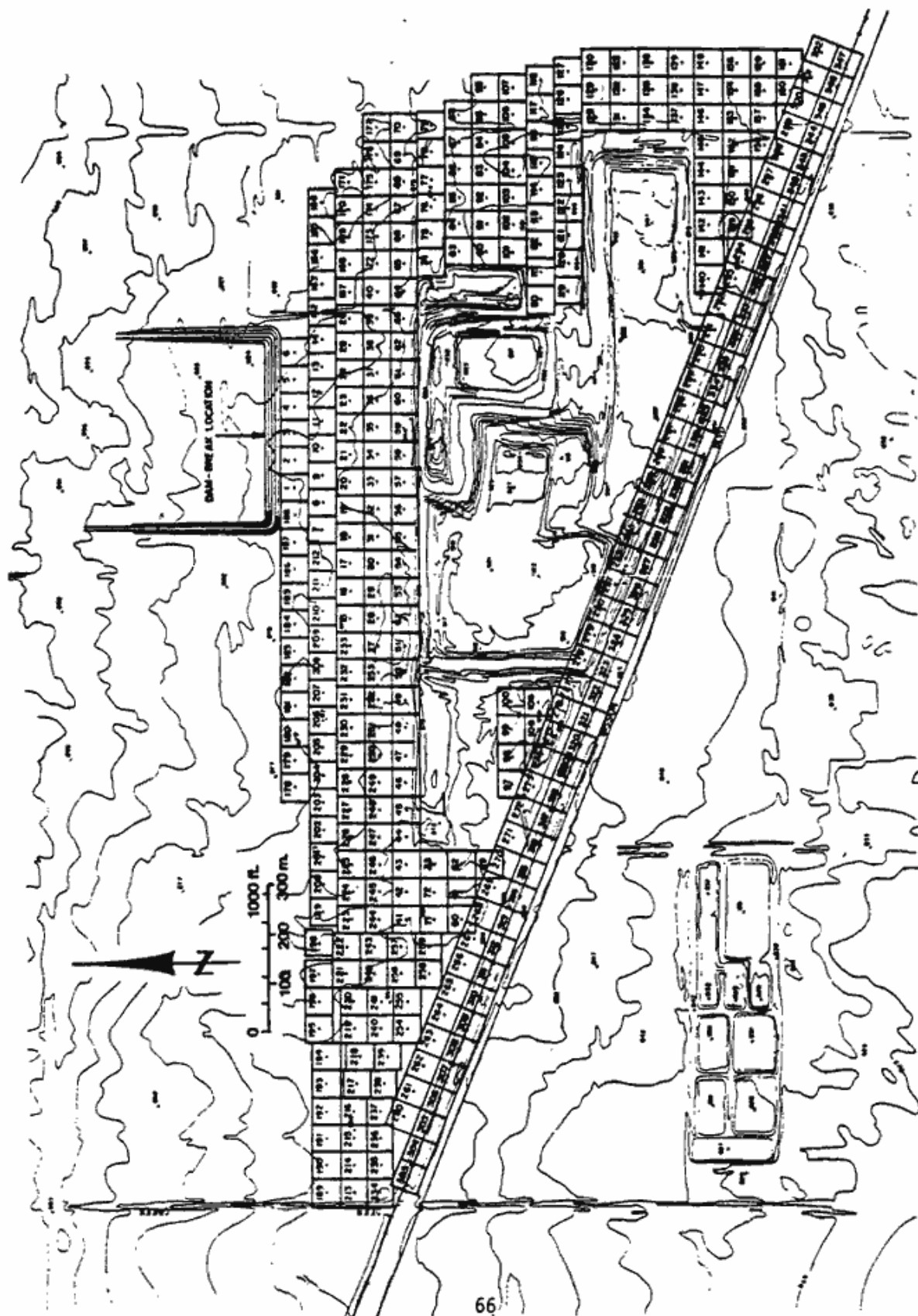


Figure 29.-- Domain discretization for Ontario Industrial Partners detention basin.

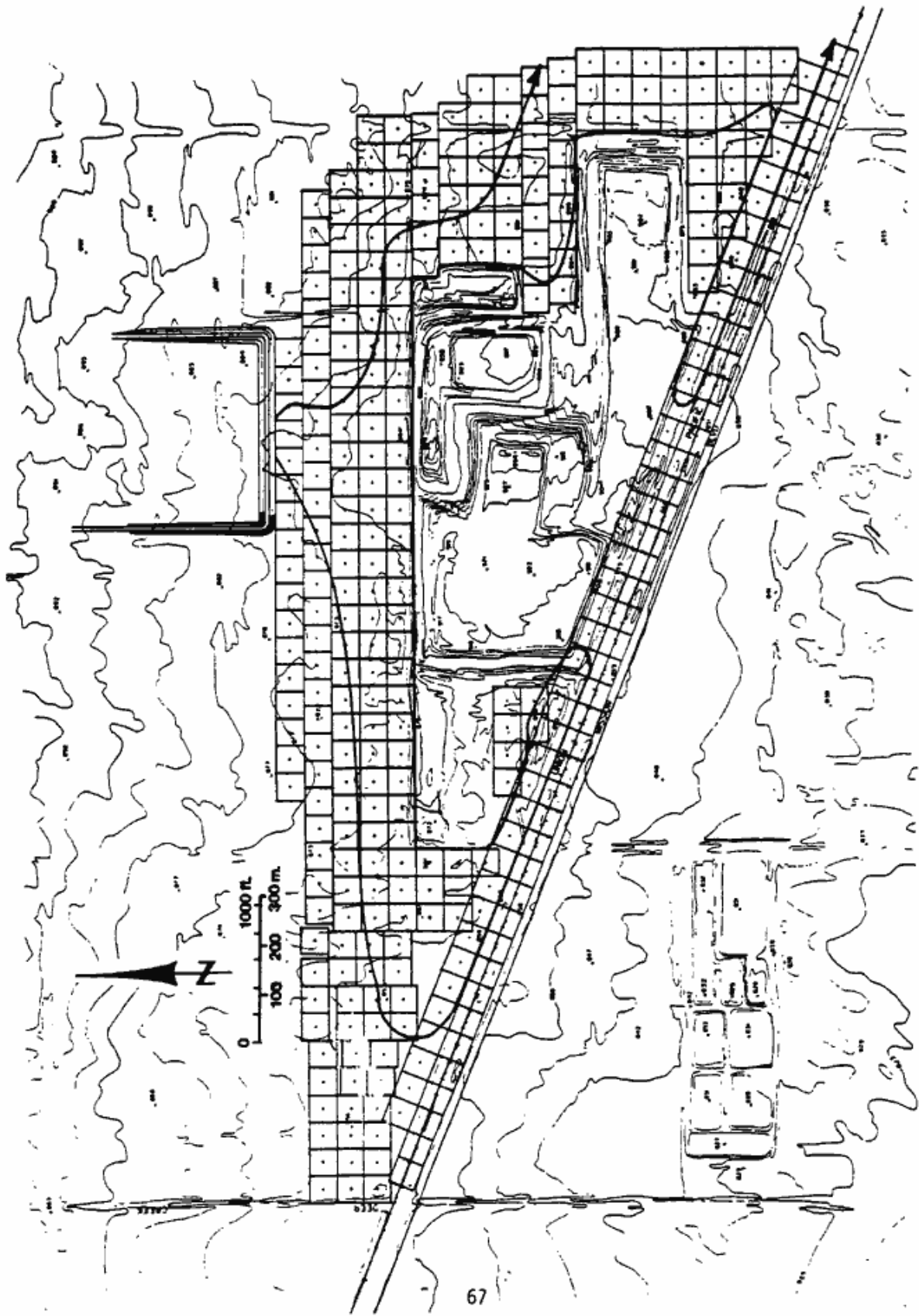


Figure 30.--Flood plain for Ontario Industrial Partners detention basin.

feet against the railroad near Milliken Avenue. Because the water spreads laterally, Milliken Avenue runs the risk of becoming flooded; however, the water only ponds to 0.6 feet along the street. A more in-depth study is needed to see if the water would remain in the gutter or flood Milliken Avenue.

By observing the arrival times of the flood plain in figure 31, it is seen that the flood plain changes very little on the west side of the landfill once it reaches the railroad (0.6 hours after the dam-break). But on the east side of the landfill it takes 2.0 hours to reach the railroad.

Application 6: Estuary Modeling

Figure 32 illustrates a hypothetical bay, which is schematized in figure 33. Stage hydrographs are available at seven stations as marked in figure 32 and are numbered 1 through 7 (counterclockwise). Stage values in this application are expressed by sinusoidal equations (see Table 1). Some DHM-predicted flow patterns in the estuary are shown in figures 34 to 36. The flow patterns appear reasonable by comparing the fluctuations of the water surface to the stage hydrographs. DHM computed flow patterns compare well to a similar study prepared by Lai (1977).

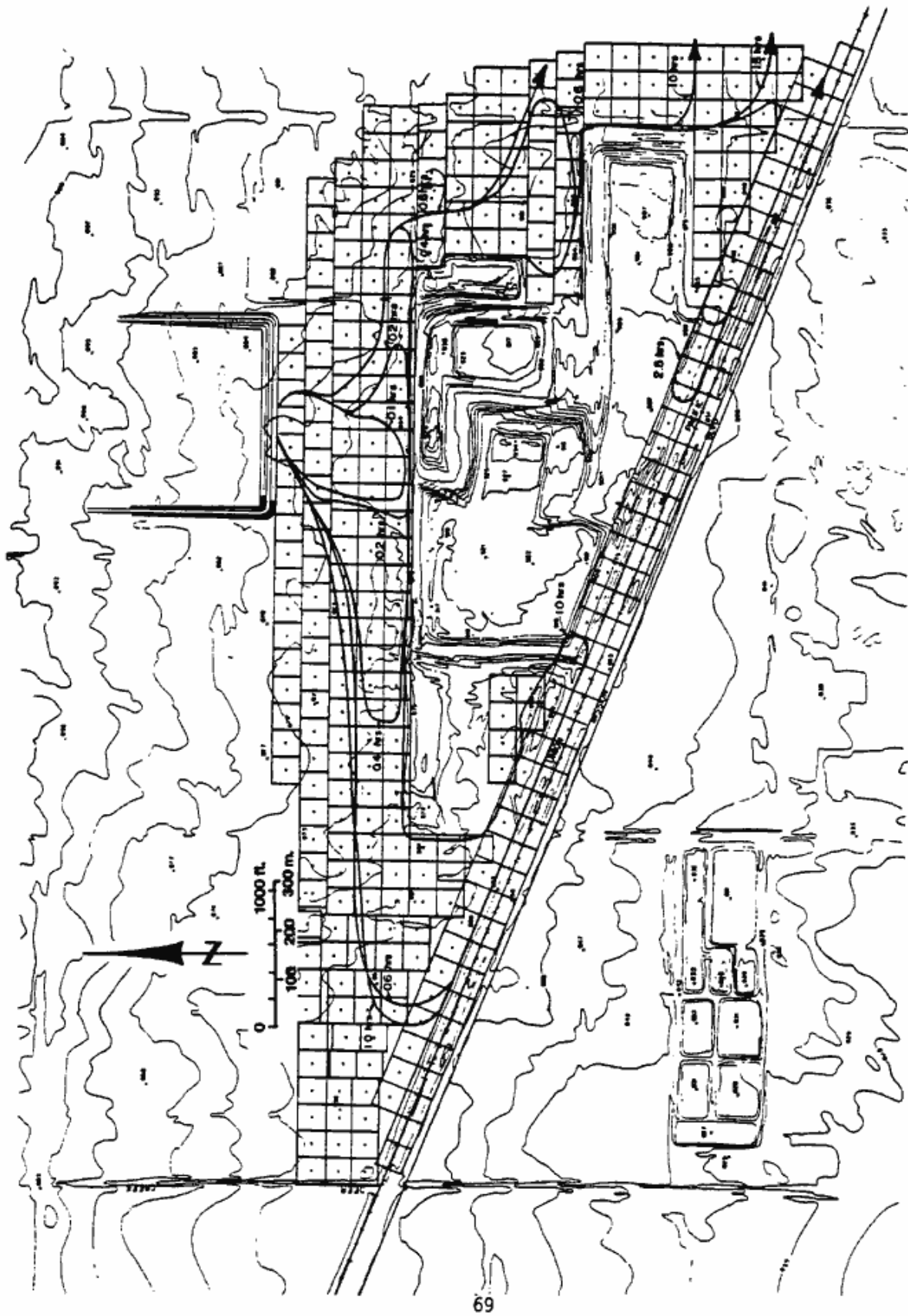


Figure 31.-- Time (hours) of maximum flooding depth for Ontario Industrial Partners detention basin.

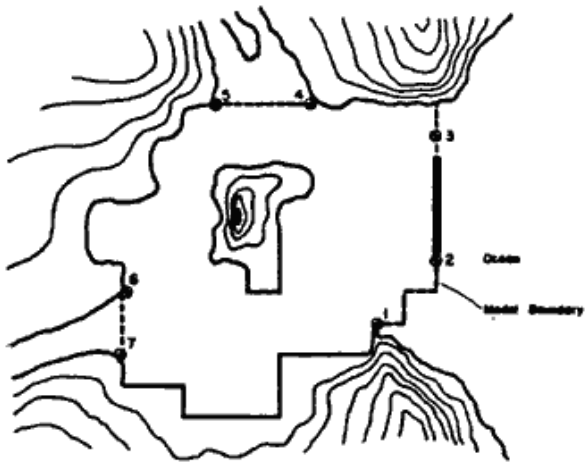


Figure 32.-- A hypothetical bay

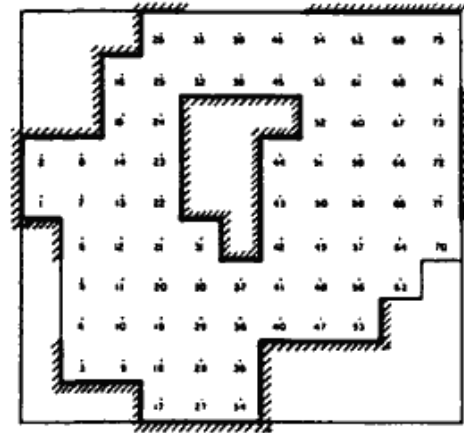
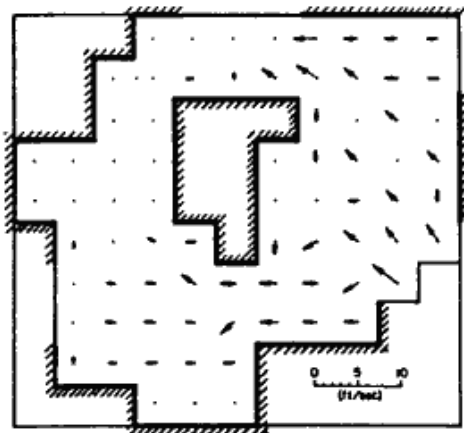
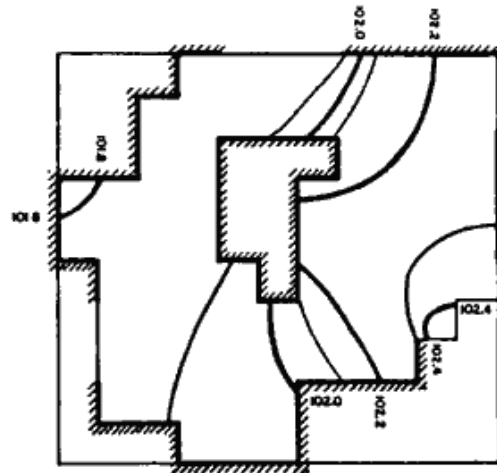


Figure 33.--The schematization of a hypothetical bay shown in figure 43



(a) Mean velocity



(b) Mean water surface

Figure 34.--Mean velocity and water surface profiles at 1-hour.

Table 1.-- Boundary values for flow computation
in a hypothetical bay

Boundary value equation:

$$z = a \sin \left[\frac{2\pi(t - \xi)}{T} \right] + M + 100.$$

in which

a = amplitude,

t = time, in second.

ξ = phase lag,

T = tidal period = 12.4 hr.

M = mean water level,

= 44640 sec.

NODE	a(ft)	ξ (sec)	M(ft)
63	5	0	0
70	4.95	60	0
74	4.85	180	0
75	4.85	180	0
46	4.75	1200	0.3
39	4.725	1260	0.35
33	4.7	1320	0.4
5	4.5	1800	0.7
4	4.45	1860	0.75

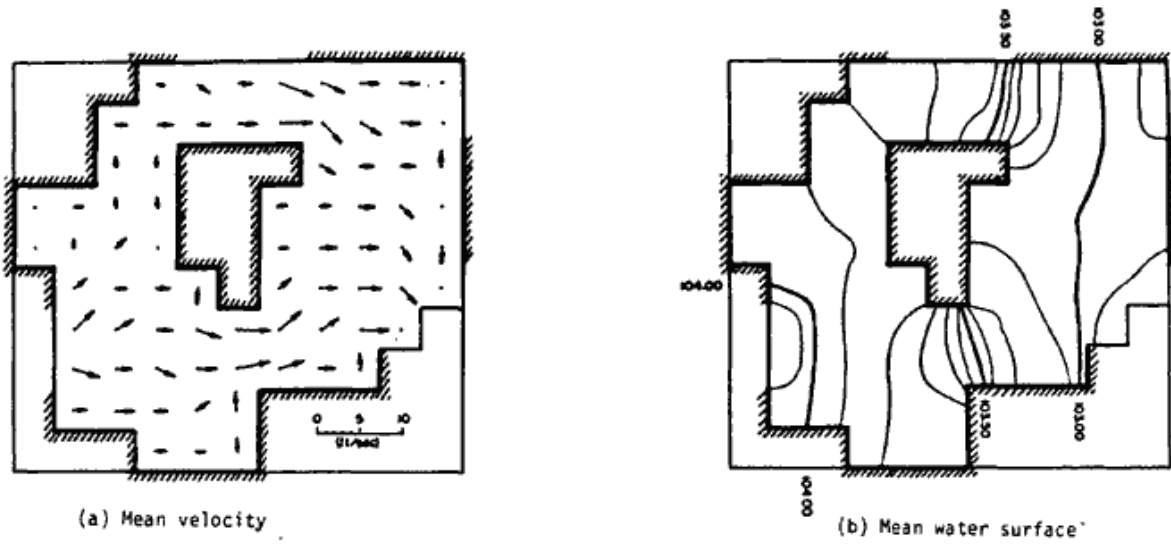


Figure 35.--Mean velocity and water surface profiles at 5-hours.

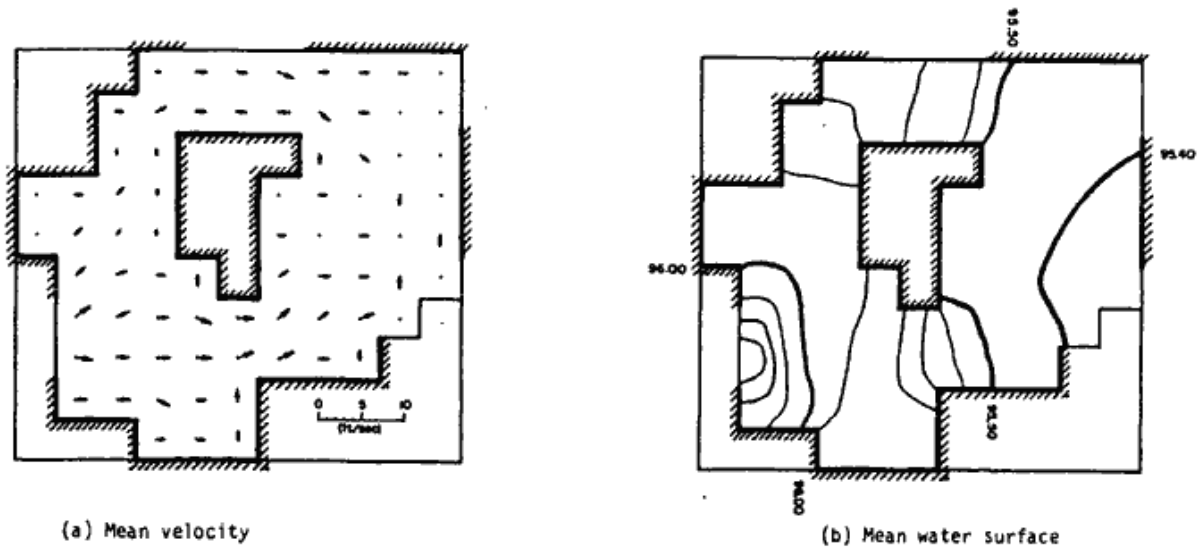


Figure 36.-- Mean velocity and water surface at 10-hours .

Application for Channel and Flood Plain Interface Model

Application 7: Channel-Flood Plain Model

Figure 37 depicts a discretization of a two-dimensional hypothetical watershed with three major channels crossing through the flood plain.

Figure 38 depicts the inflow and outflow boundary conditions for the hypothetical watershed model. Input data and partial output results of this application are included in Attachment D. Figures 39 through 44 illustrates the evolutions of the flood plain.

The shaded areas indicate which grid element are flooded. From figure 39, it is seen that the outflow rates at nodes 31, 71 and 121 are less than the corresponding inflow rates which results in a flooding situation adjacent to the outflow grid elements. The junction of channel B and B' is also flooded. At the end of the peak inflow rate (figure 41), about 1/3 of the flood plain is flooded. Figure 44 indicates a flooding situation along bottom of the basin after 10 hours of simulation. Figure 45 shows the maximum depth of water at 4 downstream cross-sections. It is needed to point out that the maximum water surface for each grid element are not necessarily incurred at the same time. Finally, figures 46 and 47 depict the outflow hydrographs for both the channel system and the flood plain system.

Until now, no existing numerical model can successfully simulate or predict the evolution of the channel-flood plain interface problem. The proposed DHM model uses a simple diffusion approach and interface scheme to simulate the channel-flood plain interface development.

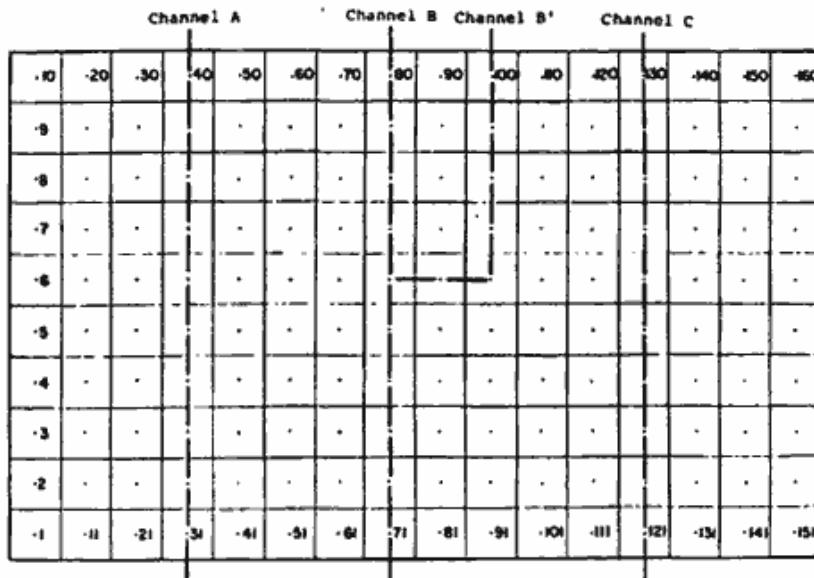


Figure 37.--Diffusion hydrodynamic model discretization of a hypothetical watershed model.

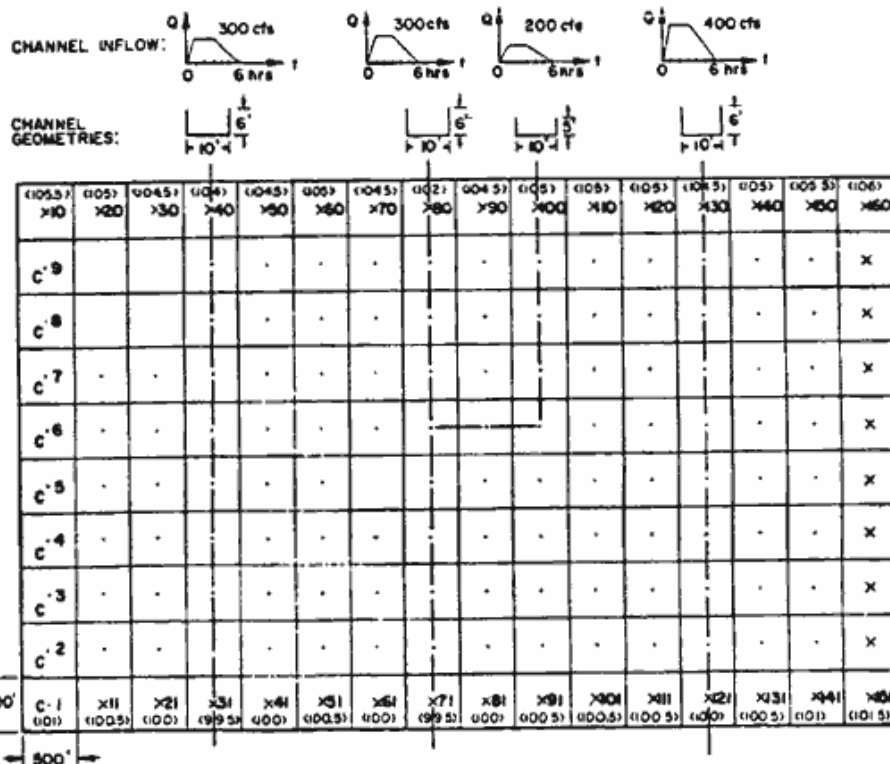


Figure 38. --Inflow and outflow boundary conditions for the hypothetical watershed model

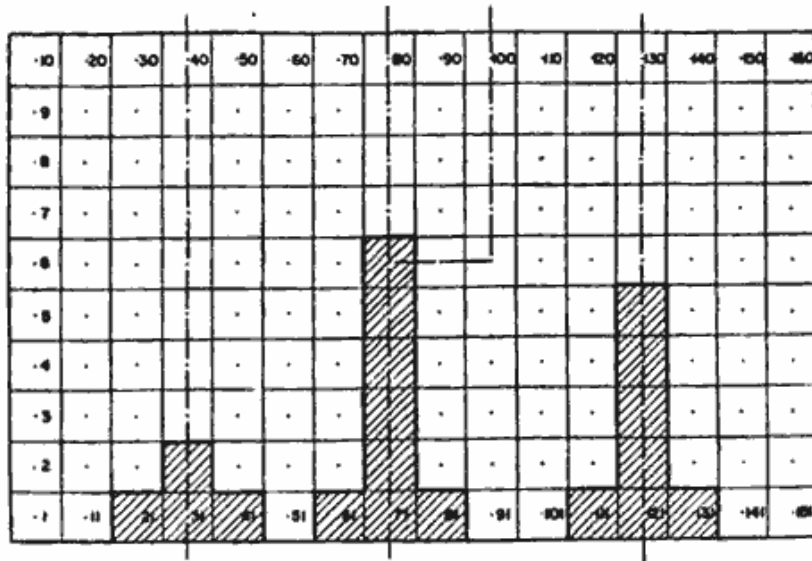


Figure 39.--Diffusion hydrodynamic modeled floodplain at time = 1-hour.

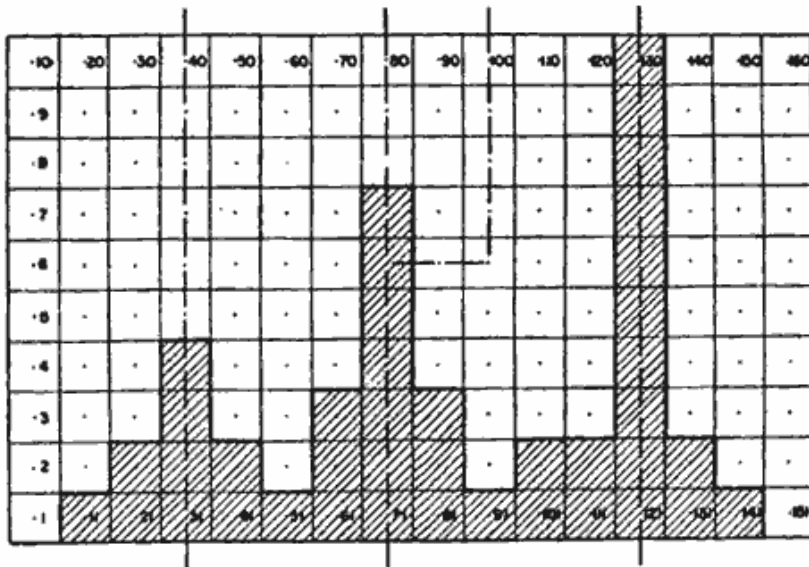


Figure 40.-- Diffusion hydrodynamic modeled floodplain at time = 2-hours.

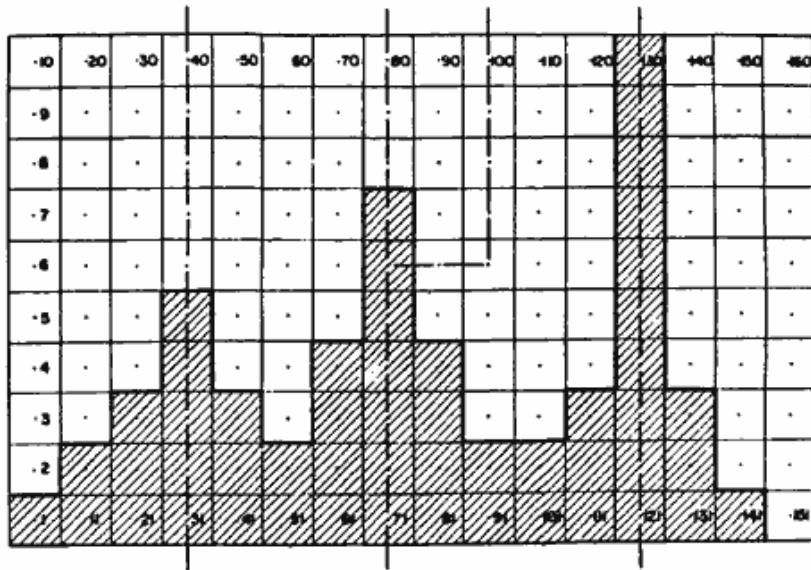


Figure 41.--Diffusion hydrodynamic modeled floodplain at time = 3 hours.

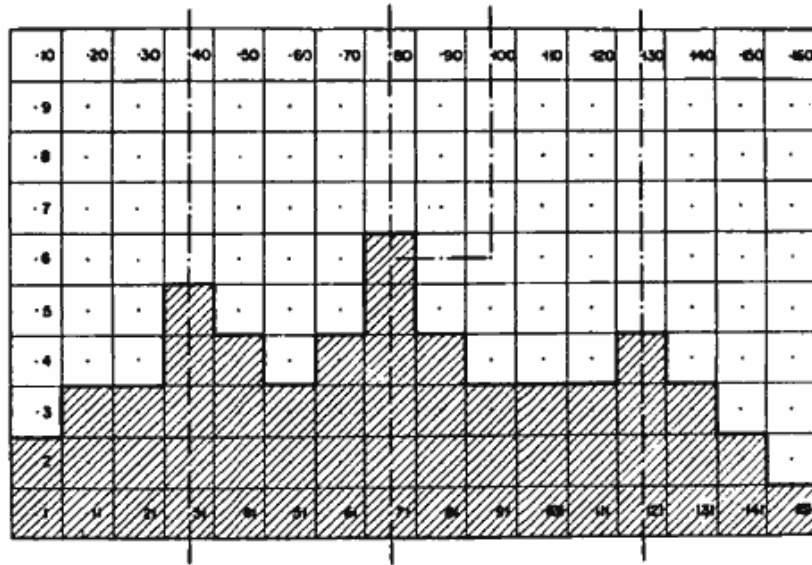


Figure 42.-- Diffusion hydrodynamic modeled floodplain at time = 5 hours.

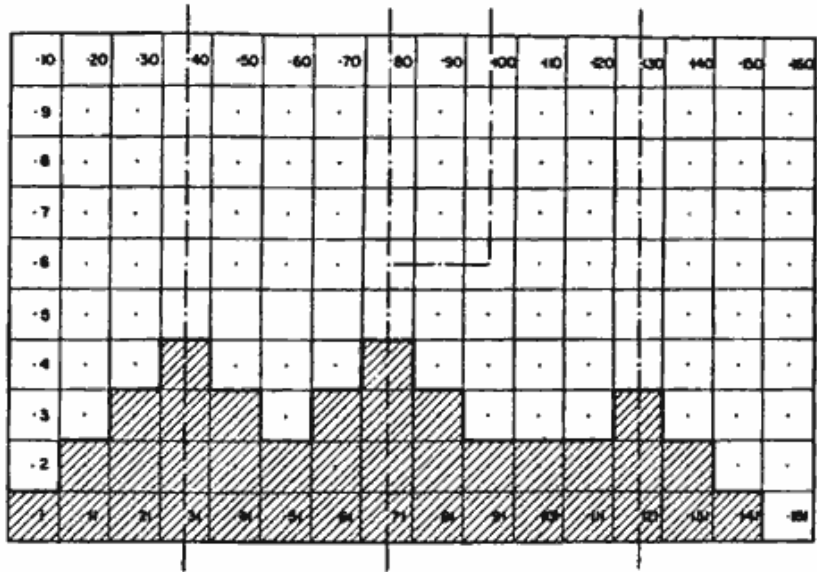


Figure 43.--Diffusion hydrodynamic modeled floodplain at time = 7 hours.

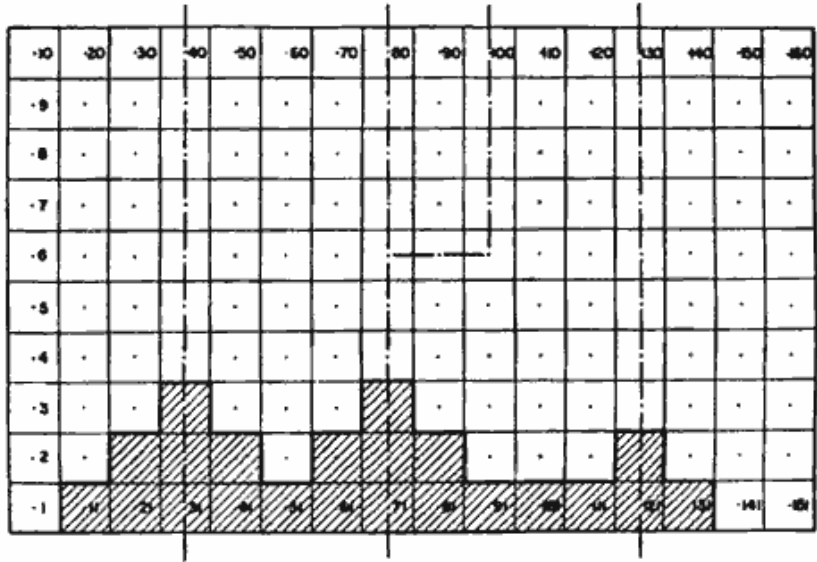
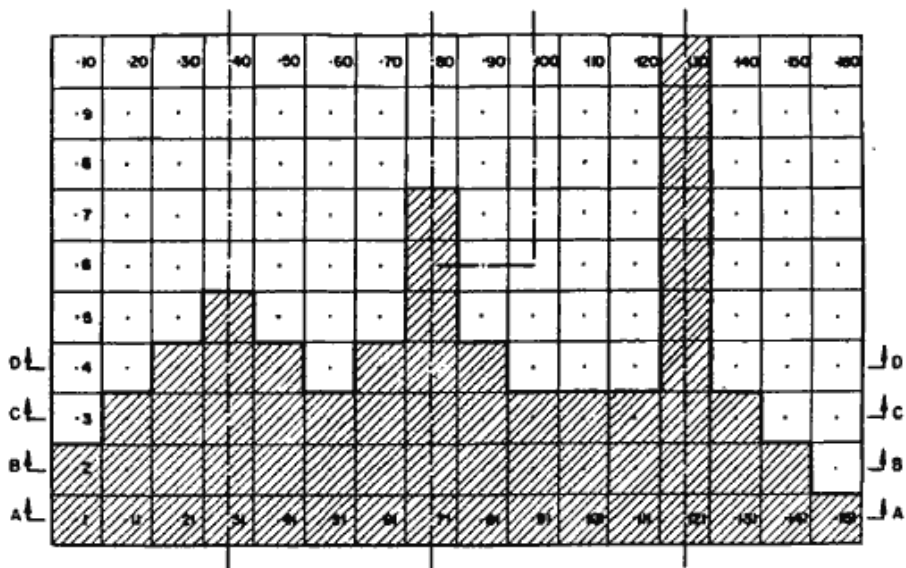
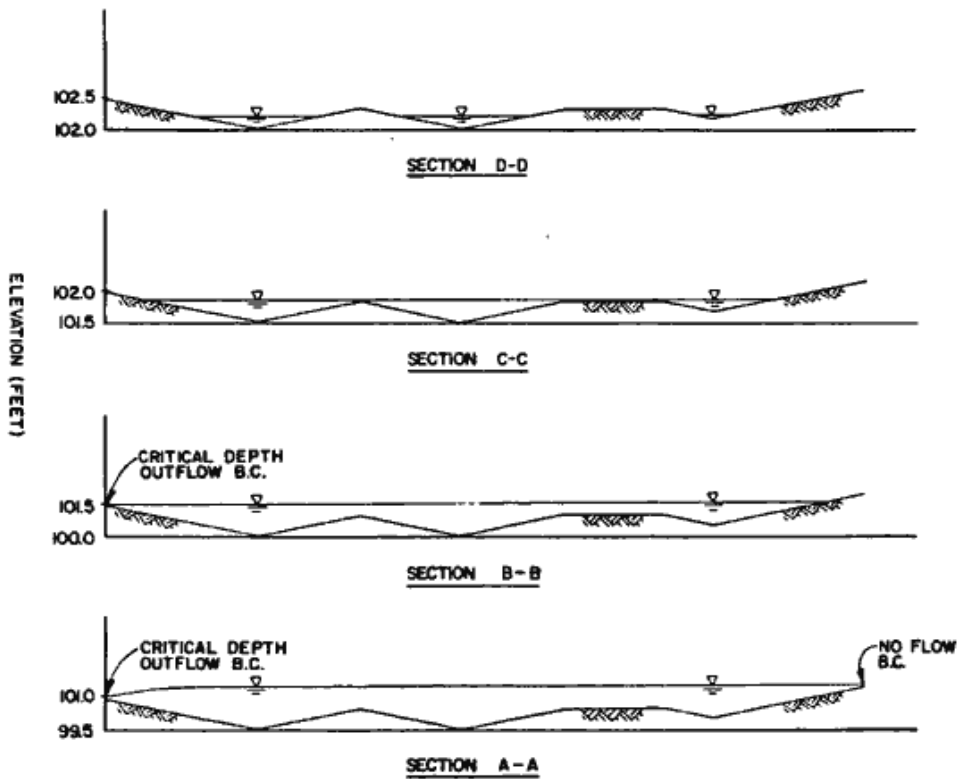


Figure 44.--Diffusion hydrodynamic modeled floodplain at time = 10 hours.



(a) Maximum floodplain



(b) Maximum water profiles

Figure 45.--Maximum water depth at different cross-sections.

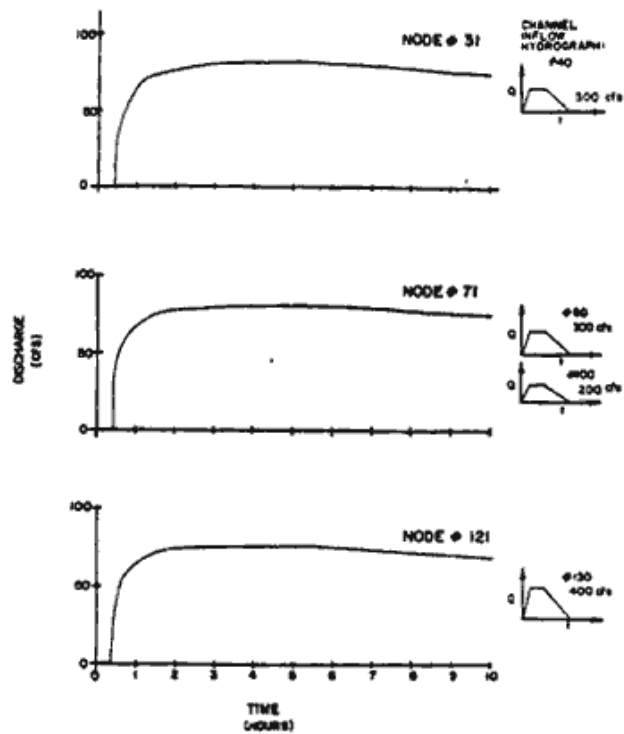


Figure 46.--Bridge flow hydrographs assumed outflow relation: $(Q = 10d)$.

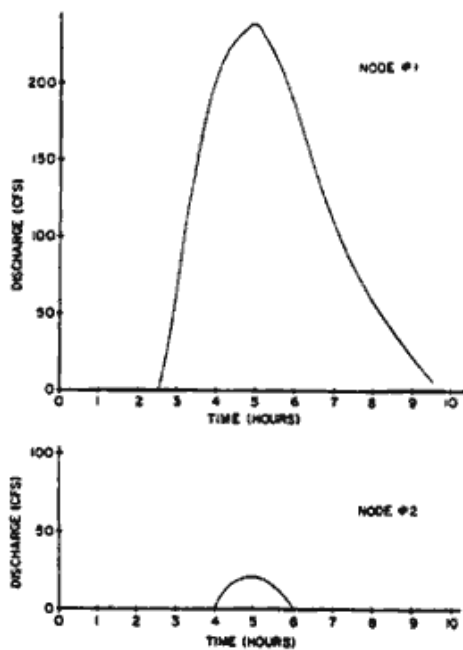


Figure 47.--Critical outflow hydrographs for floodplain.

Introduction

The two-dimensional DHM formulation of equation 32 can be simplified into a kinematic wave approximation of the two-dimensional equations of motion by using the slope of the topographic surface rather than the slope of the water surface is the friction slope in equation 28. That is, flowrates are driven by Manning's equation, while backwater effects, reverse flows, and ponding effects are entirely ignored. As a result, the kinematic wave routing approach cannot be used for flooding situations such as considered in the previous chapter. Flows which escape from the channels cannot be modeled to pond over the surrounding land surface nor move over adverse slopes, nor are backwater effects being modeled in the open channels due to constrictions which, typically, are the source of flood system deficiencies.

In a recent report by Doyle et al. (1983), an examination of approximations of the one-dimensional flow equation is presented. The authors write:

"It has been shown repeatedly in flow-routing applications that the kinematic wave approximation always predicts a steeper wave with less dispersion and attenuation than may actually occur. This can be traced to the approximations made in the development of the kinematic wave equations wherein the momentum equation is reduced to a uniform flow equation of motion that simply states the friction slope is equal to the bed slope. If the pressure term is retained in the momentum equation (diffusion wave method), then this will help to stop the accumulation of error that occurs when the kinematic wave approximation procedure is applied."

Application 8: Kinematic Routing (One-Dimensional)

To demonstrate the kinematic routing feature of the DHM, the one-dimensional channel problem used for the verification of the DHM is now used to compare results between the DHM model and the kinematic routing.

For the steep channel, both techniques show similar results up to 10 miles for the maximum water depth (figure 48) and discharge rates at 5 and 10 miles (figures 49 and 50). For the mild channel, the maximum water surface and discharge rates deviate increasingly as the distance increases downstream from the point of channel inflow.

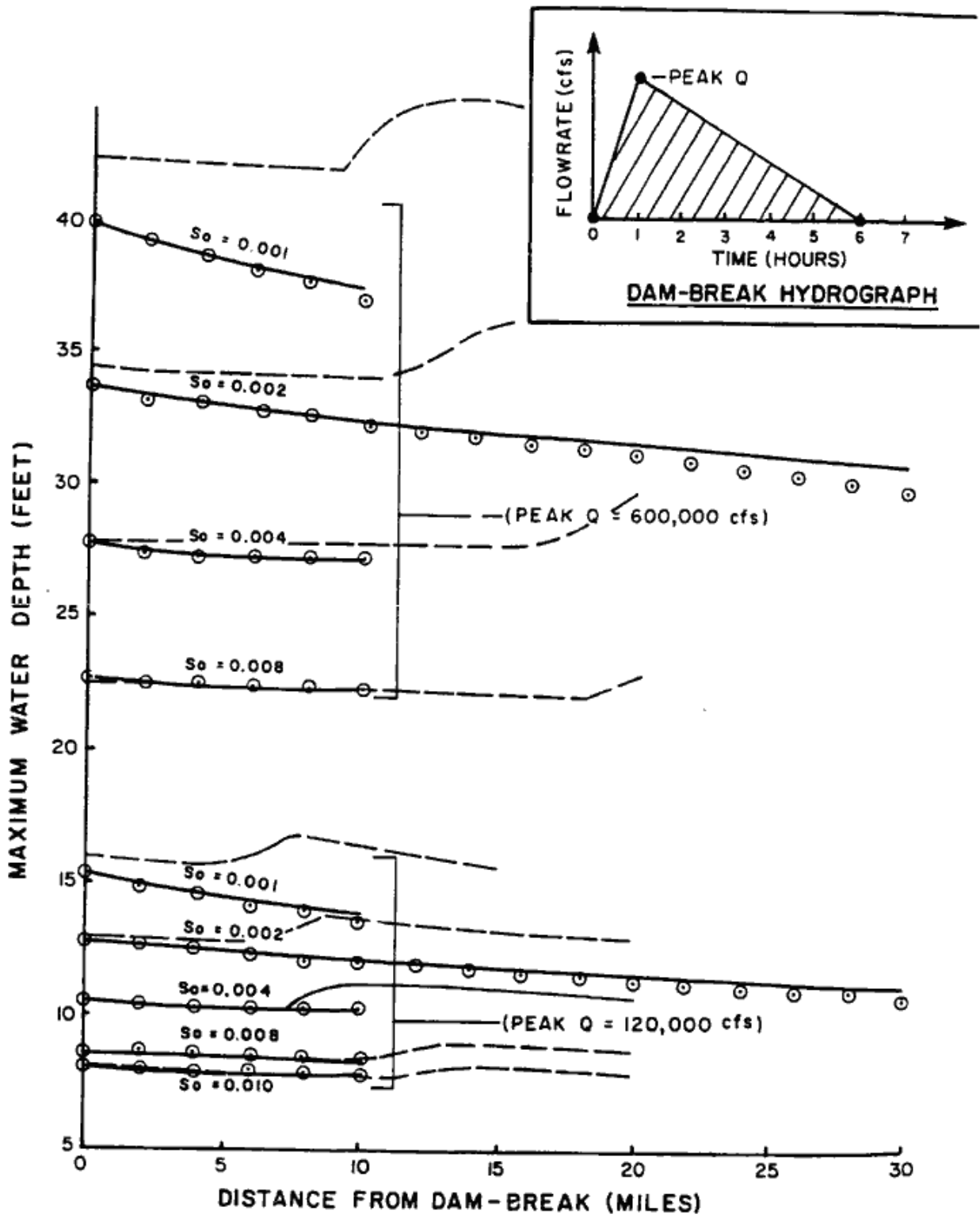


Figure 48-- Diffusion model (\odot), kinematic routing (dashed line) and K-634 model results (solid line) for 1,000-foot width channel, Manning's $n = 0.040$, for various channel slopes, S_0 .

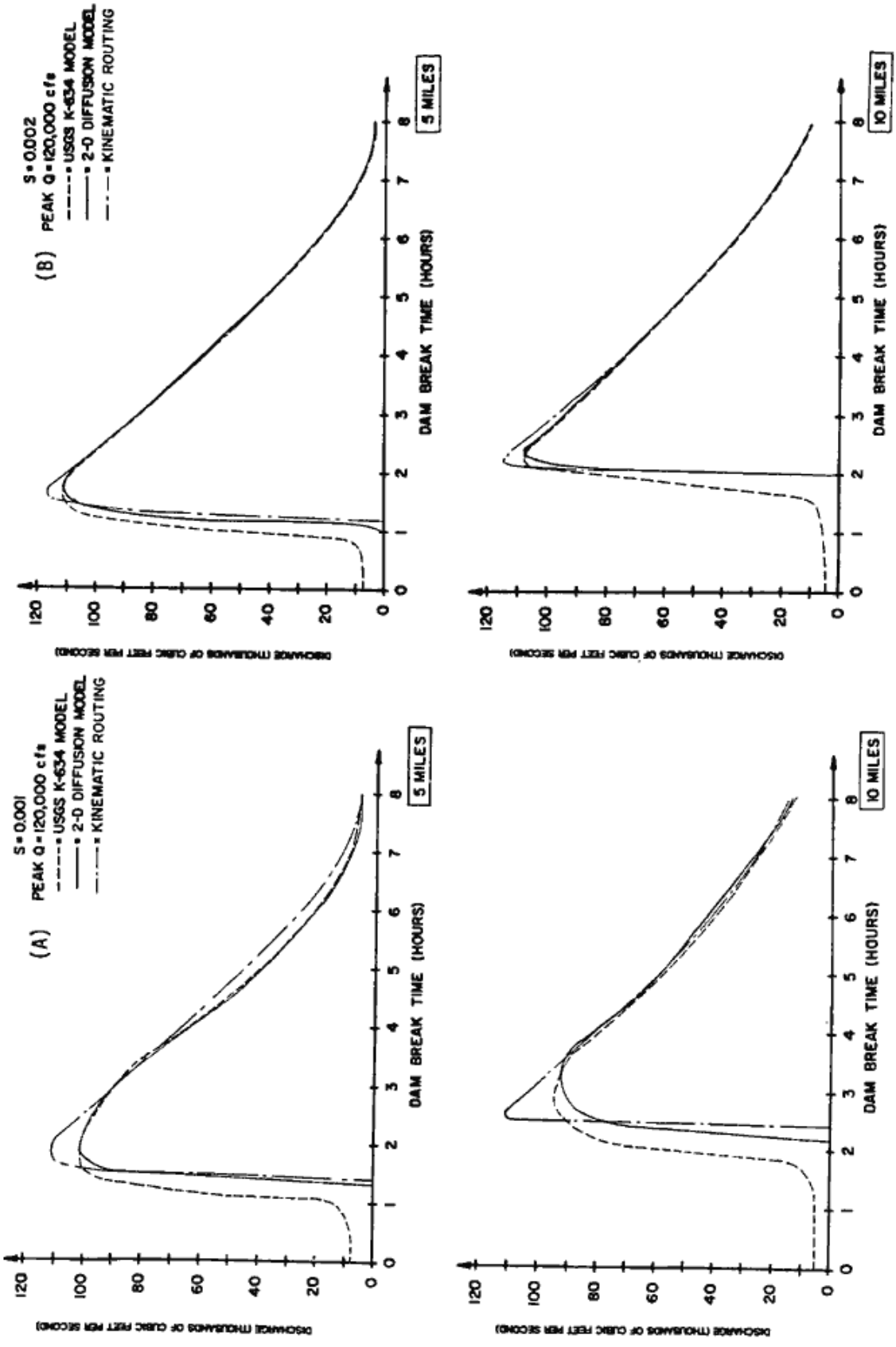


Figure 49.--Comparisons of outflow hydrographs at 5 and 10 miles downstream from the dam-break site.

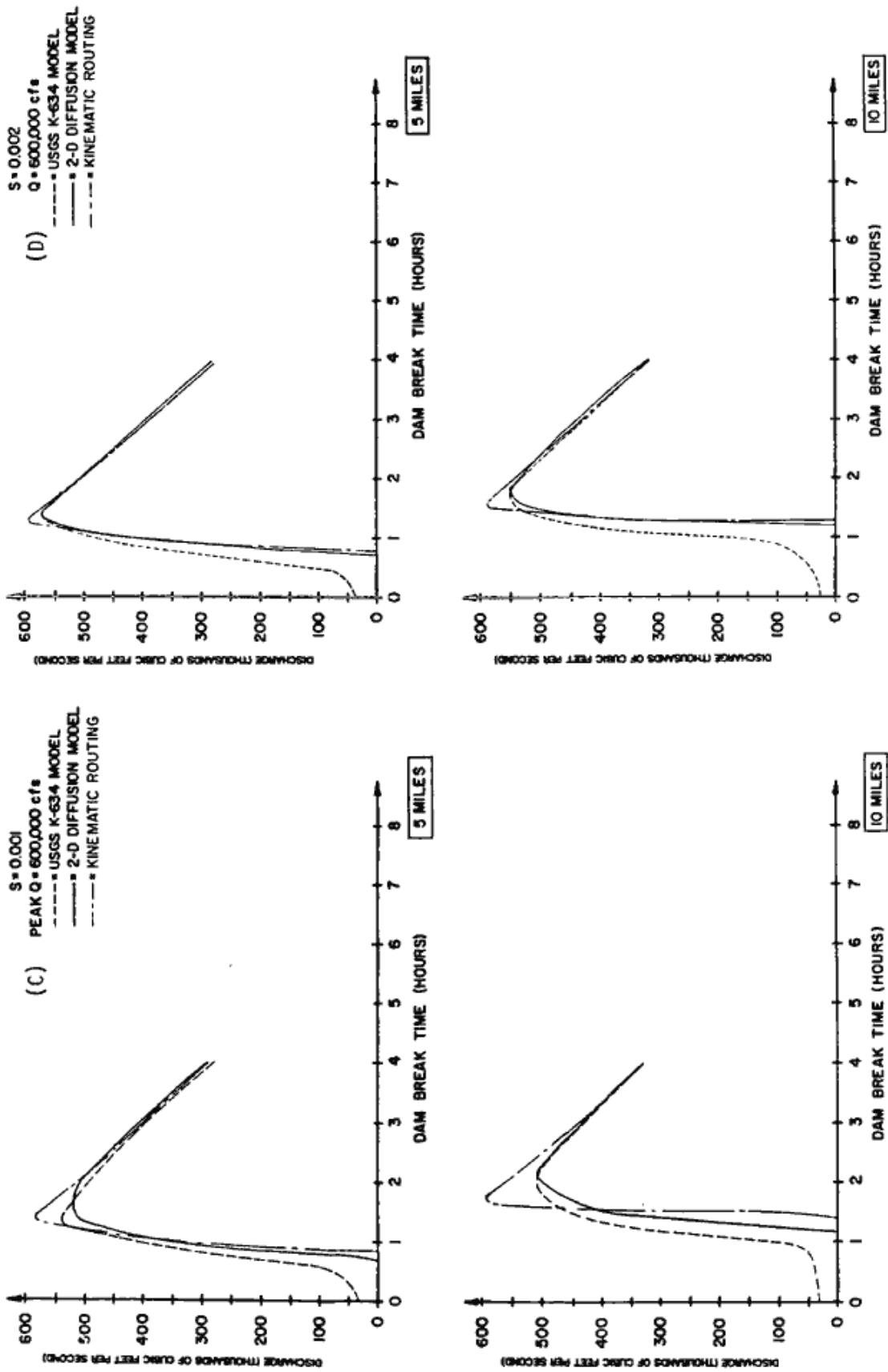


Figure 49.--Comparisons of outflow hydrographs at 5 and 10 miles downstream from the dam-break site.--(Continued)

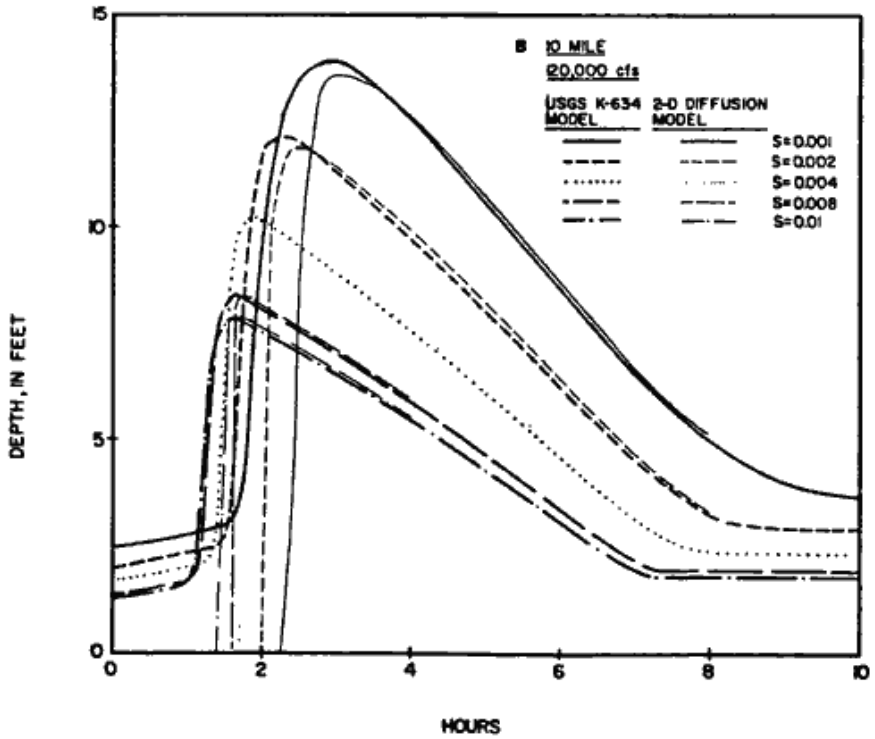
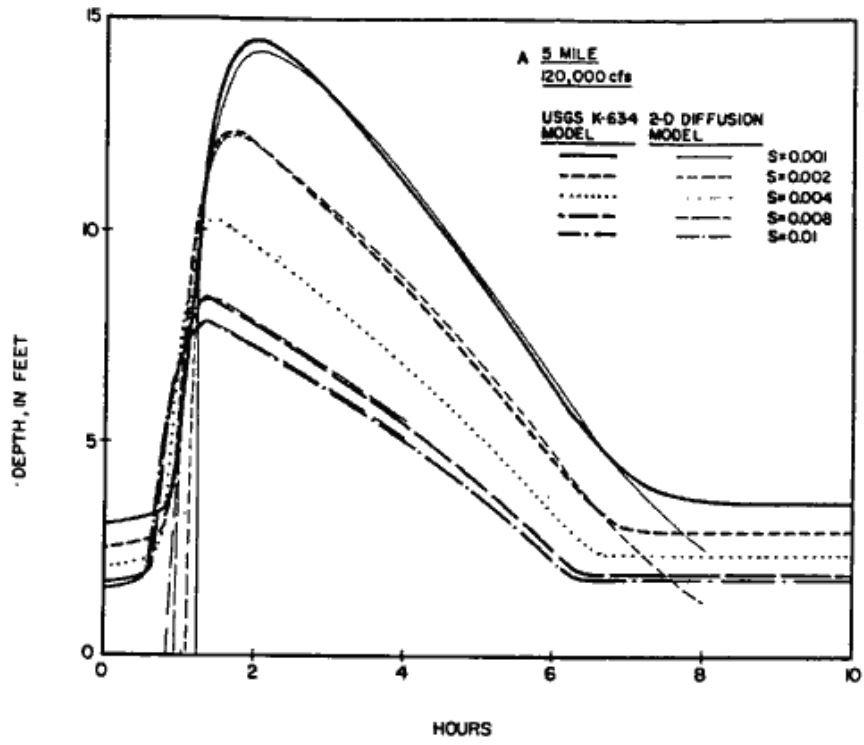


Figure 50.--Comparisons of depths of water at 5 and 10 miles downstream from the dam-break site.

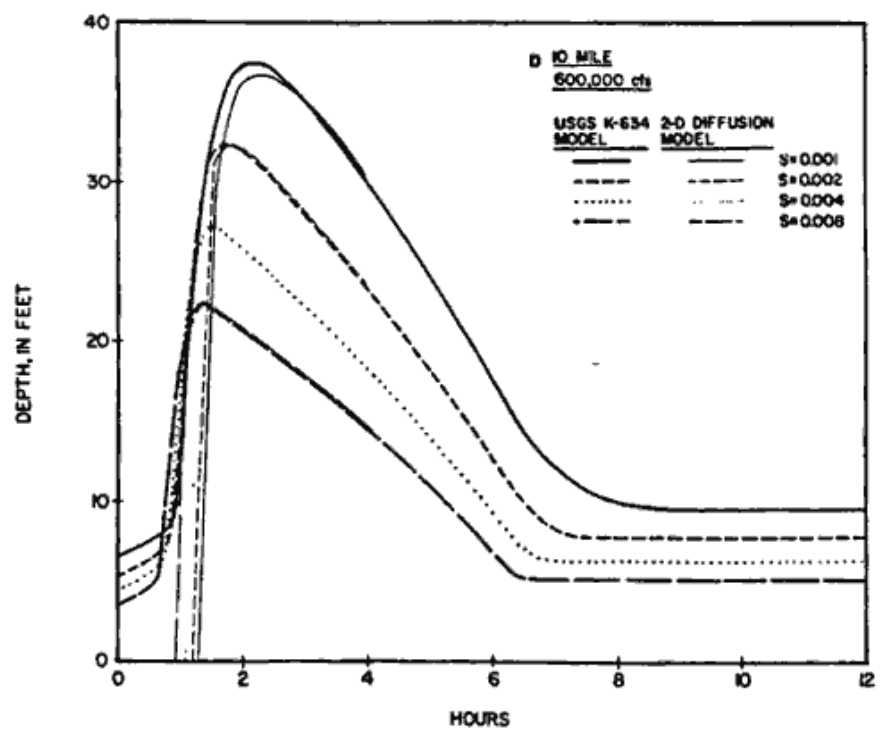
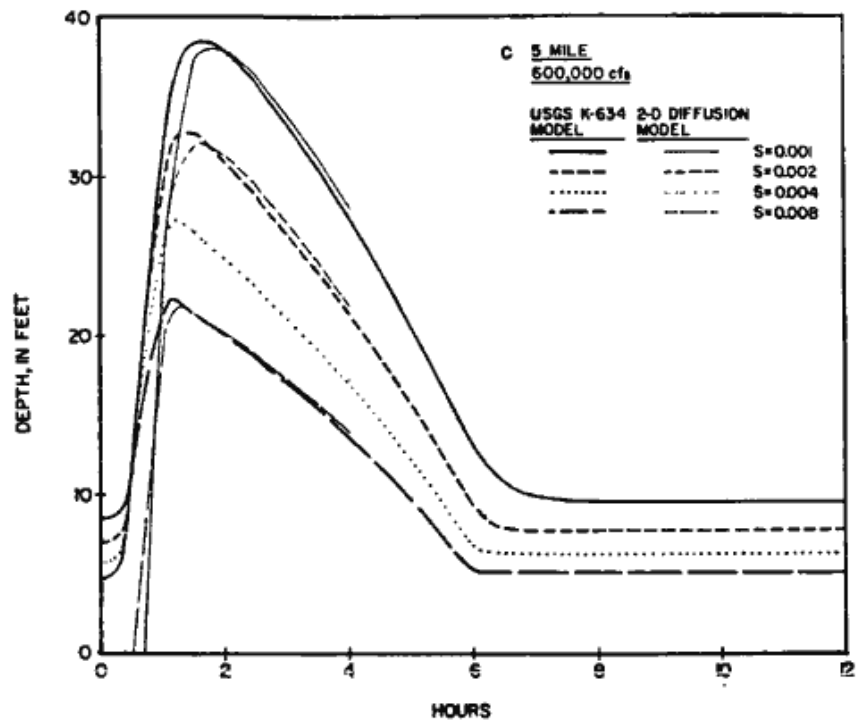


Figure 50.--Comparisons of depths of water at 5 and 10 miles downstream from the dam-break site.--(Continued)

CONCLUSIONS

A diffusion hydrodynamic model is developed for use in civil engineering flood plain studies. The diffusion hydrodynamic model capabilities may provide the practicing engineer with a flood control modeling capability not previously available, and only at the price of a home computer. Although several applications are provided in this report, further research is required for the verification of predicted flooding depths, travel times, and other important hydraulic information.

For one-dimensional unsteady flow channel routing problems where back-water effects are negligible, the comparisons made between the diffusion and kinematic routing approximations have shown significant differences, which may be important to watershed models based on the kinematic routing technique. Because the diffusion (noninertia) routing technique is simple to implement, and includes additional terms for better hydraulic approximation, it is recommended that all kinematic-wave based hydrologic models be modernized by using the diffusion-routing technique. Especially for the backwater effects, ponding and flooding due to the deficiencies of the capacities of the flood control channels can now be modeled by the DHM simultaneously.

The current version of the diffusion hydrodynamic model has been successfully applied to a collection of one- and two-dimensional unsteady flows hydraulic problems including dam-breaks, and flood system deficiency studies. Consequently, the diffusion hydrodynamic model promises to result in a highly useful, accurate, and simple to use (although considerable topographic data may be needed depending on the size of the problem) computer model, which is of immediate use of practicing flood control engineers. Use of the diffusion hydrodynamic model in surface runoff problems will result in a highly

versatile and practical tool which significantly advances the current state-of-the-art in flood control system and flood plain mapping analysis procedures, resulting in more accurate predictions in the needs of the flood control system, and potentially proving a considerable cost saving due to reduction of conservation used to compensate for the lack of proper hydraulic unsteady flow effects approximation.

REFERENCES

- Akan, A. O., and Yen, B. C., 1981, "Diffusion-Wave Flood Routing in Channel Networks," A.S.C.E., Journal of Hyd. Div., Vol. 107, No. HY6, p.719-732.
- Basco, D. R., 1978, "Introduction to Numerical Method - Part I and II," Verification of Mathematical and Physical Models in Hydraulic Engineering, A.S.C.E., Hyd., Special Conf., University of Maryland, College Park, Maryland, p. 280-302.
- Chen, C., 1980, "Laboratory Verification of a Dam-Break Flood Model," A.S.C.E., Journal of Hyd. Div., Vol. 106, No. HY4, p.535-556.
- Chen, C., and Armbruster, J. T., 1980, "Dam-Break Wave Model: Formulation and Verification," A.S.C.E., Journal of Hyd. Div., Vol. 106, No. HY5, p.747-767.
- Doyle, W. H., Shearman, J. O., Stiltner, G. J., and Krug, W. R., 1983, "A Digital Model for Streamflow Routing by Convolution Method," Wat. Res. Investigations Report 83-4160.
- Fread, D. L., 1977, "The Development and Testing of a Dam-Break Flood Forecasting Model," Dam-Break Flood routing Model Workshop, Hydrology Committee, U. S. Wat. Res. Council, Bethesda, Maryland, p.164-197.
- Henderson, F. M., 1963, "Flood Waves in Prismatic Channels," A.S.C.E., Journal of Hyd. Div., Vol. 89, No. HY4, p.39-67.
- Henderson, F. M., 1966, "Open Channel Flow," MacMillan Publishing Co., Inc., 522 p.

- Hromadka II, T. V. and Lai, C., 1985, "Solving the Two-Dimensional Diffusion Flow Model," Proceedings: ASCE Hydraulics Division Specialty Conference, Orlando, Florida.
- Hromadka II, T. V. and Nestlinger, A. J., 1985, "Using a Two-Dimensional Diffusional Dam-Break Model in Engineering Planning," Proceedings: ASCE Workshop on Urban Hydrology and Stormwater Management, Los Angeles County Flood Control District Office, Los Angeles, California.
- Hromadka II, T. V., Guymon, G. L., and Pardoen, G., 1981, "Nodal Domain Integration Model of Unsaturated Two-Dimensional Soil-Water Flow: Development," Water Resources Research, Vol. 17, pp. 1425-1430.
- Hromadka II, T. V., Berenbrock, C. E., Freckleton, J. R., and Guymon, G. L., 1985, "A Two-Dimensional Diffusion Dam-Break Model," Advances in Water Resources, Vol. 8, p.7-14.
- Hunt, T., 1982, "Asymptotic Solution for Dam-Break Problem," A.S.C.E., Journal of Hyd. Div., Vol. 108, No. HY1, p.115-126.
- Katopodes, Nikolaos and Strelkoff, Theodor, 1978, "Computing Two-Dimensional Dam-Break Flood Waves," A.S.C.E., Journal of Hyd. Div., Vol. 104, No. HY 9, p.1269-1288.
- Lai, C., 1977, "Computer Simulation of Two-Dimensional Unsteady Flows in Estuaries and Embayments by the Method of Characteristics-- Basic Theory and the Formulation of the Numerical Method," U. S. Geological Survey, Water Resources Investigation 77-85, 72p.
- Land, L. F., 1980a, "Mathematical Simulations of the Toccoa Falls, Georgia, Dam-Break Flood," Wat. Resources Bulletin, Vol. 16, No. 6, p.1041-1048.

- Land, L. F., 1980b, "Evaluation of Selected Dam-Break Flood-Wave Models by using Field Data," U.S.G.S. Wat. Res. Investigations 80-44, 54p.
- "Metropolitan Water District of Southern California," Dam-Break Inundation Study for Orange County Reservoir, 1973.
- McCuen, R. H., 1982, "A Guide to Hydrologic Analysis Using S.C.S. Methods," Prentice-Hall, 160p.
- Miller, W. A., and Cunge, J. A., 1975, "Simplified Equations of Unsteady Flow," Chapter 5 of Unsteady Flow in Open Channels, Water Resources Publications, Fort Collins, Colorado, Vol. 1, p.183-257.
- Morris, E. M., and Woolhiser, D. A., 1980, "Unsteady One-Dimensional Flow Over a Plane: Partial Equilibrium and Recession Hydrographs," Water Resources Research, AGU, Vol. 16, No. 2, p.356-360.
- Ponce, V. M., 1982, "Nature of Wave Attenuation in Open Channel Flow," A.S.C.E., Journal of Hyd. Div., Vol. 108, No. HY2, p.257-262.
- Ponce, V. M., Li, R. M., and Simons, D. B., 1978, "Applicability of Kinematic and Diffusion Models, in Verification of Mathematical and Physical Models in Hydraulic Engineering, A.S.C.E., Hyd. Div., Special Conf., University of Maryland, College Park, Maryland, p.605-613.
- Ponce, V. M., and Tsivoglou, A. J., 1981, "Modeling Gradual Dam Breaches," A.S.C.E., Journal of Hyd. Div., Vol. 107, No. HY7, p.829-838.
- Rajar, R., 1978, "Mathematical Simulation of Dam-Break Flow," A.S.C.E., Journal of Hyd. Div., Vol. 104, No. HY7, p.1011-1026.

- Sakkas, J. G., and Strelkoff, Theodor, 1973, "Dam-Break Flood in a Prismatic Dry Channel," A.S.C.E., Journal of Hyd. Div., Vol. 99, No. HY12, p.2195-2216.
- U. S. Army Corps of Engineers, 1981, "Two-Dimensional Flow Modeling Seminar," Hydrologic Engineering Center, Davis, California.
- Xanthopoulos, Th. and Koutitas, Ch., 1976, "Numerical Simulation of a Two-Dimensional Flood Wave Propagation Due to Dam Failure," A.S.C.E., Journal of Hydraulic Research, Vol. 14, No. HY4, p.321-331.

ATTACHMENT A
COMPUTER PROGRAM

Introduction

Figures A.1 and A.2 depict the simple flow chart for the DHM Model. Because the DHM computer code is relatively small, it can be handled by most current home computer that supports a FORTRAN compiler. Computer listings are included herein for reader's convenience.

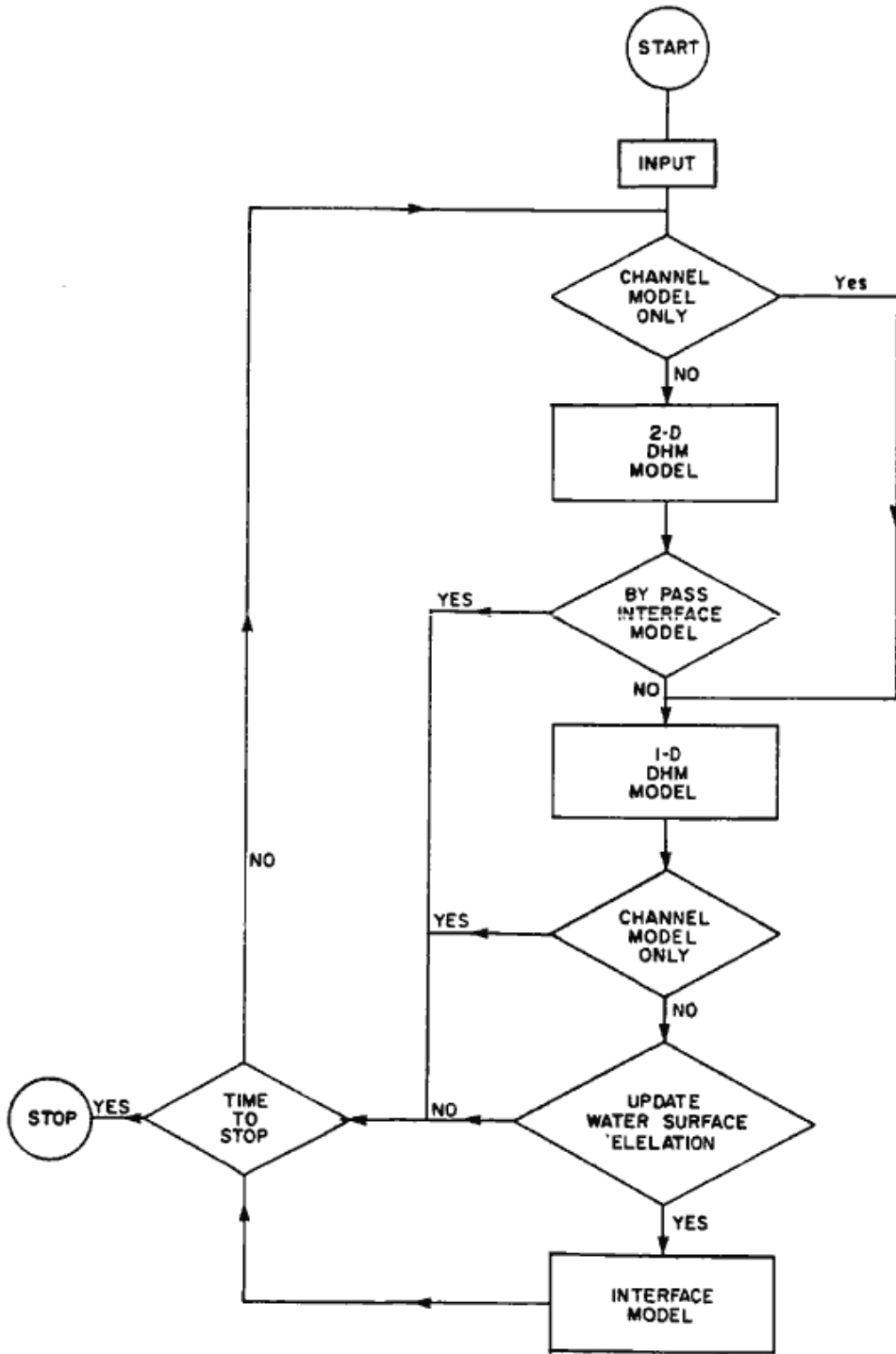


Figure A.1.--Flow chart for diffusion hydrodynamic model.

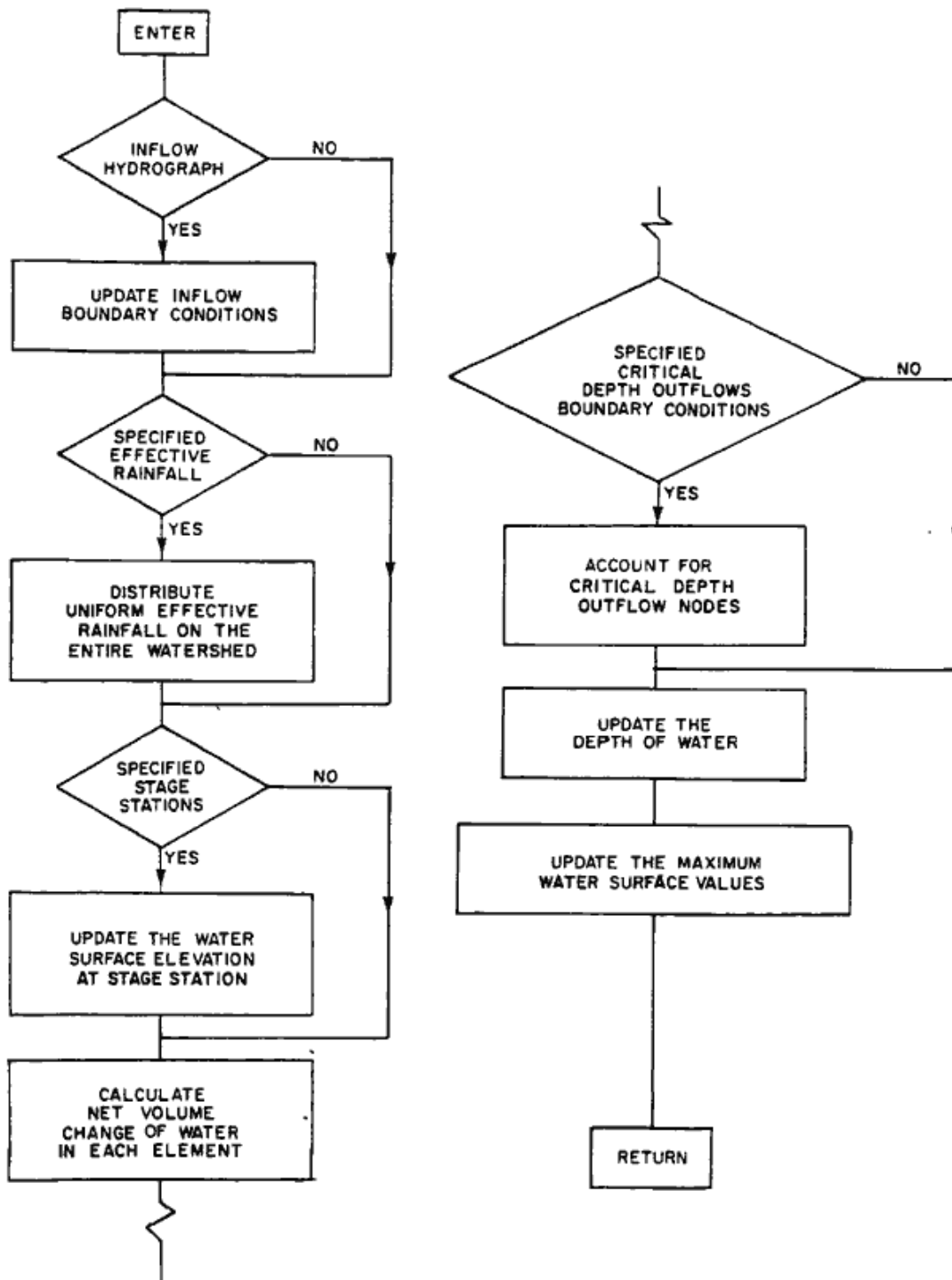


Figure A.2.- Flow chart for channel and floodplain submodel.

Input File Descriptions

The DHM model calls for the following data entries:

<u>Line</u>	<u>Variables</u>
1	DTMIN,DTMAX,DTI,DTD,SIMUL,ITER,TOUT,KODE, KMODEL
2	NNOD, NODC, SIDE, TOL, DTOL, DTOLP
3	FP(1,J), J = 1,7
.	.
.	.
.	.
NNOD+2	FP(NNOD,J), J = 1,7
NNOD+3	NERI
NNOD+4	(R(I,J), J = 1,2), I = 1,NERI
NNOD+5	NFPI, NPFPI
NNOD+6	KINP(1), (HP(1,J,1), HP(1,J,2)), J = 1, NPFPI)
.	.
.	.
.	.
NNOD+5+NFPI	KINP(NFPI), (HP(NFPI,J,1), HP(NFPI,J,2)), J = 1,NPFPI)
NNOD+NFPI+6	NDC
NNOD+NFPI+7	NODDC(I),I=1,NDC
NNOD+NFPI+8	NFLUX,NFOUT
NNOD+NFPI+9	NODFX(I),I = 1, NFLUX
NNOD+NFPI+10	KK, (FC(KK,J), J = 1,5)
.	.
.	.
.	.
NNOD+NFPI+NODC+9	KK,(FC(KK,J), J =1,5)
NNOD+NFPI+NODC+10	NCHI,NPCHI,NCHO,NPCHO,NSTA,NPSTA
NNOD+NFPI+NODC+11	KIN(1),((H(1,J,1),H(1,J,2)),J =1,NPCHI)
.	.
.	.
.	.
NNOD+NFPI+NODC+NCHI+10	KIN(NCHI),((H(NCHI,J,1),H(NCHI,J,2)),J =1,NPCHI)

```

NNOD+NFPI+NODC+NCHI+11  KOUT(1),(HOUT(1,J,1),HOUT(1,J,2),
                          HOUT(1,J,3), J = 1, NPCHO)
.
.
.
NNOD+NFPI+NODC+NCHI+   KOUT(NCHO),(HOUT(NCHO,J,1),HOUT(NCHO,J,2),
NCHO+10                 HOUT(NCHO,J,3), J = 1, NPCHO)
NNOD+NFPI+NODC+NCHI+   NOSTA(1),(STA(1,J,1),STA(1,J,2), J = 1,
NCHO+11                 NPSTA)
.
.
.
NNOD+NFPI+NODC+NCHI+   NOSTA(NSTA),(STA(NSTA,J,1),STA(NSTA,J,2),
NCHO+10+NSTA           J = 1, NPSTA)

```

where

```

DTMIN  is the minimum allowable timestep in second, (R)
DTMAX  is the maximum allowable timestep in second, (R)
DTI    is the increment of timestep in second, (R)
DTD    is the decrement of timestep in second, (R)
SIMUL  is the total simulation time in hour, (R)
ITER   is the update interval (timestep) that interface model
        is called, (I)
TOUT   is the output period in hour, (R)
KODE   { 0 , suppress the efflux velocities      (I)
        { 1 , output the efflux velocities
KMODEL { 1 , kinematic routing technique        (I)
        { otherwise , diffusion hydrodynamic model
NNOD   is the total number of nodal points for flood plain, (I)
NODC   is the number of channel element, (I)
SIDE   is the length of the uniform grid side in feet, (R)
TOL    is the specified surface detention in feet, (R)
DTOL   is the minimum change of water depth in feet for each
        timestep, (R)

```

DTOLP is defined as

$$DTOLP = \frac{\text{change of water depth}}{\text{pervious water depth}} \times 100\% \quad (R)$$

FP(I,1) is the northern nodal point of node I, (R)

FP(I,2) is the eastern nodal point of node I, (R)

FP(I,3) is the southern nodal point of node I, (R)

FP(I,4) is the western nodal point of node I, (R)

FP(I,5) is the averaged Manning's roughness coefficient for node I, (R)

FP(I,6) is the averaged ground surface elevation for node I in feet, (R)

FP(I,7) is the initial water depth for node I in feet, (R)

NERI is the number of data pairs for uniform effective rainfall rate, (I)

R(I,1) is the time (hour) corresponding to the effective rainfall rate, (R)

R(I,2) is the effective rainfall intensity (in/hr) ordinate for effective rainfall rate, (R)

NFP1 is the number of input nodal points for the flood plain, (I)

NFPPI is the number pair of inflow hydrograph rate entires, (I)

KINP(I) is the array that stores the inflow boundary condition nodal points (I)

HP(I,J,1) is the time (hour) corresponding to the inflow hydrograph, (R)

HP(I,J,2) is the inflow rate (cfs) ordinate for the inflow hydrograph, (R)

NDC is the number of critical-depth outflow nodal points, (I)

NODDC(I) is the array which stores the critical-depth outflow nodal points, (I)

NFLUX is the number of nodal points where outflow hydrograph are being printed, (I)

TFOUT is the interval for outflow hydrograph (in timesteps), (R)

NODFX(I) is the array which stores the nodal points where outflow hydrographs are being printed, (I)

KK is the nodal point for channel element, (I)

FC(KK,1) is the array which stores the averaged Manning's coefficient of the channel elements, (R)

FC(KK,2) is the array which stores the width of the channel elements, (R)

FC(KK,3) is the array which stores the depth of the channel elements, (R)

FC(KK,4) is the array which stores the bottom elevation of the channel elements, (R)

FC(KK,5) is the array which stores the initial water depth of the channel elements, (R)

NCHI is the number of the inflow boundary conditions for the channel system, (I)

NPCHI is the number of pairs of inflow hydrograph entries of the channel system, (I)

NCHO is the number of the outflow boundary conditions for the channel system, (I)

NPCHO is the number of sets of outflow hydrograph entires of the channel system, (I)

NSTA is the number of the stage station nodal points, (I)

NPSTA is the number of pair of stage curve entries, (I)

KIN(I) is the array which stores the nodes of inflow hydrograph of the channel system, (I)

H(I,J,1) is the time (hour) corresponding to the inflow hydrograph for the channel system, (R)

H(I,J,2) is the inflow rate (cfs) ordinate for the inflow hydrograph for the channel system, (R)

KOUT(I) is the array which stores the nodes of outflow hydrograph of the channel system, (I)

HOUT(I,J,1) is the array which stores the depth that a specified stage--discharge curve is used, (R)

HOUT(I,J,2) is the array which stores the coefficient of a stage--discharge curve, (R)

HOUT(I,J,3) is the array which stores the exponent of a stage--discharge curve, (R)

NOSTA(I) is the array which stores the node of stage curve for the channel system, (I)

STA(I,J,1) is the array which stores the time (hour) corresponding to the time-stage curve, (R)

STA(I,J,2) is the array which stores the water surface elevation (feet) of the time-stage curve, (R)

Note:

1. If any value of NERI, NFPI, NDC, NFLUX and NODC is equal to zero, then the values for the corresponding array need not be entered in the input file.
For an example, if NERI = 0 then R(I,J) needs not be included in the input file.
2. If NODC equals to zero, then entire channel element information need not be entered in the input file.
3. R denotes real number and I denotes integer number.

ATTACHMENT B
USER'S INSTRUCTIONS

Introduction

The DHM model has the capabilities to perform: (1) one-dimensional analysis, (2) two-dimensional analysis and (3) one- and two-dimensional interface analysis.

One-Dimensional Analysis

For one-dimensional analysis, a zero value should be entered for variable ITER. The entries for array FP(I,J) should reflect the one-dimensional representation as shown in figure B.1.

Two-Dimensional Analysis

For two-dimensional analysis, zero values should be assigned to variables ITER and NODC. The entire data entries for the channel system can be neglected in the input file.

One- and Two-Dimensional Interface Model

When variables ITER and NODC are not equal to zero, the interface model is called at each update interval to calculate the new water surface

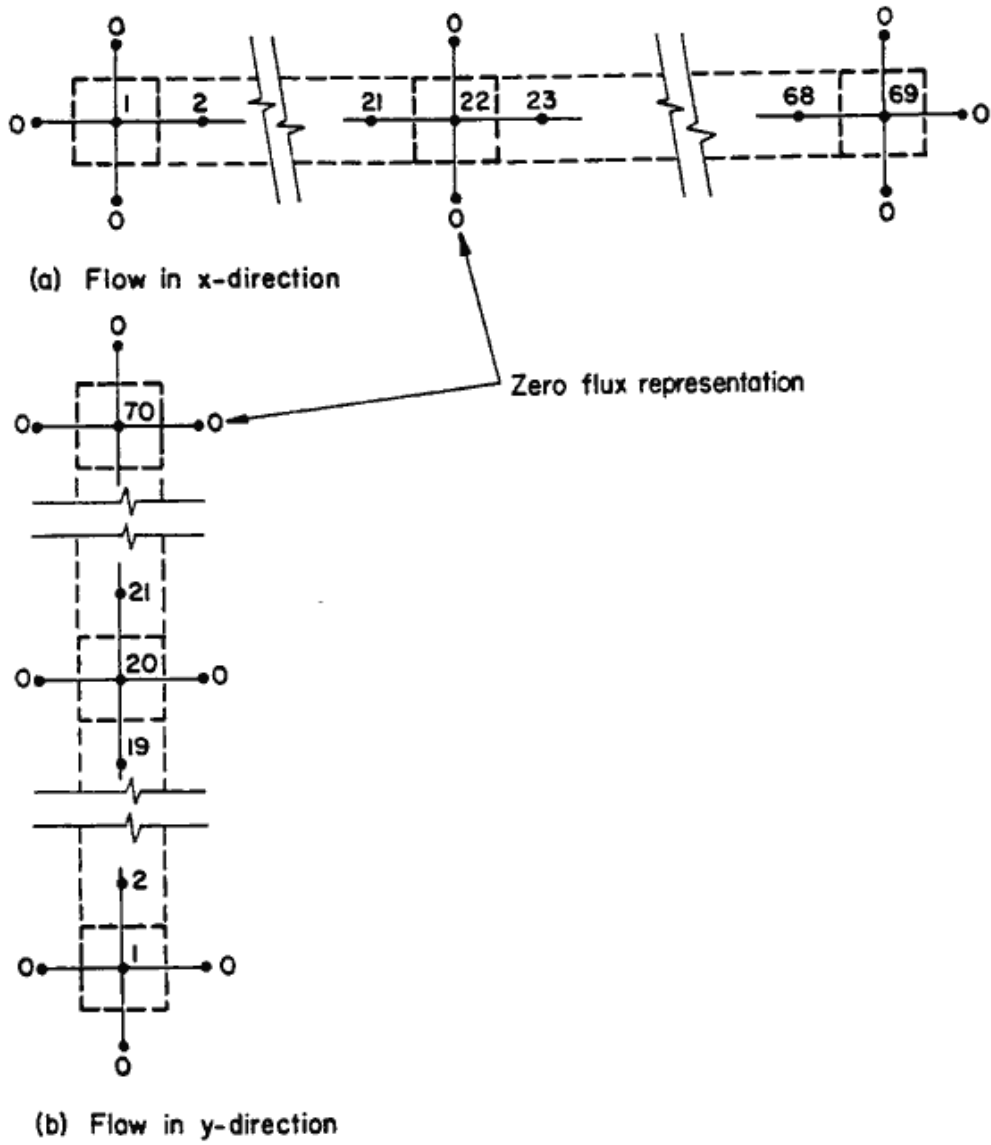


Figure B.1.-- One-dimensional grid element.

elevations for both the grid and channel elements. A negative sign should be included in the Manning's roughness coefficient for a grid element where a channel element passing through a grid element.

Inflow Boundary Conditions

Inflow boundary conditions are described by a linear time-inflow rate hydrograph for each specified inflow grid or channel element.

Outflow Boundary Conditions

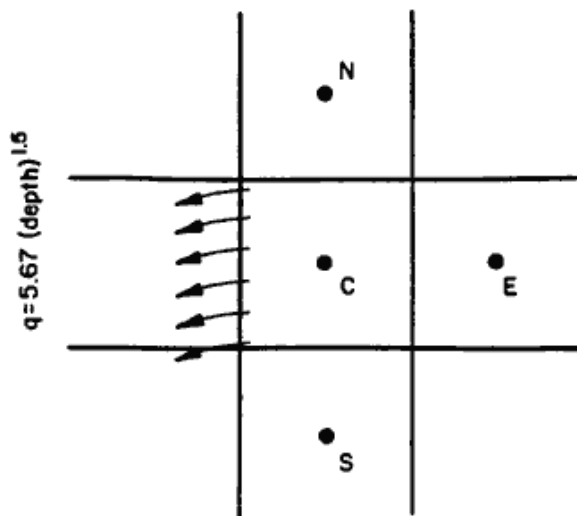
Outflow boundary conditions for channel element (figure B.2.a) are:

- (1) unidirectional critical depth assumption, i.e., discharge per unit length is $q = 5.67 (\text{depth})^{1.5}$, and
- (2) the boundary conditions where no water flows across element boundary (figure B.3).

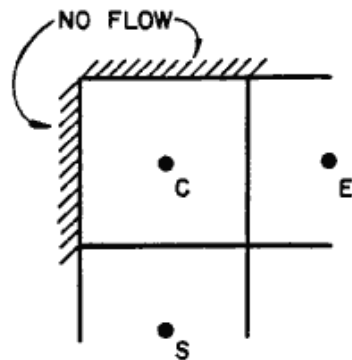
Outflow boundary condition for channel system is described by the following equation (figure (B.2.b) as:

$$Q = \begin{cases} 0 & \text{If } 0 \leq \text{depth of water} \leq \text{specified surface} \\ & \text{detention} \\ \alpha_1 (\text{depth})^{\beta_1} & \text{If specified surface detention} < \text{depth of water} \leq d_1 \\ \alpha_2 (\text{depth})^{\beta_2} & \text{If } d_1 < \text{depth of water} \leq d_2 \\ \vdots & \vdots \\ \vdots & \vdots \end{cases}$$

where d_1, d_2, \dots , are the pre-determined depth values from a stage-discharge station and up to 10 sets of data can be used to represent the stage-discharge relationship for each station.

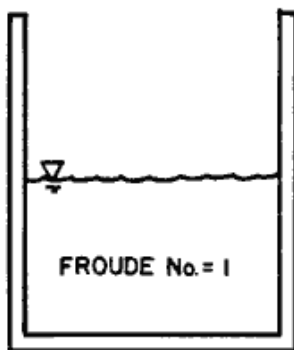


• UNIDIRECTIONAL CRITICAL DEPTH

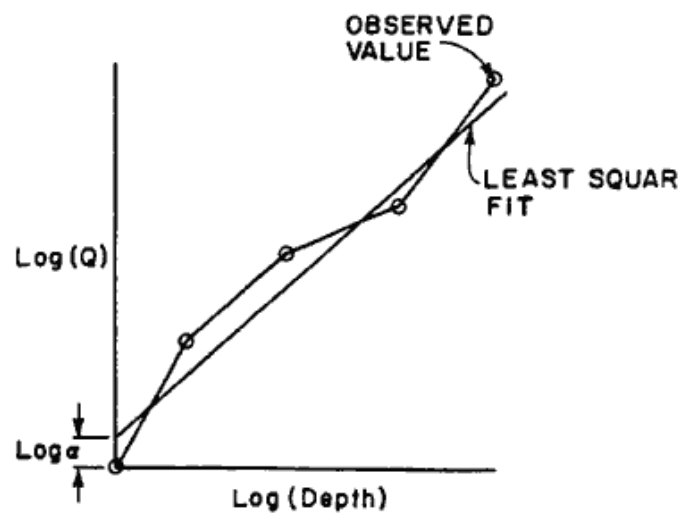


• NO FLOW

a. GRID ELEMENT MODEL



• CRITICAL DEPTH APPROXIMATION



• STAGE DISCHARGE RELATIONSHIP
($Q = a (\text{depth})^\beta$)

b. CHANNEL ELEMENTS

Figure B.2.-- Diffusion hydrodynamic boundary condition models.

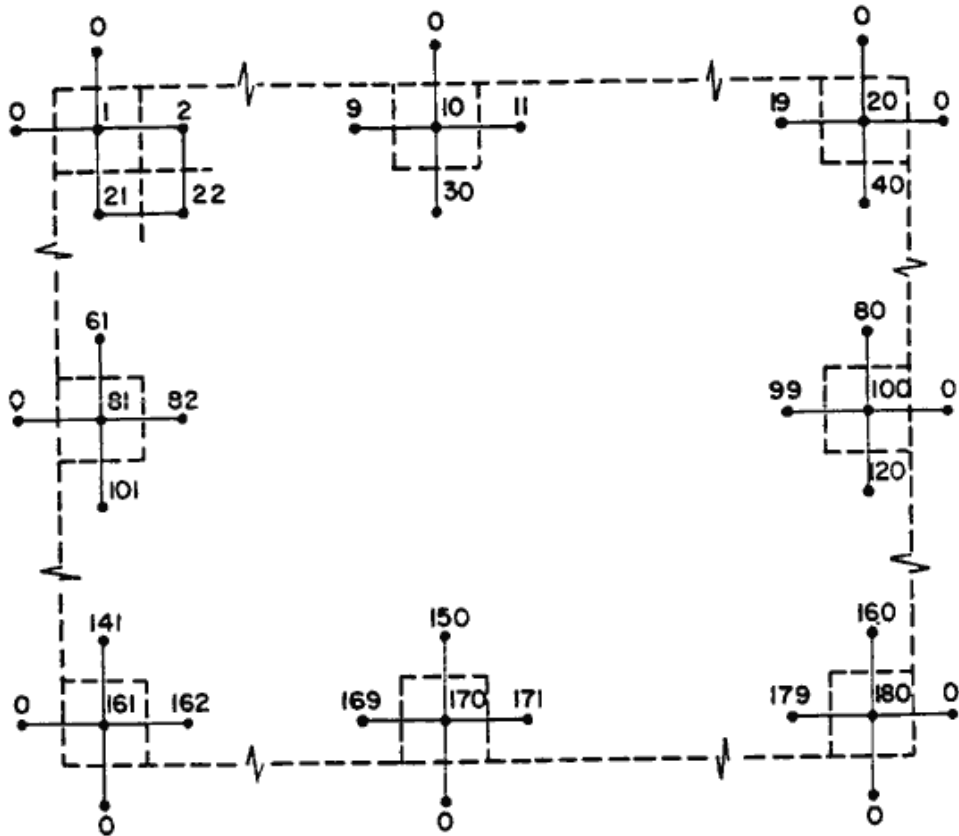


Figure B.3. -- No flux boundary nodes.

Variable Time Step

Variable time step dramatically reduces the computational time.
The algorithm of the variable time step is depicted in figure B.4.

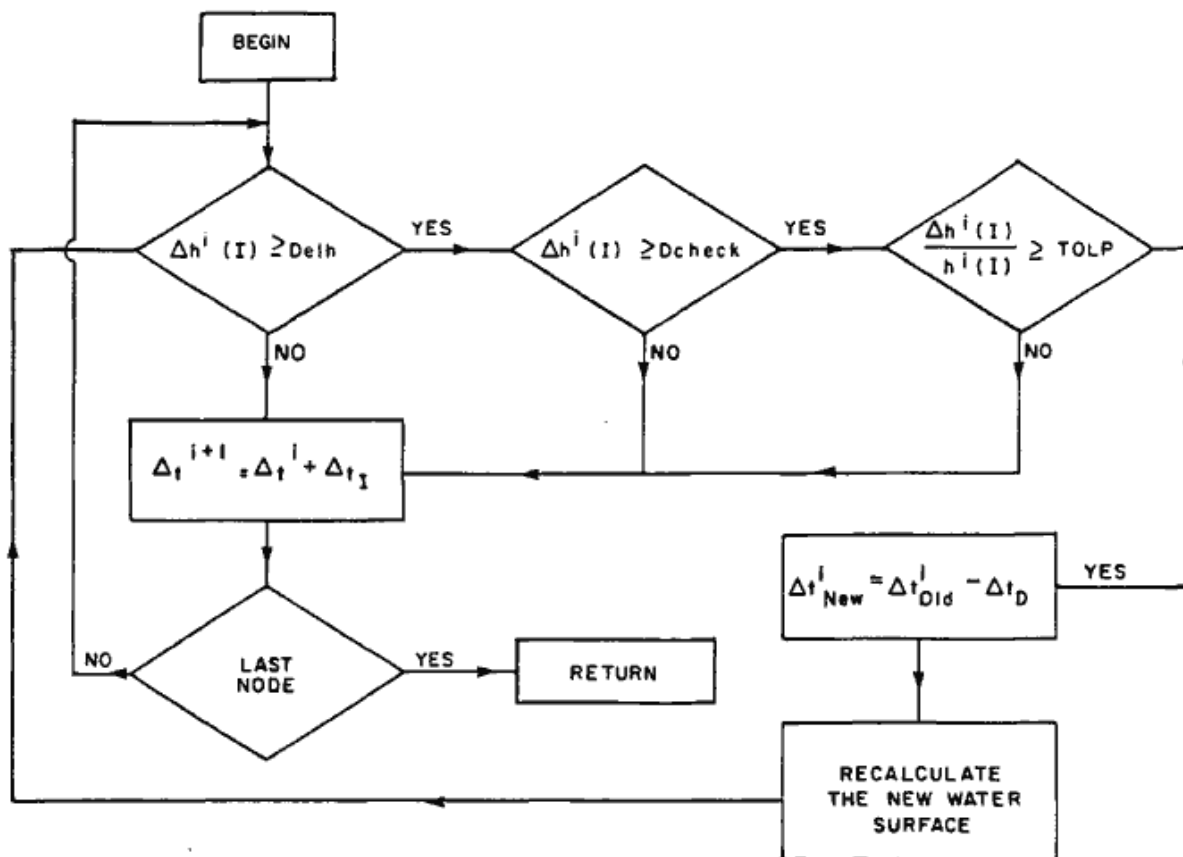


Figure B.4.-- Algorithm for the variable time step.

where

$\Delta h^i(I)$ is the change of water depth for Node I at time step i,

Delh is the user specified tolerance,

Δt^i is the interval for time step i,

Δt_I is the user specified incremental time interval,

Δt_D is the user specified decremental time interval,

TOLP is the user specified percentage of water depth, and

Dcheck is defined as Delh/TOLP.

Kinematic Routing Techniques

The kinematic routing technique is also included in the DHM model.

By setting KMODEL to 1, the kinematic routing is evoked.

ATTACHMENT C
COMPUTER LISTINGS

```
C
C   PROGRAM DMH21
C
COMMON/BLK 1/FP(250,8),FC(250,6)
COMMON/BLK 2/KIN(10),H(10,15,2),KOUT(10),HOUT(10,15,3)
COMMON/BLK 3/NOSTA(10),STA(10,15,2),NODFX(50)
COMMON/BLK 4/DMAX(250,2),TIMEX(250,2)
COMMON/BLK 5/KINP(10),HP(10,15,2)
COMMON/BLK 6/NODC,NCHI,NCHO,NPCHI,NPCHO,NSTA,NPSTA
COMMON/BLK 7/DTOL,DTOLP,NFLUX,KFLUX,CHECKD,ITER
DIMENSION NODDC(50),VEL(250,4),R(10,2),Q(4)
DATA NR/1/,NW/2/

C
C   DEFINITIONS
C
C   FLOODPLAIN INFORMATION:
C
C   FP(I,J)=N,E,S,W,MANNINGS,ELEV.,INITIAL DEPTH,TEMPORARY MEMORY
C   Q(I)=FLOWRATE PER UNIT WIDTH OF FLOW
C   R(I,1)=TIME COORDINATE FOR EFFECTIVE RAINFALL INTENSITY IN HOUR
C   R(I,2)=EFFECTIVE RAINFALL INTENSITY(IN/HR)
C   KINP(I)=INFLOW NODAL POINTS
C   HP(I,J,K)=INFLOW HYDROGRAPH FOR NODE I
C   DMAX(I,J)=MAXIMUM WATER DEPTH
C   TIMEX(I,J)=TIME CORRESPONDS TO MAXIMUM WATER DEPTH
C   NODDC(I)=CRITICAL DEPTH OUTFLOW NODES
C   VEL(I,J)=N-,E-,S-,AND W-EFFLUX VELOCITIES
C
C.....OPEN INPUT AND OUTPUT FILES
OPEN (UNIT=NR,FILE='DHM21.DAT',STATUS='OLD')
OPEN (UNIT=NW,FILE='DHM21.ANS',STATUS='NEW')

C
C   DATA INPUT
C
C.....READ PROGRAM CONTROL DATA
READ (NR,*)DTMIN,DTMAX,DTI,DTD,SIMUL,ITER,TOUT,KODE,KMODEL
READ (NR,*)NNOD,NODC,SIDE,TOL,DTOL,DTOLP
C.....INPUT FLOODPALIN INFORMATION
READ (NR,*)((FP(I,J),J=1,7),I=1,NNOD)
C.....READ EFFECTIVE RAINFALL INTENSITY (LINEAR FUNCTION)
READ (NR,*)NERI
IF(NERI.GE.1)READ (NR,*)((R(I,J),J=1,2),I=1,NERI)
C.....READ INFLOW HYDROGRAPHS (LINEAR FUNCTION)
READ (NR,*)NFPI,NPFPI
IF(NFPI.LT.1)GOTO 10
DO 20 I=1,NFPI
READ (NR,*)KINP(I),(HP(I,J,1),HP(I,J,2),J=1,NPFPI)
20 CONTINUE
```



```

C.....READ OUTFLOW CRITICAL DEPTH NODES
10  READ (NR,*)NDC
    IF(NDC.GE.1)READ (NR,*)(NODDC(I),I=1,NDC)
C.....READ SPECIFIED OUTFLOW NODES
    READ (NR,*)NFLUX,TFOUT
    IF(NFLUX.GE.1)READ (NR,*) (NODFX(I),I=1,NFLUX)
    IF(NODC.LT.1)GOTO 30
C.....INPUT CHANNEL INFORMATION
    DO 25 I=1,NODC
    READ (NR,*)KK,(FC(KK,J),J=1,3),FC(KK,5)
    FC(KK,4)=FP(KK,6)-FC(KK,3)
25  CONTINUE
    READ (NR,*)NCHI,NPCHI,NCHO,NPCHO,NSTA,NPSTA
    IF(NCHI.LT.1)GOTO 40
C.....READ INFLOW HYDROGRAPHS (LINEAR FUNCTION)
    DO 50 I=1,NCHI
    READ (NR,*)KIN(I),(H(I,J,1),H(I,J,2),J=1,NPCHI)
50  CONTINUE
40  IF(NCHO.LT.1)GOTO 60
    DO 70 I=1,NCHO
C.....READ OUTFLOW BOUNDARY CONDITION NODES
C.....  QOUT = ALPHA*(DEPTH OF WATER)**BETA
    READ (NR,*)KOUT(I),(HOUT(I,J,1),HOUT(I,J,2),
    C  HOUT(I,J,3),J=1,NPCHO)
70  CONTINUE
60  IF(NSTA.LT.1)GOTO 30
C.....READ STAGE CURVE (LINEAR FUNCTION)
    DO 80 I=1,NSTA
80  READ (NR,*) NOSTA(I),(STA(I,J,1),STA(I,J,2),J=1,NPSTA)
30  CONTINUE
C.....END OF INPUT DATA
    ITTER=ITER
    IF(ITTER.EQ.0)ITTER=1

C
C  WRITE BASIC INFORMATION TO OUTPUT FILE
C
C.....FORMATS
2001  FORMAT(/,10X,'*** KINEMATIC ROUTING ***',/)
2002  FORMAT(/,10X,'*** DIFFUSION ROUTING ***',/)
2003  FORMAT(10X,'MIN. TIMESTEP(SEC.) = ',F5.2,/,
    C  10X,'MAX. TIMESTEP(SEC.) = ',F5.2,/,
    C  10X,'INCREASED TIMESTEP INTERVAL (SEC.) = ',F5.2,/,
    C  10X,'DECREASED TIMESTEP INTERVAL (SEC.) = ',F5.2,/,
    C  10X,'TOTAL SIMULATION(HOUR) = ',F5.2,/,
    C  10X,'UPDATE INTERVAL(TIMESTEPS) = ',I5,/,
    C  10X,'OUTPUT INTERVAL(HOUR) = ',F5.2)
2004  FORMAT(10X,'NUMBER OF NODAL POINTS FOR FLOOD PLAIN = ',I5,/,
    C  10X,'UNIFORM GRID SIDE(FEET) = ',F10.3,/,
    C  10X,'NUMBER OF NODAL POINTS FOR CHANNEL = ',I5,/,
    C  10X,'RETENTION WATER DEPTH(FEET) = ',F5.4,/,
    C  10X,'TOLERANCE OF CHANGE IN WATER DEPTH(FEET) = ',F5.4,/,
    C  10X,'PERCENTAGE OF CHANGE IN WATER DEPTH = ',F5.1,' %')

```

```

2005  FORMAT(130('-',))
2006  FORMAT(/,10X,'NODAL POINT DATA ENTRY:',//,
C    7X,'*** FLOOD PLAIN INFORMATION ***',/,
C    10X,'NC = CENTRAL GRID NODE',/,
C    10X,'NN,NE,NS,NW = NORTH, EAST, SOUTH, WEST NODAL POINTS',/,
C    10X,'NBAR = NODAL POINT MANNINGS ROUGHNESS COEFFICIENT',/,
C    12X,'(NEGATIVE SIGN INDICATES A CHANNEL PASSING THROUGH)',/,
C    10X,'ELEV = NODAL POINT ELEVATION',/,
C    10X,'DEPTH = INITIAL WATER DEPTH AT NODE',//)
2007  FORMAT(11X,' NC NN NE NS NW NBAR ELEV. DEPTH')
2008  FORMAT(10X,5I4,1X,F6.4,2X,F6.1,1X,F5.1)
2009  FORMAT(/,10X,'NUMBER OF EFFECTIVE RAINFALL INTENSITY ',
C    'ENTRIES = ',I2,/,4X,'LINEAR FUNCTION IN EFFECTIVE RAINFALL',
C    ' INTENSITY (IN/HR) ON WATERSHED:',/,10X,'HOUR INTENSITY')
2010  FORMAT(8X,F6.2,4X,F6.2)
2011  FORMAT(/,10X,'INFLOW HYDROGRAPH AT NODE #',I3,/,
C    12X,'HOUR CFS')
2012  FORMAT(10X,F5.1,4X,F7.0)
2013  FORMAT(/,10X,'NUMBER OF CRITICAL-DEPTH OUTFLOW NODES = ',I4,/,
C    10X,'CRITICAL-DEPTH OUTFLOW NODE NUMBERS:')
2014  FORMAT(10X,I3,1X,I3)
2015  FORMAT(/,7X,'***CHANNEL INFORMATION***',/.
C    10X,'NODE NBAR WIDTH DEPTH BOTTOM INITIAL DEPTH')
2016  FORMAT(10X,I3,2X,F5.4,1X,F7.1,1X,F7.1,1X,F7.1,5X,F7.1)
2017  FORMAT(10X,'OUTFLOW IS APPROXIMATED AS THE FOLLOWING EQUATION:',
C    /,12X,'QOUT = ALPHA*(DEPTH)**BETA')
2018  FORMAT(10X,'OUTFLOW NODE # ',I3,
C    /,9X,'DEPTH LESS THAN',
C    /,9X,' OR EQUAL TO ALPHA BETA')
2019  FORMAT(15X,F4.1,6X,F7.3,1X,F7.3)
2020  FORMAT(/,10X,'STAGE CURVE AT NODE #',I3,/,
C    12X,'HOUR FEET')
2021  FORMAT(10X,F5.1,4X,F7.3)
2022  FORMAT(/,5X,'MODEL TIME(HOURS) = ',F10.2)
2023  FORMAT(11X,'EFFECTIVE RAINFALL(IN/HR) = ',F6.2,/)
2024  FORMAT(/,5X,'AVERAGE FLOW RATE FOR SPECIFIED FLOOD PLAIN ',
C    'NODES :',/,10X,'NODE',5X,'QN',9X,'QE',9X,'QS',9X,'QW')
2025  FORMAT(10X,I4,4(2X,E9.3))
2026  FORMAT(/,5X,'MODEL TIME(HOURS) = ',F10.2,' (SECONDS) = ',E9.3,
C    ' (TOTAL TIMESTEP NUMBER) = ',IPE9.1)
2027  FORMAT(7X,'***FLOOD PLAIN RESULTS***')
2028  FORMAT(10X,'INFLOW RATE AT NODE ',I3,' IS EQUAL TO ',F10.2)
2029  FORMAT(/,5X,'NODE',7X,10(I3,8X))
2030  FORMAT(5X,'DEPTH',10(3X,F8.3))
2031  FORMAT(3X,'ELEVATION',F9.3,10(2X,F9.3))
2032  FORMAT(5X,'VEL-N',10(3X,F8.3))
2033  FORMAT(5X,'VEL-E',10(3X,F8.3))
2034  FORMAT(5X,'VEL-S',10(3X,F8.3))
2035  FORMAT(5X,'VEL-W',10(3X,F8.3))
2036  FORMAT(/,5X,'OUTFLOW RATE AT CRITICAL-DEPTH NODES:',
C    /,10X,'NODE OUTFLOW RATE(CFS)')

```

```

2037 FORMAT(10X,14,5X,F10.2)
2038 FORMAT(//,7X,'***CHANNEL RESULTS***',/)
2039 FORMAT(10X,'OUTFLOW RATE AT NODE ',I3,' IS EQUAL TO ',F10.2)
2040 FORMAT(//,5X,'MIN. TIMESTEP(SEC.) = ',F5.2,
C   5X,'MAX. TIMESTEP(SEC.) = ',F5.2,
C   5X,'MEAN TIMESTEP(SEC.) = ',F5.2,/)
2041 FORMAT(130('='))
2042 FORMAT(///,10X,'MAXIMUM WATER SURFACE VALUES FOR FLOOD',
C   ' PLAIN',/)
2043 FORMAT(5X,'TIME ',10(3X,F8.3))
2044 FORMAT(///,10X,'MAXIMUM WATER SURFACE VALUES FOR CHANNEL',/)
2045 FORMAT(2X,'*** DEPTH OF WATER IS EITHER GREATER THAN',
1   ' 150 OR LESS THAN 0 ***',/,2X,'*** PROGRAM STOP ***')
2046 FORMAT(2X,'*** MINIMUM TIMESTEP ',F4.1,' SEC. IS TOO LARGE!!',
1   /,2X,' ==> A SMALLER TIMESTEP SHOULD BE USED ***')
C
IF(KMODEL.EQ.1)WRITE(NW,2001)
IF(KMODEL.NE.1)WRITE(NW,2002)
WRITE(NW,2003)DTMIN,DTMAX,DTI,DTD,SIMUL,ITTER,TOUT
WRITE(NW,2004)NNOD,SIDE,NODC,TOL,DTOL,DTOLP
WRITE(NW,2005)
WRITE(NW,2006)
WRITE(NW,2007)
DO 90 I=1,NNOD
NN=IFIX(FP(I,1))
NE=IFIX(FP(I,2))
NS=IFIX(FP(I,3))
NNW=IFIX(FP(I,4))
WRITE(NW,2008)I,NN,NE,NS,NNW,(FP(I,J),J=5,7)
90 CONTINUE
WRITE(NW,2005)
IF(NERI.LT.1)GOTO 100
WRITE(NW,2009)NERI
WRITE(NW,2010)((R(I,J),J=1,2),I=1,NERI)
WRITE(NW,2005)
100 IF(NFPI.LT.1)GOTO 110
DO 120 I=1,NFPI
WRITE(NW,2011)KINP(I)
DO 120 J=1,NPFPI
WRITE(NW,2012)HP(I,J,1),HP(I,J,2)
120 CONTINUE
WRITE(NW,2005)
110 IF(NDC.LT.1)GOTO 130
WRITE(NW,2013)NDC
WRITE(NW,2014)(NODDC(I),I=1,NDC)
WRITE(NW,2005)
130 IF(NODC.LT.1)GOTO 140
WRITE(NW,2015)
DO 135 I=1,NNOD
IF(FC(I,1).EQ.0.)GO TO 135
WRITE(NW,2016)I,(FC(I,J),J=1,5)
135 CONTINUE
WRITE(NW,2005)
IF(NCHI.LT.1)GOTO 150

```

```

DO 160 I=1,NCHI
WRITE(NW,2011)KIN(I)
DO 160 J=1,NPCHI
WRITE(NW,2012)H(I,J,1),H(I,J,2)
160 CONTINUE
WRITE(NW,2005)
150 IF(NCHO.LT.1)GOTO 170
WRITE(NW,2017)
DO 180 I=1,NCHO
WRITE(NW,2018)KOUT(I)
DO 180 J=1,NPCHO
WRITE(NW,2019)HOUT(I,J,1),HOUT(I,J,2),HOUT(I,J,3)
180 CONTINUE
WRITE(NW,2005)
170 IF(NSTA.LT.1)GOTO 140
DO 190 I=1,NSTA
WRITE(NW,2020)NOSTA(I)
DO 190 J=1,NPSTA
WRITE(NW,2021)STA(I,J,1),STA(I,J,2)
190 CONTINUE
WRITE(NW,2005)
140 CONTINUE
C
C
C MAIN PROGRAM
C
C
C.....INITIALIZE CONSTANTS
ITERA=0
DSEC=DTMIN
DT=DTMIN/3600.
DTOLP=DTOLP*.01
CHECKD=DTOL/DTOLP
TTIME=0.
QBC=0.
QTEMP=0.
KK=0
TTOUT=TOUT
TTFOUT=TFOUT
KIT=0
TIME=0.
DO 200 J=1,NNOD
DMAX(J,1)=0.
TIMEX(J,1)=0.
DMAX(J,2)=0.
TIMEX(J,2)=0.
FP(J,8)=0.
200 CONTINUE
C
C.....MAIN LOOP FOR MODEL
C
210 KKOUT=0
TMIN=99.
TMAX=-99.
TMEAN=0.

```

```

C
C.....FLOODPLAIN MODEL

C
220   KFLUX=0
      IKODE=0
      TIME=TIME+DT
230   FPMAX=0.
      ITERA=ITERA+1
      FCMAX=0.
      IJK=0
      IF(ITER.EQ.0 .AND. NODC.NE.0)GO TO 240
      TTIME=DSEC
      GO TO 250
C.....UPDATE TIME AND BOUNDARY CONDITION VALUES
240   IF(NFPI.LT.1)GOTO 260
      DO 270 J=1,NFPI
      DO 280 I=2,NPFPI
      IF(TIME.GT.HP(J,I,1))GOTO 280
      QTEMP=HP(J,I-1,2)+(HP(J,I,2)-HP(J,I-1,2))*(TIME-HP(J,I-1,1))/
C      (HP(J,I,1)-HP(J,I-1,1))
      GO TO 290
280   CONTINUE
      QTEMP=HP(J,NPFPI,2)
290   QBC=QTEMP/SIDE
      IF(QBC.LT.0.)QBC=0.
      JJ=KINP(J)
      FP(JJ,8)=FP(JJ,8)+QBC
270   CONTINUE
C.....INCLUDE THE EFFECITIVE RAINFALL ON THE WATERSHED
260   IF(NERI.LT.1)GOTO 300
      DO 310 J=2,NERI
      IF(TIME.GT.R(J,1))GOTO 310
      RRATE=R(J-1,2)+(R(J,2)-R(J-1,2))*(TIME-R(J-1,1))/
C      (R(J,1)-R(J-1,1))
      GO TO 320
310   CONTINUE
320   QRAIN=RRATE*SIDE*SIDE/(12.*3600.)
      DO 330 J=1,NNOD
      FP(J,8)=FP(J,8)+QRAIN/SIDE
330   CONTINUE
300   IF(NFLUX.EQ.0)GOTO 340
      IF(TIME.LT.TTFOUT)GOTO 340
      TTFOUT=TTFOUT+TFOUT
      IF(ITER.EQ.0 .AND. NODC.NE.0)GO TO 340
      WRITE(NW,2005)
      WRITE(NW,2022)TIME
      IF(RRATE.NE.0.)WRITE(NW,2023)RRATE
      IJK=1
      WRITE(NW,2024)
340   CONTINUE

```

```

C.....CALCULATE FLOW VELOCITIES AND FLOWRATES
DO 350 I=1,NNOD
DO 360 II=1,4
NQ=FP(I,II)
IF(NQ.EQ.0.)GOTO 360
CALL QFP(I,NQ,SIDE,QQ,ID,VV,TOL,KMODEL)
IF(ID.EQ.1)GOTO 370
360   Q(II)=QQ
C.....ADJUST FLOWRATES FOR DIRECTION
Q(3)=-Q(3)
Q(4)=-Q(4)
C.....ESTIMATE ACCUMULATION OF INFLOW
QNET=Q(3)+Q(4)-Q(1)-Q(2)
IF(NFLUX.EQ.0)GOTO 380
IF(IJK.NE.1)GOTO 380
QN=Q(1)*SIDE
QE=Q(2)*SIDE
QS=Q(3)*SIDE
QW=Q(4)*SIDE
DO 390 J=1,NFLUX
IF(I.EQ.NODFX(J))WRITE(NW,2025)I,QN,QE,QS,QW
390   CONTINUE
380   FP(I,8)=QNET+FP(I,8)
350   CONTINUE
C.....ACCOUNT FOR CRITICAL-DEPTH OUTFLOW NODES
IF(NDC.LT.1)GOTO 400
DO 410 J=1,NDC
JJ=NODDC(J)
QOUT=5.67*(FP(JJ,7)**0.5)*(FP(JJ,7)-TOL)
IF(FP(JJ,7).LT.TOL)QOUT=0.
FP(JJ,8)=FP(JJ,8)-QOUT
410   CONTINUE
C.....UPDATE CHANGE OF WATER DEPTH
400   DO 420 J=1,NNOD
FP(J,8)=FP(J,8)*DSEC/SIDE
TEMP=ABS(FP(J,8))
IF(TEMP.LT.DTOL)GOTO 420
IF(FP(J,7).LT.CHECKD)FPMAX=99.
IF(FP(J,7).LT.CHECKD)GOTO 430
TOLP=TEMP/FP(J,7)
IF(TOLP.GE.DTOLP)FPMAX=99.
IF(TOLP.GE.DTOLP)GOTO 430
420   CONTINUE
C.....CALCULATE THE EFFLUX VELOCITIES
IF(KODE.NE.1)GOTO 440
DO 450 J=1,NNOD
DO 450 II=1,4
NQ=FP(J,II)
IF(NQ.EQ.0.)GOTO 450
CALL QFP(J,NQ,SIDE,QQ,ID,VV,TOL,KMODEL)
VEL(J,II)=VV
450   CONTINUE

```

```

C.....CHECK INTERFACE MODEL UPDATE REQUEST
440   IF(IKODE.EQ.0)KIT=KIT+1
      IF(IKODE.EQ.0)TTIME=TTIME+DSEC
      IF(KIT.EQ.ITER .AND. NODC.GE.1)GOTO 430
C
C.....UPDATE WATER DEPTH FOR CHANNEL
C
250   CALL FLOODC(TIME,TTIME,NNOD,SIDE,TOL,FCMAX,NW,KMODEL)
C.....UPDATE NEW TIMESTEP SIZE
430   DD=AMAX1(FPMAX,FCMAX)
      IF(DD.GT.0.)DSECP=DSEC-DTD
      IF(DD.LE.0.)DSECP=DSEC+DTI
      IF(DSECP.LT.DTMIN)DSECP=DTMIN
      IF(DSECP.GT.DTMAX)DSECP=DTMAX
      DTT=DSECP/3600.
      IF(DD.LE.DTOL)GOTO 460
      IF(DSEC.EQ.DTMIN)IKODE=1+IKODE
      IF(DSEC.NE.DTMIN)IKODE=1
      IF(IKODE.GE.3)GOTO 470
      TIME=TIME-DT+DTT
      IF(TTIME.EQ.0.)GOTO 480
      TTIME=TTIME-DSEC+DSECP
      IF(TTIME.LT.DTMIN)TTIME=DTMIN
480   DO 490 J=1,NNOD
      FP(J,8)=0.
490   CONTINUE
      DT=DTT
      DSEC=DSECP
      GO TO 230
C.....UPDATE DEPTH OF WATER
460   DO 500 J=1,NNOD
      FP(J,7)=FP(J,7)+FP(J,8)
      IF(FP(J,7).LT.0.)FP(J,7)=0.
      FP(J,8)=0.
      IF(NODC.LT.1)GOTO 500
      FC(J,5)=FC(J,5)+FC(J,6)
      IF(FC(J,5).LT.0.)FC(J,5)=0.
      FC(J,6)=0.
500   CONTINUE
      IF(DSEC.GT.TMAX)TMAX=DSEC
      IF(DSEC.LT.TMIN)TMIN=DSEC
C.....INTERFACE BETWEEN FLOOD PLAIN AND CHANNEL DEPTHS
      IF(KIT.NE.ITER)GOTO 510
      IF(NODC.LT.1)GOTO 510
      IF(ITER.NE.0)CALL CHANPL(NNOD,SIDE,TOL)
      TTIME=0.
      KIT=0
C.....CHECK OUTPUT REQUEST
510   IF(TIME.LT.TTOUT)GOTO 520
C.....USE FC(I,6) AND FP(I,8) TO STORE WATER SURFACE ELEVATIONS
      DO 530 J=1,NNOD
      IF(NODC.LT.1)GOTO 540
      FC(J,6)=FC(J,5)+FC(J,4)
      IF(ITER.EQ.0)GOTO 530
540   FP(J,8)=FP(J,7)+FP(J,6)
530   CONTINUE

```

```

C.....UPDATE MAXIMUM WATER SURFACE VALUES
520 DO 550 J=1,NNOD
    IF(FP(J,7).LT.DMAX(J,1))GOTO 550
    DMAX(J,1)=FP(J,7)
    TIMEX(J,1)=TIME
550 CONTINUE
    IF(NODC.LT.1)GOTO 560
    DO 570 J=1,NNOD
    IF(FC(J,5).LT.DMAX(J,2))GOTO 570
    DMAX(J,2)=FC(J,5)
    TIMEX(J,2)=TIME
570 CONTINUE
560 TMEAN=TMEAN+DSEC
    KKOUT=KKOUT+1
    DT=DTT
    DSEC=DSECP
    IF(TIME.GE.TI .AND. TIME.LE.TO)GOTO 370
    IF(TIME.LT.TTOUT)GOTO 220
C.....STORE FLOODPLAIN AND CHANNEL RESULTS IN OUTPUT FILE
370 WRITE(NW,2005)
    XTIME=TIME*3600.
    XTERA=REAL(ITERA)
    WRITE(NW,2026)TIME,XTIME,XTERA
    WRITE(NW,2022)TIME
    IF(RRATE.NE.0.)WRITE(NW,2023)RRATE
    IF(ITER.EQ.0 .AND. NODC.NE.0)GOTO 580
    WRITE(NW,2027)
    IF(NFPI.LT.1)GOTO 590
    DO 600 J=1,NFPI
    DO 610 I=2,NPFPI
    IF(TIME.GT.HP(J,I,1))GOTO 610
    QIN=HP(J,I-1,2)+(HP(J,I,2)-HP(J,I-1,2))*(TIME-HP(J,I-1,1))/
    C      (HP(J,I,1)-HP(J,I-1,1))
    GO TO 620
610 CONTINUE
620 WRITE(NW,2028)KINP(J),QIN
600 CONTINUE
590 KO=1
    IO=1
    JO=10
630 DO 615 II=IO,JO
    IF(FP(II,7).GT.0.)GOTO 625
615 CONTINUE
    GO TO 635
625 WRITE(NW,2029)(J,J=IO,JO)
    WRITE(NW,2030)(FP(J,7),J=IO,JO)
    WRITE(NW,2031)(FP(J,8),J=IO,JO)
    IF(KODE.EQ.1)WRITE(NW,2032)(VEL(J,1),J=IO,JO)
    IF(KODE.EQ.1)WRITE(NW,2033)(VEL(J,2),J=IO,JO)
    IF(KODE.EQ.1)WRITE(NW,2034)(VEL(J,3),J=IO,JO)
    IF(KODE.EQ.1)WRITE(NW,2035)(VEL(J,4),J=IO,JO)

```



```

635      KO=KO+1
        IO=IO+10
        JO=10*KO
        IF(JO.LE.NNOD)GOTO 630
        IF(JO-NNOD.GE.10)GOTO 640
        JO=NNOD
        GO TO 630
640      DO 650 J=1,NNOD
650      FP(J,8)=0.
C.....OUTPUT OUTFLOW RATE AT CRITICAL-DEPTH NODES
        IF(NDC.LT.1)GOTO 580
        WRITE(NW,2036)
        DO 660 J=1,NDC
        JJ=NODDC(J)
        QOUT=5.67*(FP(JJ,7)**0.5)*SIDE*(FP(JJ,7)-TOL)
        IF(FP(JJ,7).LT.TOL)QOUT=0.
        WRITE(NW,2037)JJ,QOUT
660      CONTINUE
        WRITE(NW,2005)
580      IF(NODC.LT.1)GOTO 670
        WRITE(NW,2038)
        IF(NCHI.LT.1)GOTO 680
        DO 690 J=1,NCHI
        DO 700 I=2,NPCHI
        IF(TIME.GT.H(J,I,1))GOTO 700
        QIN=H(J,I-1,2)+(H(J,I,2)-H(J,I-1,2))*(TIME-H(J,I-1,1))/
C          (H(J,I,1)-H(J,I-1,1))
        GO TO 710
700      CONTINUE
710      WRITE(NW,2028)KIN(J),QIN
690      CONTINUE
680      IF(NCHO.LT.1)GOTO 720
        DO 730 J=1,NCHO
        JJ=KOUT(J)
        DO 740 KJ=1,NPCHO
        IF(FC(JJ,5).GT.HOUT(J,KJ,1))GOTO 740
        QOUT=HOUT(J,KJ,2)*(FC(JJ,5)**HOUT(J,KJ,3))
        IF(FC(JJ,5).LT.TOL)QOUT=0.
        GO TO 750
740      CONTINUE
750      WRITE(NW,2039)JJ,QOUT
730      CONTINUE
720      CONTINUE

```

```

      KO=1
      IO=1
      JO=10
760   DO 770 I1=IO,JO
      IF(FC(I1,5).GT.0.)GOTO 780
770   CONTINUE
      GO TO 790
780   WRITE(NW,2029)(J,J=IO,JO)
      WRITE(NW,2030)(FC(J,5),J=IO,JO)
      WRITE(NW,2031)(FC(J,6),J=IO,JO)
790   KO=KO+1
      IO=IO+10
      JO=10*KO
      IF(JO.LE.NNOD)GOTO 760
      IF(JO-NNOD.GE.10)GOTO 800
      JO=NNOD
      GO TO 760
800   DO 810 J=1,NNOD
810   FC(J,6)=0.
      C
      C.....END OF MAIN LOOP
      C
670   IF(ID.EQ.1)GOTO 470
      TMEAN=TMEAN/FLOAT(KKOUT)
      WRITE(NW,2040)TMIN,TMAX,TMEAN
      TTOUT=TTOUT+TOUT
      IF(TIME.LT.SIMUL)GOTO 210
470   WRITE(NW,2041)
      C.....OUTPUT THE MAXIMUM WATER SURFACE
      IF(ITER.EQ.0 .AND. NODC.NE.0)GOTO 820
      WRITE(NW,2042)
      KO=1
      IO=1
      JO=10
830   WRITE(NW,2029)(J,J=IO,JO)
      WRITE(NW,2030)(DMAX(J,1),J=IO,JO)
      WRITE(NW,2043)(TIMEX(J,1),J=IO,JO)
      KO=KO+1
      IO=IO+10
      JO=10*KO
      IF(JO.LE.NNOD)GOTO 830
      IF(JO-NNOD.GE.10)GOTO 840
      JO=NNOD
      GO TO 830

```

```

840 WRITE(NW,2041)
820 IF(NODC.LT.1)GOTO 850
      WRITE(NW,2044)
      KO=1
      IO=1
      JO=10
860 DO 870 II=IO,JO
      IF(DMAX(II,2).GT.0.)GOTO 880
870 CONTINUE
      GO TO 890
880 WRITE(NW,2029)(J,J=IO,JO)
      WRITE(NW,2030)(DMAX(J,2),J=IO,JO)
      WRITE(NW,2043)(TIMEX(J,2),J=IO,JO)
890 KO=KO+1
      IO=IO+10
      JO=10*KO
      IF(JO.LE.NNOD)GOTO 880
      IF(JO-NNOD.GE.10)GOTO 850
      JO=NNOD
      GO TO 880
850 WRITE(NW,2041)
C.....END OF PROGRAM
      IF(ID.EQ.1)WRITE(NW,2045)
      IF(IKODE.GE.3)WRITE(NW,2046)DSEC
C
      STOP
      END

```

```

SUBROUTINE FLOODC(TIME,TTIME,NNOD,SIDE,TOL,FCMAX,NW,KMODEL)
C
C THIS SUBROUTINE CALCULATES THE DEPTH OF WATER FOR
C THE CHANNEL MODEL
C
COMMON/BLK 1/FP(250,8),FC(250,6)
COMMON/BLK 2/KIN(10),H(10,15,2),KOUT(10),HOUT(10,15,3)
COMMON/BLK 3/NOSTA(10),STA(10,15,2),NODFX(50)
COMMON/BLK 4/DMAX(250,2),TIMEX(250,2)
COMMON/BLK 6/NODC,NCHI,NCHO,NPCHI,NPCHO,NSTA,NPSTA
COMMON/BLK 7/DTOL,DTOLP,NFLUX,KFLUX,CHECKD,ITER
DIMENSION Q(4)
C
C DEFINITIONS
C
C FC(I,J)=MANNINGS,WIDTH,DEPTH,BOTTOM ELEVATION,INITIAL DEPTH,
C TEMPORARY MEMORY
C KIN(I)=ARRAY OF INFLOW NODE
C H(I,J,1)=TIME COORDINATE FOR INFLOW RATE IN HOUR
C H(I,J,2)=INFLOW RATE(CFS)
C KOUT(I)=ARRAY OF OUTFLOW NODE
C HOUT(I,J)=PARAMETERS FOR OUTFLOW NODE
C Q(I)=VOLUME OF FLOW
C NOSTA(I)=ARRAY OF STAGE STATION
C STA(I,J,1)=TIME COORDINATE FOR STAGE CURVE
C STA(I,J,2)=DEPTH OF WATER IN FEET
C
C CHANNEL MODEL
C
C.....INITIALIZE CONSTANTS
QBC=0.
QTEMP=0.
DO 30 J=1,NNOD
FC(J,6)=0.
30 CONTINUE
C
C.....FORMATS
C
212 FORMAT(/,130('-'),/,5X,'MODEL TIME(HOUR) = ',F10.2,/)
213 FORMAT(/,5X,'AVERAGE FLOW RATE FOR SPECIFIED CHANNEL NODES :',
C /,10X,'NODE',5X,'QN',9X,'QE',9X,'QS',9X,'QW')
214 FORMAT(10X,I4,4(2X,E9.3))
C
IF(KFLUX.EQ.1 .AND. ITER.EQ.0)WRITE(NW,212)TIME
IF(KFLUX.EQ.1)WRITE(NW,213)
C
C.....MAIN LOOP FOR CHANNEL MODEL
C
C.....UPDATE TIME AND BOUNDARY CONDITION VALUES
IF(NCHI.LT.1)GOTO 40
DO 50 J=1,NCHI
DO 60 I=2,NPCHI
IF(TIME.GT.H(J,I,1))GOTO 60
QTEMP=H(J,I-1,2)+(H(J,I,2)-H(J,I-1,2))*(TIME-H(J,I-1,1))/
C (H(J,I,1)-H(J,I-1,1))
GO TO 70

```

```

60     CONTINUE
70     QBC=QTEMP*TTIME
      IF(QBC.LT.0.)QBC=0.
C.....UPDATE INFLOW BOUNDARY CONDITION NODES
      JJ=KIN(J)
      FC(JJ,6)=QBC
50     CONTINUE
C.....CALCULATE FLOW VELOCITIES AND FLOWRATES
40     DO 80 I=1,NNOD
      QNET=0.
      IF(FP(I,5).GT.0.)GOTO 80
      DO 90 II=1,4
      NQ=FP(I,II)
      IF(NQ.EQ.0)GOTO 90
      IF(FP(NQ,5).GT.0.)NQ=0
      IF(NQ.EQ.0)GOTO 90
      CALL QFC(I,NQ,QQ,SIDE,TOL,KMODEL)
90     Q(II)=QQ
C.....ADJUST FLOWRATES FOR DIRECTION
      Q(3)=-Q(3)
      Q(4)=-Q(4)
C.....ESTIMATE ACCUMULATION OF INFLOW
      QNET=(Q(3)+Q(4)-Q(1)-Q(2))*TTIME
      IF(NFLUX.EQ.0)GOTO 80
      IF(KFLUX.EQ.0)GOTO 80
      DO 100 J=1,NFLUX
      IF(I.NE.NODFX(J))GOTO 100
      WRITE(NW,214)I,Q(1),Q(2),Q(3),Q(4)
100    CONTINUE
80     FC(I,6)=QNET+FC(I,6)
C.....ACCOUNT DISCHARGE AT OUTFLOW NODES
      IF(NCHO.LT.1)GOTO 110
      DO 120 J=1,NCHO
      JJ=KOUT(J)
      DO 130 K=1,NPCHO
      IF(FC(JJ,5).GT.HOUT(J,K,1))GOTO 130
      QOUT=HOUT(J,K,2)*(FC(JJ,5)**HOUT(J,K,3))*TTIME
      IF(FC(JJ,5).LT.TOL)QOUT=0.
      GO TO 140
130    CONTINUE
140    FC(JJ,6)=FC(JJ,6)-QOUT
120    CONTINUE
C.....UPDATE THE WATER ELEVATIONS AT STAGE STATIONS
110    IF(NSTA.LT.1)GOTO 150
      DO 160 I=1,NSTA
      NN=NOSTA(I)
      DO 170 J=2,NPSTA
      IF(TIME.GT.STA(I,J,1))GOTO 170
      DE=STA(I,J-1,2)+(STA(I,J,2)-STA(I,J-1,2))*(TIME-STA(I,J-1,1))
      C    /(STA(I,J,1)-STA(I,J-1,1))
      GO TO 180

```

```

170    CONTINUE
180    CONTINUE
      FC(NN,5)=DE-FC(NN,4)
      FC(NN,6)=0.
160    CONTINUE
C.....CHECK MAXIMUM CHANGE OF WATER DEPTH
150    DO 190 J=1,NNOD
      IF(NSTA.LT.1)GOTO 200
      DO 210 JJ=1,NSTA
      IF(J.EQ.NOSTA(JJ))GOTO 190
210    CONTINUE
200    IF(FP(J,5).GT.0.)GOTO 190
      A=0.
      KCO=0
      DO 220 JJ=1,4
      NQ=FP(J,JJ)
      IF(FP(NQ,5).GT.0.)GOTO 220
      A=A+(.25*FC(NQ,2)+.75*FC(J,2))* .5*SIDE
      KCO=KCO+1
220    CONTINUE
      IF(KCO.EQ.1)A=2,*A
      FC(J,6)=FC(J,6)/A
190    CONTINUE
      DO 230 I=1,NNOD
      TEMP=ABS(FC(I,6))
      IF(TEMP.LT.DTOL)GOTO 230
      IF(FC(I,5).LT.CHECKD)FCMAX=99.
      IF(FC(I,5).LT.CHECKD)RETURN
      TOLP=TEMP/FC(I,5)
      IF(TOLP.GE.DTOLP)FCMAX=99.
      IF(TOLP.GE.DTOLP)RETURN
230    CONTINUE
      RETURN
      END

```

```

SUBROUTINE CHANPL(NNOD,SIDE,TOL)
C
C THIS SUBROUTINE UPDATES THE WATER SUFRACE ELEVATION
C BETWEEN THE FLOODPLAIN AND CHANNEL MODELS
C
COMMON/BLK 1/FP(250,8),FC(250,6)
C
DO 100 I=1,NNOD
C.....CHECK INTERFACE BETWEEN CHANNEL AND FLOOD PLAIN
IF(FP(I,5).GT.0.)GOTO 100
C.....A IS WATER LEVEL AT FLOOD PLAIN
C.....B IS WATER LEVEL AT CHANNEL
C.....FC(I,3) IS THE DEPTH OF CHANNEL
A=FP(I,6)+FP(I,7)
B=FC(I,4)+FC(I,5)
IF(A.GT.B)GOTO 110
C.....FLOODING OF CHANNEL, B > A
FP(I,7)=FP(I,7)+(B-A)*FC(I,2)/SIDE
FC(I,5)=FP(I,7)+FC(I,3)
GO TO 100
C.....FLOW INTO CHANNEL FROM GRID ELEMENT, A > B
110 IF(FC(I,3).LT.FC(I,5))GOTO 120
VAL=(FC(I,3)-FC(I,5)+TOL)*FC(I,2)
VW=(SIDE-FC(I,2))*(FP(I,7)-TOL)
C.....CASE 1 - NO FLOW INTO CHANNEL
IF(VW.LT.0.)GOTO 100
IF(VAL.GE.VW)GOTO 130
C.....CASE 2 - CHANNEL IS FULL AFTER FILLING
FP(I,7)=TOL+(VW-VAL)/SIDE
FC(I,5)=FC(I,3)+FP(I,7)
GO TO 100
C.....CASE 3 - FC(I,3) > FC(I,5)
130 FC(I,5)=FC(I,5)+VW/FC(I,2)
FP(I,7)=TOL
GOTO 100
C.....CASE 4 - FC(I,5) > FC(I,3)
120 FP(I,7)=B+(A-B)*(SIDE-FC(I,2))/SIDE-FP(I,6)
FC(I,5)=FP(I,7)+FC(I,3)
100 CONTINUE
RETURN
END

```

```

SUBROUTINE QFC(I,NQ,QQ,SIDE,TOL,KMODEL)
C
C THIS SUBROUTINE CALCULATES VOLUME OF WATER THAT
C FLOWS ACROSS THE ADJACENT CONTROL VOLUMES FOR
C CHANNEL FLOW
C
COMMON/BLK 1/FP(250,8),FC(250,6)
QQ=0.
DCH=.5*(FC(I,3)+FC(NQ,3))
WID=.5*(FC(I,2)+FC(NQ,2))
H=FC(I,4)+FC(I,5)
IF(KMODEL.EQ.1)H=FC(I,4)
IF(FC(I,5).EQ.0..AND.FC(NQ,5).EQ.0.)GOTO 200
C..... DEPTHS ARE NONZERO
HN=FC(NQ,4)+FC(NQ,5)
IF(KMODEL.EQ.1)HN=FC(NQ,4)
GRAD=(HN-H)/SIDE
IF(GRAD)150,200,170
C..... H > HN
150 IF(FC(I,5).LT.TOL)GOTO 200
YBAR=FC(I,5)
GOTO 180
C..... HN > H
170 IF(FC(NQ,5).LT.TOL)GOTO 200
YBAR=FC(NQ,5)
180 HBAR=.5*(FC(I,5)+FC(NQ,5))
WETT=2.*HBAR+WID
WETC=2.*DCH+WID
WET=AMIN1(WETC,WETT)
A=WID*HBAR
R=A/WET
IF(HBAR.LT.TOL)GOTO 200
XNBAR=.5*(FC(I,1)+FC(NQ,1))
AGRAD=ABS(GRAD)
IF(AGRAD.LT..00001)GOTO 200
XK=(1.486/XNBAR)*R**0.667/SQRT(AGRAD)
VEL=-XK*GRAD
QQ=VEL*WID*YBAR
200 CONTINUE
RETURN
END

```



```

C      SUBROUTINE QFP(I,NQ,SIDE,QQ, ID,VEL,TOL,KMODEL)
C      THIS SUBROUTINE CALCULATES THE EFFLUX PER UNIT WIDTH
C      WHICH FLOWS ACROSS THE ADJACENT CONTORL VOLUMES FOR
C      FLOODPLAIN FLOW
C
C      COMMON/BLK 1/FP(250,8),FC(250,6)
C      VEL=0.
C      ID=0
C      QQ=0.
C      H=FP(I,7)+FP(I,6)
C      IF(KMODEL.EQ.1)H=FP(I,6)
C      IF(FP(I,7).EQ.0. .AND.FP(NQ,7).EQ.0.)GOTO 200
C..... DEPTHS ARE NONZERO
C      HN=FP(NQ,7)+FP(NQ,6)
C      IF(KMODEL.EQ.1)HN=FP(NQ,6)
C      GRAD=(HN-H)/SIDE
C      HBAR=.5*(FP(I,7)+FP(NQ,7))
C      IF(GRAD)150,200,170
C..... H > HN
150    IF(FP(I,7).LT.TOL)GOTO 200
C      YBAR=FP(I,7)-TOL
C      GOTO 180
C..... HN > H
170    IF(FP(NQ,7).LT.TOL)GOTO 200
C      YBAR=FP(NQ,7)-TOL
180    XNBAR=.5*(ABS(FP(I,5))+ABS(FP(NQ,5)))
C      AGRAD=ABS(GRAD)
C      IF(AGRAD.LT..00001)GOTO 200
C      XK=(1.486/XNBAR)*YBAR*HBAR**.667/SQRT(AGRAD)
C      IF(HBAR.LT.O. .OR. HBAR.GT.150.)ID=1
C      QQ=-XK*GRAD
C      VEL=QQ/YBAR
200    CONTINUE
C      RETURN
C      END

```

ATTACHMENT D

EXAMPLE RUN (APPLICATION 7)
Input File

```

1. 30. 1. 10. 10. 1 .5 0 2
160 36 500 .0001 .1 10.
  2 11 0 0 .040 101.000 0.
  3 12 1 0 .040 101.500 0.
  4 13 2 0 .040 102.000 0.
  5 14 3 0 .040 102.500 0.
  6 15 4 0 .040 103.000 0.
  7 16 5 0 .040 103.500 0.
  8 17 6 0 .040 104.000 0.
  9 18 7 0 .040 104.500 0.
10 19 8 0 .040 105.000 0.
  0 20 9 0 .040 105.500 0.
12 21 0 1 .040 100.500 0.
13 22 11 2 .040 101.000 0.
14 23 12 3 .040 101.500 0.
15 24 13 4 .040 102.000 0.
16 25 14 5 .040 102.500 0.
17 26 15 6 .040 103.000 0.
18 27 16 7 .040 103.500 0.
19 28 17 8 .040 104.000 0.
20 29 18 9 .040 104.500 0.
  0 30 19 10 .040 105.000 0.
22 31 0 11 .040 100.000 0.
23 32 21 12 .040 100.500 0.
24 33 22 13 .040 101.000 0.
25 34 23 14 .040 101.500 0.
26 35 24 15 .040 102.000 0.
27 36 25 16 .040 102.500 0.
28 37 26 17 .040 103.000 0.
29 38 27 18 .040 103.500 0.
30 39 28 19 .040 104.000 0.
  0 40 29 20 .040 104.500 0.
32 41 0 21 -.040 99.500 0.
33 42 31 22 -.040 100.000 0.
34 43 32 23 -.040 100.500 0.
35 44 33 24 -.040 101.000 0.
36 45 34 25 -.040 101.500 0.
37 46 35 26 -.040 102.000 0.
38 47 36 27 -.040 102.500 0.
39 48 37 28 -.040 103.000 0.
40 49 38 29 -.040 103.500 0.
  0 50 39 30 -.040 104.000 0.
42 51 0 31 .040 100.000 0.
43 52 41 32 .040 100.500 0.
44 53 42 33 .040 101.000 0.
45 54 43 34 .040 101.500 0.
46 55 44 35 .040 102.000 0.
47 56 45 36 .040 102.500 0.
48 57 46 37 .040 103.000 0.

```

49	58	47	38	.040	103.500	0.
50	59	48	39	.040	104.000	0.
0	60	49	40	.040	104.500	0.
52	61	0	41	.040	100.500	0.
53	62	51	42	.040	101.000	0.
54	63	52	43	.040	101.500	0.
55	64	53	44	.040	102.000	0.
56	65	54	45	.040	102.500	0.
57	66	55	46	.040	103.000	0.
58	67	56	47	.040	103.500	0.
59	68	57	48	.040	104.000	0.
60	69	58	49	.040	104.500	0.
0	70	59	50	.040	105.000	0.
62	71	0	51	.040	100.000	0.
63	72	61	52	.040	100.500	0.
64	73	62	53	.040	101.000	0.
65	74	63	54	.040	101.500	0.
66	75	64	55	.040	102.000	0.
67	76	65	56	.040	102.500	0.
68	77	66	57	.040	103.000	0.
69	78	67	58	.040	103.500	0.
70	79	68	59	.040	104.000	0.
0	80	69	60	.040	104.500	0.
72	81	0	61	-.040	99.500	0.
73	82	71	62	-.040	100.000	0.
74	83	72	63	-.040	100.500	0.
75	84	73	64	-.040	101.000	0.
76	85	74	65	-.040	101.500	0.
77	86	75	66	-.040	102.000	0.
78	87	76	67	-.040	102.500	0.
79	88	77	68	-.040	103.000	0.
80	89	78	69	-.040	103.500	0.
0	90	79	70	-.040	104.000	0.
82	91	0	71	.040	100.000	0.
83	92	81	72	.040	100.500	0.
84	93	82	73	.040	101.000	0.
85	94	83	74	.040	101.500	0.
86	95	84	75	.040	102.000	0.
87	96	85	76	-.040	102.500	0.
88	97	86	77	.040	103.000	0.
89	98	87	78	.040	103.500	0.
90	99	88	79	.040	104.000	0.
0	100	89	80	.040	104.500	0.
92	101	0	81	.040	100.500	0.
93	102	91	82	.040	101.000	0.
94	103	92	83	.040	101.500	0.
95	104	93	84	.040	102.000	0.
96	105	94	85	.040	102.500	0.
97	106	95	86	-.040	103.000	0.
98	107	96	87	-.040	103.500	0.
99	108	97	88	-.040	104.000	0.

100	109	98	89	-.040	104.500	0.
0	110	99	90	-.040	105.000	0.
102	111	0	91	.040	101.000	0.
103	112	101	92	.040	101.500	0.
104	113	102	93	.040	102.000	0.
105	114	103	94	.040	102.500	0.
106	115	104	95	.040	103.000	0.
107	116	105	96	.040	103.500	0.
108	117	106	97	.040	104.000	0.
109	118	107	98	.040	104.500	0.
110	119	108	99	.040	105.000	0.
0	120	109	100	.040	105.500	0.
112	121	0	101	.040	100.500	0.
113	122	111	102	.040	101.000	0.
114	123	112	103	.040	101.500	0.
115	124	113	104	.040	102.000	0.
116	125	114	105	.040	102.500	0.
117	126	115	106	.040	103.000	0.
118	127	116	107	.040	103.500	0.
119	128	117	108	.040	104.000	0.
120	129	118	109	.040	104.500	0.
0	130	119	110	.040	105.000	0.
122	131	0	111	-.040	100.000	0.
123	132	121	112	-.040	100.500	0.
124	133	122	113	-.040	101.000	0.
125	134	123	114	-.040	101.500	0.
126	135	124	115	-.040	102.000	0.
127	136	125	116	-.040	102.500	0.
128	137	126	117	-.040	103.000	0.
129	138	127	118	-.040	103.500	0.
130	139	128	119	-.040	104.000	0.
0	140	129	120	-.040	104.500	0.
132	141	0	121	.040	100.500	0.
133	142	131	122	.040	101.000	0.
134	143	132	123	.040	101.500	0.
135	144	133	124	.040	102.000	0.
136	145	134	125	.040	102.500	0.
137	146	135	126	.040	103.000	0.
138	147	136	127	.040	103.500	0.
139	148	137	128	.040	104.000	0.
140	149	138	129	.040	104.500	0.
0	150	139	130	.040	105.000	0.
142	151	0	131	.040	101.000	0.
143	152	141	132	.040	101.500	0.
144	153	142	133	.040	102.000	0.
145	154	143	134	.040	102.500	0.
146	155	144	135	.040	103.000	0.
147	156	145	136	.040	103.500	0.
148	157	146	137	.040	104.000	0.
149	158	147	138	.040	104.500	0.
150	159	148	139	.040	105.000	0.

0	160	149	140	.040	105.500	0.		
152	0	0	141	.040	101.500	0.		
153	0	151	142	.040	102.000	0.		
154	0	152	143	.040	102.500	0.		
155	0	153	144	.040	103.000	0.		
156	0	154	145	.040	103.500	0.		
157	0	155	146	.040	104.000	0.		
158	0	156	147	.040	104.500	0.		
159	0	157	148	.040	105.000	0.		
160	0	158	149	.040	105.500	0.		
0	0	159	150	.040	106.000	0.		
0								
0	0							
9								
1	2	3	4	5	6	7	8	9
0	0							
31	.015	10.	6.	93.5	0.			
32	.015	10.	6.	94.0	0.			
33	.015	10.	6.	94.5	0.			
34	.015	10.	6.	95.0	0.			
35	.015	10.	6.	95.5	0.			
36	.015	10.	6.	96.0	0.			
37	.015	10.	6.	96.5	0.			
38	.015	10.	6.	97.0	0.			
39	.015	10.	6.	97.5	0.			
40	.015	10.	6.	98.0	0.			
71	.015	10.	6.	93.5	0.			
72	.015	10.	6.	94.0	0.			
73	.015	10.	6.	94.5	0.			
74	.015	10.	6.	95.0	0.			
75	.015	10.	6.	95.5	0.			
76	.015	10.	6.	96.0	0.			
77	.015	10.	6.	96.5	0.			
78	.015	10.	6.	97.0	0.			
79	.015	10.	6.	97.5	0.			
80	.015	10.	6.	98.0	0.			
86	.015	10.	5.5	97.0	0.			
96	.015	10.	5.	98.0	0.			
97	.015	10.	5.	98.5	0.			
98	.015	10.	5.	99.0	0.			
99	.015	10.	5.	99.5	0.			
100	.015	10.	5.	100.0	0.			
121	.015	10.	6.	94.0	0.			
122	.015	10.	6.	94.5	0.			
123	.015	10.	6.	95.0	0.			
124	.015	10.	6.	95.5	0.			
125	.015	10.	6.	96.0	0.			
126	.015	10.	6.	96.5	0.			
127	.015	10.	6.	97.0	0.			
128	.015	10.	6.	97.5	0.			
129	.015	10.	6.	98.0	0.			

130 .015 10. 6 98.5 0.

4 5 3 1 0 0

40 0 0 1 300 3 300 5 0 12 0

80 0 0 1 300 3 300 5 0 12 0

100 0 0 1 200 3 200 5 0 12 0

130 0 0 1 400 3 400 5 0 12 0

31 30 30 1

71 30 30 1

121 30 30 1

Output File (partial results)

*** DIFFUSION ROUTING ***

```

MIN. TIMESTEP(SEC.) = 1 00
MAX. TIMESTEP(SEC.) = 30 00
INCREASED TIMESTEP INTERVAL (SEC.) = 1.00
DECREASED TIMESTEP INTERVAL (SEC.) = 10.00
TOTAL SIMULATION(HOUR) = 10 00
UPDATE INTERVAL(TIMESTEPS) = 1
OUTPUT INTERVAL(HOUR) = 50
NUMBER OF NODAL POINTS FOR FLOOD PLAIN = 160
UNIFORM GRID SIDE(FEET) = 500 000
NUMBER OF NODAL POINTS FOR CHANNEL = 36
RETARDING WATER DEPTH(FEET) = 0001
TOLERANCE OF CHANGE IN WATER DEPTH(FEET) = .1000
PERCENTAGE OF CHANGE IN WATER DEPTH = 10.0 %
    
```

NODAL POINT DATA ENTRY:

*** FLOOD PLAIN INFORMATION ***

```

NC = CENTRAL GRID NODE
NN,NE,NS,NW = NORTH, EAST, SOUTH, WEST NODAL POINTS
NBAR = NODAL POINT MANNINGS FRICTION FACTOR
(NEGATIVE SIGN INDICATES A CHANNEL PASSING THROUGH)
ELEV = NODAL POINT ELEVATION
DEPTH = INITIAL WATER DEPTH AT NODE
    
```

NC	NN	NE	NS	NW	NBAR	ELEV.	DEPTH
1	2	11	0	0	.0400	101.0	.0
2	3	12	1	0	.0400	101.5	.0
3	4	13	2	0	.0400	102.0	.0
4	5	14	3	0	.0400	102.5	.0
5	6	15	4	0	.0400	103.0	.0
6	7	16	5	0	.0400	103.5	.0
7	8	17	6	0	.0400	104.0	.0
8	9	18	7	0	.0400	104.5	.0
9	10	19	8	0	.0400	105.0	.0
10	0	20	9	0	.0400	105.5	.0
11	12	21	0	1	.0400	100.5	.0
12	13	22	11	2	.0400	101.0	.0
13	14	23	12	3	.0400	101.5	.0
14	15	24	13	4	.0400	102.0	.0
15	16	25	14	5	.0400	102.5	.0
16	17	26	15	6	.0400	103.0	.0
17	18	27	16	7	.0400	103.5	.0
18	19	28	17	8	.0400	104.0	.0
19	20	29	18	9	.0400	104.5	.0
20	0	30	19	10	.0400	105.0	.0
21	22	31	0	11	.0400	100.0	.0
22	23	32	21	12	.0400	100.5	.0
23	24	33	22	13	.0400	101.0	.0
24	25	34	23	14	.0400	101.5	.0
25	26	35	24	15	.0400	102.0	.0
26	27	36	25	16	.0400	102.5	.0
27	28	37	26	17	.0400	103.0	.0
28	29	38	27	18	.0400	103.5	.0
29	30	39	28	19	.0400	104.0	.0
30	0	40	29	20	.0400	104.5	.0
31	32	41	0	21	.0400	99.5	.0
32	33	42	31	22	.0400	100.0	.0
33	34	43	32	23	.0400	100.5	.0
34	35	44	33	24	.0400	101.0	.0
35	36	45	34	25	.0400	101.5	.0
36	37	46	35	26	.0400	102.0	.0
37	38	47	36	27	.0400	102.5	.0
38	39	48	37	28	.0400	103.0	.0
39	40	49	38	29	.0400	103.5	.0
40	0	50	39	30	.0400	104.0	.0
41	42	51	0	31	.0400	100.0	.0
42	43	52	41	32	.0400	100.5	.0
43	44	53	42	33	.0400	101.0	.0
44	45	54	43	34	.0400	101.5	.0
45	46	55	44	35	.0400	102.0	.0
46	47	56	45	36	.0400	102.5	.0
47	48	57	46	37	.0400	103.0	.0
48	49	58	47	38	.0400	103.5	.0

INFLOW HYDROGRAPH AT NODE # 40

HOUR	CFS
0	0
1 0	300
3 0	300
6 0	0
12 0	0

INFLOW HYDROGRAPH AT NODE # 80

HOUR	CFS
0	0
1 0	300
3 0	300
6 0	0
12 0	0

INFLOW HYDROGRAPH AT NODE #100

HOUR	CFS
0	0
1 0	200
3 0	200
6 0	0
12 0	0

INFLOW HYDROGRAPH AT NODE #130

HOUR	CFS
0	0
1 0	400
3 0	400
6 0	0
12 0	0

OUTFLOW IS APPROXIMATED AS THE FOLLOWING EQUATION:

$Q_{OUT} = \text{ALPHA} * (\text{DEPTH}) ** \text{BETA}$

OUTFLOW NODE #	DEPTH LESS THAN OR EQUAL TO	ALPHA	BETA
31	30 0	30 000	1 000
71	30 0	30 000	1 000
121	30 0	30 000	1 000

MODEL TIME (HOURS) = 3 00
 FLOOD PLAIN RESULTS

NODE	1	2	3	4	5	6	7	8	9	10
DEPTH	.000	.000	.000	.000	.000	.000	.000	.000	.000	.000
ELEVATION	101.000	101.500	102.000	102.500	103.000	103.500	104.000	104.500	105.000	105.500
NODE	11	12	13	14	15	16	17	18	19	20
DEPTH	.062	.000	.000	.000	.000	.000	.000	.000	.000	.000
ELEVATION	100.562	101.000	101.500	102.000	102.500	103.000	103.500	104.000	104.500	105.000
NODE	21	22	23	24	25	26	27	28	29	30
DEPTH	.571	.107	.000	.000	.000	.000	.000	.000	.000	.000
ELEVATION	100.571	100.607	101.000	101.500	102.000	102.500	103.000	103.500	104.000	104.500
NODE	31	32	33	34	35	36	37	38	39	40
DEPTH	1.078	.617	.276	.058	.000	.000	.000	.000	.000	.000
ELEVATION	100.578	100.617	100.776	101.059	101.500	102.000	102.500	103.000	103.500	104.000
NODE	41	42	43	44	45	46	47	48	49	50
DEPTH	.599	.109	.000	.000	.000	.000	.000	.000	.000	.000
ELEVATION	100.599	100.609	101.000	101.500	102.000	102.500	103.000	103.500	104.000	104.500
NODE	51	52	53	54	55	56	57	58	59	60
DEPTH	.336	.000	.000	.000	.000	.000	.000	.000	.000	.000
ELEVATION	100.836	101.000	101.500	102.000	102.500	103.000	103.500	104.000	104.500	105.000
NODE	61	62	63	64	65	66	67	68	69	70
DEPTH	.869	.409	.078	.000	.000	.000	.000	.000	.000	.000
ELEVATION	100.869	100.909	101.078	101.500	102.000	102.500	103.000	103.500	104.000	104.500

NODE	71	72	73	74	75	76	77	78	79	80
DEPTH	1.381	.918	.585	.415	.336	.304	.087	.000	.000	.00
ELEVATION	100.881	100.918	101.085	101.415	101.836	102.304	102.587	103.000	103.500	104.00
NODE	81	82	83	84	85	86	87	88	89	90
DEPTH	.880	.411	.078	.000	.000	.000	.000	.000	.000	.00
ELEVATION	100.880	100.911	101.078	101.500	102.000	102.500	103.000	103.500	104.000	104.50
NODE	91	92	93	94	95	96	97	98	99	100
DEPTH	.376	.000	.000	.000	.000	.000	.000	.000	.000	.00
ELEVATION	100.876	101.000	101.500	102.000	102.500	103.000	103.500	104.000	104.500	105.00
NODE	101	102	103	104	105	106	107	108	109	110
DEPTH	.000	.000	.000	.000	.000	.000	.000	.000	.000	.00
ELEVATION	101.000	101.500	102.000	102.500	103.000	103.500	104.000	104.500	105.000	105.50
NODE	111	112	113	114	115	116	117	118	119	120
DEPTH	.351	.000	.000	.000	.000	.000	.000	.000	.000	.00
ELEVATION	100.851	101.000	101.500	102.000	102.500	103.000	103.500	104.000	104.500	105.00
NODE	121	122	123	124	125	126	127	128	129	130
DEPTH	.854	.434	.120	.000	.000	.000	.000	.000	.000	.01
ELEVATION	100.854	100.939	101.120	101.500	102.000	102.500	103.000	103.500	104.000	104.48
NODE	131	132	133	134	135	136	137	138	139	140
DEPTH	.351	.000	.000	.000	.000	.000	.000	.000	.000	.00
ELEVATION	100.851	101.000	101.500	102.000	102.500	103.000	103.500	104.000	104.500	105.00
NODE	141	142	143	144	145	146	147	148	149	150
DEPTH	.000	.000	.000	.000	.000	.000	.000	.000	.000	.00
ELEVATION	101.000	101.500	102.000	102.500	103.000	103.500	104.000	104.500	105.000	105.50
NODE	151	152	153	154	155	156	157	158	159	160
DEPTH	.000	.000	.000	.000	.000	.000	.000	.000	.000	.00
ELEVATION	101.500	102.000	102.500	103.000	103.500	104.000	104.500	105.000	105.500	106.00

OUTFLOW RATE AT CRITICAL-DEPTH NODES

NODE	OUTFLOW RATE(CFS)
1	.00
2	.00
3	.00
4	.00
5	.00
6	.00
7	.00
8	.00
9	.00

CHANNEL RESULTS

INFLOW RATE AT NODE 40 IS EQUAL TO 299.81
 INFLOW RATE AT NODE 80 IS EQUAL TO 299.81
 INFLOW RATE AT NODE 100 IS EQUAL TO 199.87
 INFLOW RATE AT NODE 130 IS EQUAL TO 399.75
 OUTFLOW RATE AT NODE 31 IS EQUAL TO 212.34
 OUTFLOW RATE AT NODE 71 IS EQUAL TO 221.42
 OUTFLOW RATE AT NODE 121 IS EQUAL TO 205.63

NODE	31	32	33	34	35	36	37	38	39	40
DEPTH	7.078	6.617	6.276	6.058	5.903	5.789	5.657	5.561	5.482	5.410
ELEVATION	100.578	100.617	100.776	101.059	101.403	101.769	102.157	102.561	102.952	103.410
NODE	71	72	73	74	75	76	77	78	79	80
DEPTH	7.381	6.918	6.585	6.415	6.336	6.304	6.087	5.929	5.793	5.670
ELEVATION	100.881	100.918	101.085	101.415	101.836	102.304	102.587	102.929	103.293	103.670
NODE	81	82	83	84	85	86	87	88	89	90
DEPTH	.000	.000	.000	.000	.000	3.480	.000	.000	.000	.000
ELEVATION	.000	.000	.000	.000	.000	102.480	.000	.000	.000	.000
NODE	91	92	93	94	95	96	97	98	99	100
DEPTH	.000	.000	.000	.000	.000	4.743	4.548	4.385	4.252	4.140
ELEVATION	.000	.000	.000	.000	.000	102.743	103.048	103.385	103.752	104.140
NODE	121	122	123	124	125	126	127	128	129	130
DEPTH	6.854	6.434	6.120	5.882	5.675	5.488	5.331	5.194	5.080	4.980
ELEVATION	100.854	100.935	101.120	101.382	101.675	101.988	102.331	102.694	103.080	103.480

MIN TIMESTEP(SEC.) = 1.00 MAX. TIMESTEP(SEC.) = 15.00 MEAN TIMESTEP(SEC.) = 7.45

MAXIMUM WATER SURFACE VALUES FOR FLOOD PLAIN

NODE	1	2	3	4	5	6	7	8	9	10
DEPTH	.000	.000	.000	.000	.000	.000	.000	.000	.000	.000
TIME	10.006	10.006	10.006	10.006	10.006	10.006	10.006	10.006	10.006	10.006
NODE	11	12	13	14	15	16	17	18	19	20
DEPTH	.378	.000	.000	.000	.000	.000	.000	.000	.000	.000
TIME	4.905	10.006	10.006	10.006	10.006	10.006	10.006	10.006	10.006	10.006
NODE	21	22	23	24	25	26	27	28	29	30
DEPTH	.883	.389	.000	.000	.000	.000	.000	.000	.000	.000
TIME	4.759	4.606	10.006	10.006	10.006	10.006	10.006	10.006	10.006	10.006
NODE	31	32	33	34	35	36	37	38	39	40
DEPTH	1.382	.892	.424	.071	.003	.000	.000	.000	.000	.000
TIME	4.646	4.603	4.524	3.214	1.851	10.006	10.006	10.006	10.006	10.006
NODE	41	42	43	44	45	46	47	48	49	50
DEPTH	.896	.396	.000	.000	.000	.000	.000	.000	.000	.000
TIME	4.647	4.671	10.006	10.006	10.006	10.006	10.006	10.006	10.006	10.006
NODE	51	52	53	54	55	56	57	58	59	60
DEPTH	.495	.033	.000	.000	.000	.000	.000	.000	.000	.000
TIME	4.454	4.383	10.006	10.006	10.006	10.006	10.006	10.006	10.006	10.006
NODE	61	62	63	64	65	66	67	68	69	70
DEPTH	1.020	.538	.140	.000	.000	.000	.000	.000	.000	.000
TIME	4.255	4.188	3.829	10.006	10.006	10.006	10.006	10.006	10.006	10.006
NODE	71	72	73	74	75	76	77	78	79	80
DEPTH	1.524	1.047	.647	.429	.339	.304	.088	.002	.000	.000
TIME	4.334	4.253	3.766	3.342	3.141	3.048	3.016	3.361	10.006	10.006
NODE	81	82	83	84	85	86	87	88	89	90
DEPTH	1.027	.540	.140	.000	.000	.000	.000	.000	.000	.000
TIME	4.320	4.334	3.829	10.006	10.006	10.006	10.006	10.006	10.006	10.006
NODE	91	92	93	94	95	96	97	98	99	100
DEPTH	.524	.035	.000	.000	.000	.000	.000	.000	.000	.000
TIME	4.388	4.306	10.006	10.006	10.006	10.006	10.006	10.006	10.006	10.006
NODE	101	102	103	104	105	106	107	108	109	110
DEPTH	.019	.000	.000	.000	.000	.000	.000	.000	.000	.000
TIME	4.598	10.006	10.006	10.006	10.006	10.006	10.006	10.006	10.006	10.006
NODE	111	112	113	114	115	116	117	118	119	120
DEPTH	.513	.053	.000	.000	.000	.000	.000	.000	.000	.000
TIME	4.484	4.383	10.006	10.006	10.006	10.006	10.006	10.006	10.006	10.006
NODE	121	122	123	124	125	126	127	128	129	130
DEPTH	1.009	.558	.202	.005	.001	.000	.000	.000	.000	.000
TIME	4.503	4.402	4.167	3.313	1.740	10.006	10.006	10.006	10.006	10.006
NODE	131	132	133	134	135	136	137	138	139	140
DEPTH	.511	.053	.000	.000	.000	.000	.000	.000	.000	.000
TIME	4.580	4.383	10.006	10.006	10.006	10.006	10.006	10.006	10.006	10.006
NODE	141	142	143	144	145	146	147	148	149	150
DEPTH	.006	.000	.000	.000	.000	.000	.000	.000	.000	.000
TIME	4.747	10.006	10.006	10.006	10.006	10.006	10.006	10.006	10.006	10.006
NODE	151	152	153	154	155	156	157	158	159	160
DEPTH	.000	.000	.000	.000	.000	.000	.000	.000	.000	.000
TIME	10.006	10.006	10.006	10.006	10.006	10.006	10.006	10.006	10.006	10.006

MAXIMUM WATER SURFACE VALUES FOR CHANNEL

NODE	1	2	3	4	5	6	7	8	9	10
DEPTH	.000	.000	.000	.000	.000	.000	.000	.000	.000	.000
TIME	10.006	10.006	10.006	10.006	10.006	10.006	10.006	10.006	10.006	10.006
NODE	11	12	13	14	15	16	17	18	19	20
DEPTH	.000	.000	.000	.000	.000	.000	.000	.000	.000	.000
TIME	10.006	10.006	10.006	10.006	10.006	10.006	10.006	10.006	10.006	10.006
NODE	21	22	23	24	25	26	27	28	29	30
DEPTH	.000	.000	.000	.000	.000	.000	.000	.000	.000	.000
TIME	10.006	10.006	10.006	10.006	10.006	10.006	10.006	10.006	10.006	10.006
NODE	31	32	33	34	35	36	37	38	39	40
DEPTH	7.382	6.892	6.424	6.071	6.003	5.880	5.880	5.596	5.522	5.420
TIME	4.646	4.603	4.524	3.214	1.851	1.376	1.851	1.849	1.851	2.987
NODE	41	42	43	44	45	46	47	48	49	50
DEPTH	.000	.000	.000	.000	.000	.000	.000	.000	.000	.000
TIME	10.006	10.006	10.006	10.006	10.006	10.006	10.006	10.006	10.006	10.006
NODE	51	52	53	54	55	56	57	58	59	60
DEPTH	.000	.000	.000	.000	.000	.000	.000	.000	.000	.000
TIME	10.006	10.006	10.006	10.006	10.006	10.006	10.006	10.006	10.006	10.006
NODE	61	62	63	64	65	66	67	68	69	70
DEPTH	.000	.000	.000	.000	.000	.000	.000	.000	.000	.000
TIME	10.006	10.006	10.006	10.006	10.006	10.006	10.006	10.006	10.006	10.006
NODE	71	72	73	74	75	76	77	78	79	80
DEPTH	7.524	7.047	6.647	6.429	6.339	6.304	6.088	6.002	5.921	5.686
TIME	4.334	4.253	3.766	3.342	3.141	3.048	2.916	3.561	3.004	2.987
NODE	81	82	83	84	85	86	87	88	89	90
DEPTH	.000	.000	.000	.000	.000	3.485	.000	.000	.000	.000
TIME	10.006	10.006	10.006	10.006	10.006	2.987	10.006	10.006	10.006	10.006
NODE	91	92	93	94	95	96	97	98	99	100
DEPTH	.000	.000	.000	.000	.000	4.744	4.550	4.385	4.253	4.147
TIME	10.006	10.006	10.006	10.006	10.006	2.982	2.987	2.982	2.987	2.999
NODE	101	102	103	104	105	106	107	108	109	110
DEPTH	.000	.000	.000	.000	.000	.000	.000	.000	.000	.000
TIME	10.006	10.006	10.006	10.006	10.006	10.006	10.006	10.006	10.006	10.006
NODE	111	112	113	114	115	116	117	118	119	120
DEPTH	.000	.000	.000	.000	.000	.000	.000	.000	.000	.000
TIME	10.006	10.006	10.006	10.006	10.006	10.006	10.006	10.006	10.006	10.006
NODE	121	122	123	124	125	126	127	128	129	130
DEPTH	7.009	6.558	6.202	6.005	6.001	5.879	5.522	5.347	5.116	5.000
TIME	4.503	4.402	4.167	3.313	1.740	3.313	1.740	3.957	1.740	3.985
NODE	131	132	133	134	135	136	137	138	139	140
DEPTH	.000	.000	.000	.000	.000	.000	.000	.000	.000	.000
TIME	10.006	10.006	10.006	10.006	10.006	10.006	10.006	10.006	10.006	10.006
NODE	141	142	143	144	145	146	147	148	149	150
DEPTH	.000	.000	.000	.000	.000	.000	.000	.000	.000	.000
TIME	10.006	10.006	10.006	10.006	10.006	10.006	10.006	10.006	10.006	10.006
NODE	151	152	153	154	155	156	157	158	159	160
DEPTH	.000	.000	.000	.000	.000	.000	.000	.000	.000	.000
TIME	10.006	10.006	10.006	10.006	10.006	10.006	10.006	10.006	10.006	10.006